Appendix A: Estimation of the total in-place gas resource in the Bowland-Hodder shales, central Britain

Aim

The aim of this study is to estimate the P10-P50-P90[1] range of **total gas-in-place volumes** for the upper and lower Bowland-Hodder (Early Carboniferous) shale units across the Pennine Basin of central Britain.

This analysis forms the appendix to the main Bowland-Hodder report, which provides the detailed geological background to this shale gas play. This specific study applies a Monte Carlo simulation to a suite of input parameters, some of which come from the geology-based methodology described in the main report, and others which are based on information from published analogues.

Introduction

The total gas content of a shale is made up of two main components:

Free gas – the gas contained in pore spaces; this volume is very pressure dependent, and pressure is related to depth (assuming no overpressure).

Adsorbed gas – the gas which is adsorbed in the organic matter in the shale. The quantity of gas adsorbed is dependent on the quantity, type and distribution of the organic content within the shale, it is largely pressure independent.

In the USA shale gas plays, the ratio of adsorbed gas to free gas varies from 60:40 to 10:90 (Jarvie 2012).

Equations[2]

Free gas at standard conditions is calculated using the equation:

$GIIP_f = A * h * \phi * Bg$

Where A = area
       h = thickness
       ϕ = gas-filled porosity
       B_g = gas expansion factor (depth dependant)

---

[1] P10, P50 and P90 correspond to the 10%, 50% or 90% probability of more than that amount being present. In the case of P10, there is a 10% probability that the actual result will be higher, or a 90% chance the result will be lower.
[2] In this project, metric units have been used throughout the calculation stages, with the conversion to imperial units only given for the presentation of the output (Table 3b and Figures 1 and 2).

Adsorbed gas is calculated using the equation:

$GIIP_a = A * h * \rho * G$

Where A = area

h = thickness

ρ = rock density

G = adsorbed gas content of shale (volume of gas/weight of shale)

Where experimental analysis of core samples is available, the Langmuir equation is used to calculate G:

$$G = \frac{G_l * P}{P_l + P}$$

Where G_l = Langmuir volume [volume of adsorbed gas at infinite pressure]

P_l = Langmuir pressure [pressure where one-half of the gas at infinite pressure has been desorbed]

P = Reservoir pressure

Total gas in place (GIIP) (at standard conditions) **= Free gas (GIIP $_f$) + Adsorbed gas (GIIP$_a$)**

Values used

Free gas

The controlling factors for free gas are **area**, **thickness**, *gas-filled porosity* and **depth** (and overpressure, if present). Those factors that are estimated in this study are shown in bold; those that rely on analogues are shown in italics.

Rather than inputting parameters for area and thickness separately, a figure for net shale volume has been used. This is the volume of organic-rich shale (TOC>2%) which is considered mature for gas generation (R_o>1.1). The explanation of how this volume was derived can be found in Section 3.9 of the main report. Error bars of ± 15% have been used to take into account uncertainties in the seismic mapping.

Specific information on the gas-filled porosities of UK shales is not available. Reported gas-filled porosities for US gas shales are in the range 1-5% (Curtis 2002) and 2.9-6% (Jarvie 2012) (Table 1). Lewis *et al.* (2004) quotes a figure of 4-6% porosity for gas shales. For an undeveloped play in the Netherlands, TNO (2009) used the Curtis (2002) figures of 1-5% gas-filled porosity. These conservative figures are used in this analysis: a log-normal distribution with a mean of 3% porosity with a two standard-deviation variation and cut-offs at 0.5% and 10%.

The gas expansion factor (B_g) converts the volume of free gas under reservoir conditions into a volume under atmospheric conditions using the formula:

B_g = depth (m) /10.7

It is not known whether the UK shales are overpressured, and hydrostatic pressure has been assumed. Any overpressure would increase the quantity of free gas stored in the pore spaces. Shale gas accumulations in the USA are commonly overpressured.

Adsorbed gas

The controlling factors are **area**, **thickness**, **shale density** and *adsorbed gas content of shale*. Those factors that are estimated in this study are shown in bold; those that rely on analogues are shown in italics.

Langmuir volumes can be obtained experimentally from core samples, but none have been published for shales in the UK. Published values of adsorbed gas contents of shales in the USA are as follows:

Source	Basin/area	Gas-filled porosity (%)	Total gas content (scf/ton)	Adsorbed gas (%)	Adsorbed gas content (scf/ton)	Adsorbed gas content (m^3/ton)
Curtis (2002)	Antrim	4	40 - 100	70	28 - 70	0.8 - 2.0
Curtis (2002)	Ohio	2	60 - 100	50	30 - 50	0.8 - 1.4
Curtis (2002)	New Albany	5	40 - 80	40 - 60	16 - 32	0.5 - 0.9
Curtis (2002)	Barnett	2.5	300 - 350	20	60 - 70	1.7 - 2.0
Curtis (2002)	Lewis	1 - 3.5	15 - 45	60 - 85	9 - 27	0.3 - 0.8
Jarvie (2012)	Marcellus	4	60 - 150	45	27 - 67.5	0.8 - 1.9
Jarvie (2012)	Haynesville	6	100 - 330	25	25 - 82.5	0.7 - 2.3
Jarvie (2012)	Bossier	4	50 - 150	55	27.5 - 82.5	0.8 - 2.3
Jarvie (2012)	Barnett	5	300 - 350	55	165 - 192.5	4.7 - 5.5
Jarvie (2012)	Fayetteville	4.5	60 - 220	50 - 70	30 - 110	0.8 - 3.1
Jarvie (2012)	Muskwa	4	90 - 110	20	18 - 22	0.5 - 0.6
Jarvie (2012)	Woodford	3	200 - 300	60	120 - 180	3.4 - 5.1
Jarvie (2012)	Eagle Ford	4.5	200 - 220	25	50 - 55	1.4 - 1.6
Jarvie (2012)	Utica	2.9	70	60	42	1.2
Jarvie (2012)	Montney	3.5	300	10	30	0.8

Table 1. Summary of parameters for various shales in the USA that are relevant to gas resource calculations in this study (from Curtis 2002, Jarvie 2012).

For the modelling undertaken in this report, a fairly conservative range of adsorbed gas contents of 0.5 to 2.0 m^3/ton (18-71 scf/ton) has been taken. There is a linear relationship between gas contents and TOC values, and the use of a lower gas content value relative to the US examples (which tend to have a slightly higher TOC) is reasonable. See Section 3.8 of the main report for a discussion on UK TOC values.

Published shale densities are in the range 2.4-2.8 g/cm³. This study has used 2.55 – 2.6 – 2.65 g/cm³ as a range of values for calcareous shale. This is supported by downhole geophysical well logs in the study area.

Monte Carlo input parameters

For free gas-in-place (GIIP$_f$)

	Net mature shale volume (m³)			Median depth (m)			Gas-filled porosity (%)		
	cut-off	ml	cut-off	min	ml	max	cut-off	mean	cut-off
Upper unit	7.90E+11	9.31E+11	1.15E+12	1800	2100	2400	0.5	3	10
Lower unit	2.90E+12	3.45E+12	3.97E+12	2100	2400	2700	0.5	3	10

For adsorbed gas-in-place (GIIP$_a$)

	Net mature shale volume (m³)			Density (g/cm³)			Adsorbed gas content (m³/t)	
	cut-off	ml	cut-off	min	ml	max	min	max
Upper unit	7.90E+11	9.31E+11	1.15E+12	2.55	2.6	2.65	0.5	2
Lower unit	2.90E+12	3.45E+12	3.97E+12	2.55	2.6	2.65	0.5	2

Table 2. Input parameters for the Monte Carlo simulation used to determine the total gas content and total gas in place in the upper and lower parts of the Bowland-Hodder unit, central Britain.

Monte Carlo results

(a) Metric	Total gas content estimates (m³/m³)			Total gas in-place estimates (tcm)		
	Low (P90)	Central (P50)	High (P10)	Low (P90)	Central (P50)	High (P10)
Upper unit	3.9	7.9	14.8	4.6	7.5	12.7
Lower unit	4.2	8.7	16.3	18.6	30.2	51.9

(b) Imperial	Total gas content estimates (bcf/mile²m)			Total gas in-place estimates (tcf)		
	Low (P90)	Central (P50)	High (P10)	Low (P90)	Central (P50)	High (P10)
Upper unit	0.36	0.73	1.35	164	264	447
Lower unit	0.39	0.79	1.49	658	1065	1834

Table 3. Results of a Monte Carlo simulation (500,000 iterations) to determine the total gas content and total in-place gas resource in the upper and lower parts of the Bowland-Hodder unit, central Britain. The results are given in (a) metric and (b) imperial units.

Note that USEIA (2001a) used a figure of 48 bcf/mile² with a thickness of 148 ft (45.1 m), which gives an equivalent value of 1.06 bcf/mile²m.
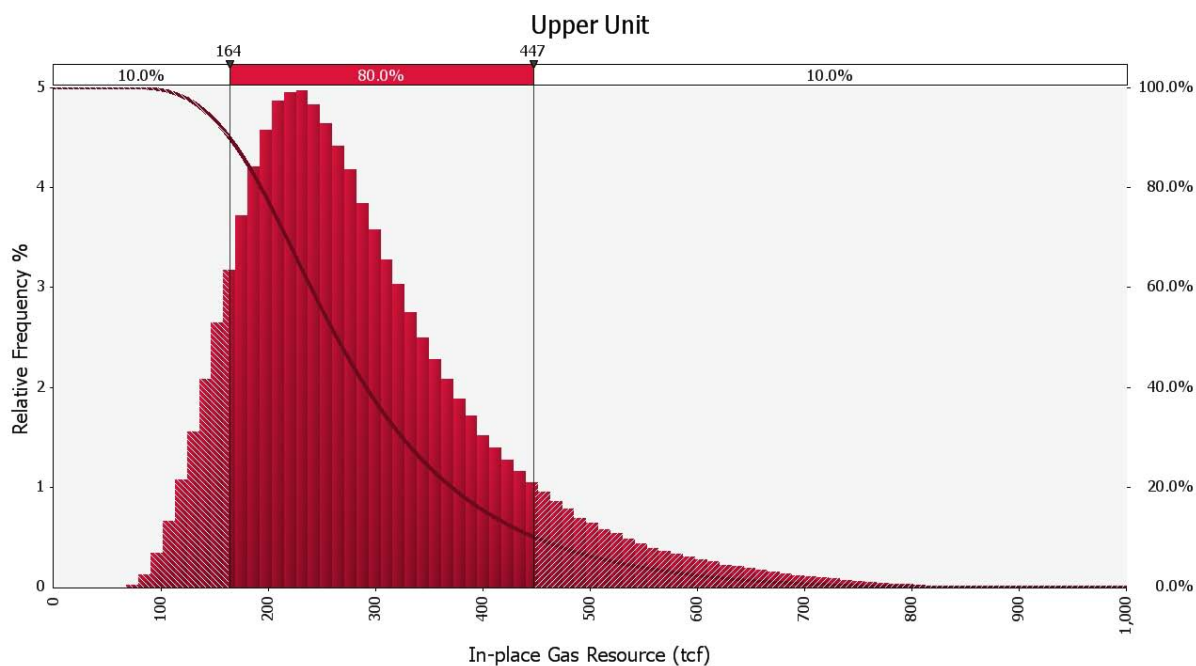
Figure 1. Probabilistic distribution and cumulative probability curve representing the result of a Monte Carlo analysis for the in-place resource estimation of shale gas in the upper Bowland-Hodder unit.
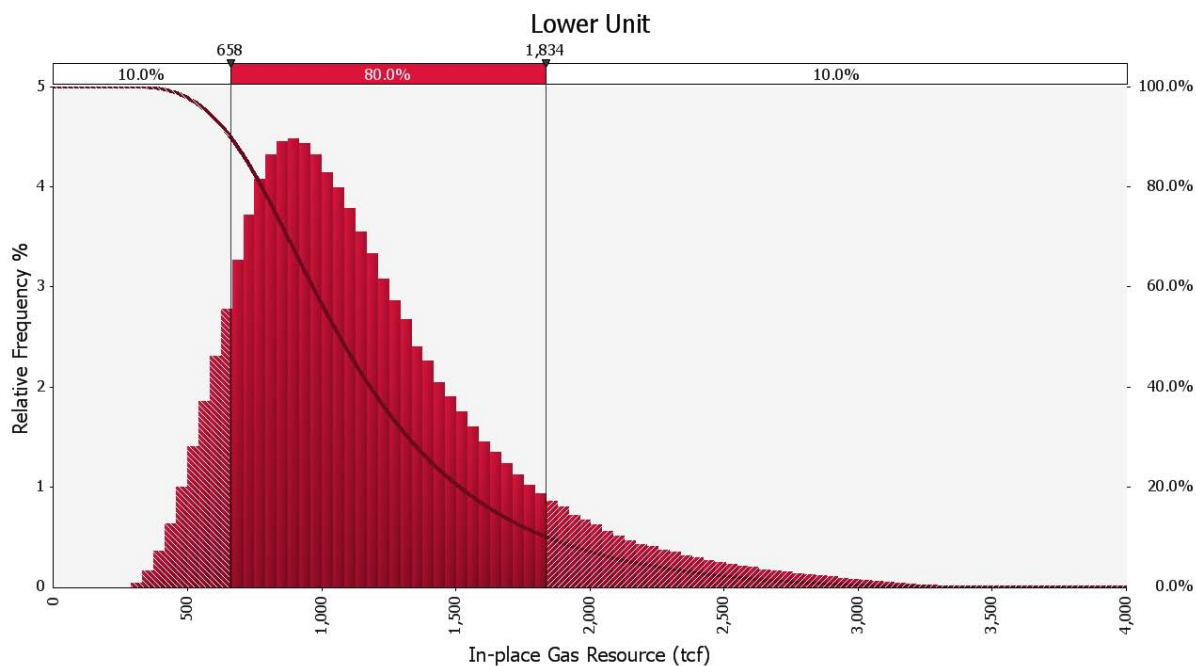
Figure 2. Probabilistic distribution and cumulative probability curve representing the result of a Monte Carlo analysis for the in-place resource estimation of shale gas in the lower Bowland-Hodder unit.

© DECC 2013

Key variables and their effect on the estimated gas volume

Variable	Uncertainty
Gross rock volume/3D geological model	The 2D seismic data interpreted in the study area is of variable quality, and is generally poor to moderate. A two-standard-deviation variation has been used on the gross rock volume, but it could be greater, resulting in a wider range of estimated gas volumes.
Definition of prospective shale	The definition of net prospective shale used in this report could be optimistic; it includes a wide variety of shales and not just those with the highest gamma-log response (and hence highest TOC). This definition is influenced by the fact that the most suitable shales for current extraction techniques are not necessarily those with the highest TOC. Any approach which is more pessimistic would have the greatest effect on the *lower* Bowland-Hodder unit volumes.
Definition of gas maturity	The use of R_o > 1.1% as the top of the gas window is possibly optimistic. It could be 1.4% which would reduce the estimated gas volume.
Shallow depth cut-off	The use of 5000 ft is based on USGS global screening criteria. If this were deeper, this would reduce the estimated gas volume.
Gas-filled porosity of the shale	The use of a mean of 3% is a conservative estimate. It could be greater, which would increase the estimated gas volume. The large range of values has a significant effect on the calculated in-place gas figure (see Figures 3 & 4).
Reservoir pressure	The assumption that the shales are at hydrostatic pressure is conservative. Any amount of overpressure would increase the estimated gas volume.
Adsorbed gas content	The use of 0.5-2.0 m³/ton is lower than some US analogues. Any increase in this range of values would increase the estimated gas volume.
Bulk density	The average density of 2.6 g/cm³ is a robust estimate. If the density is higher this will increase the estimated gas volume (and vice versa).
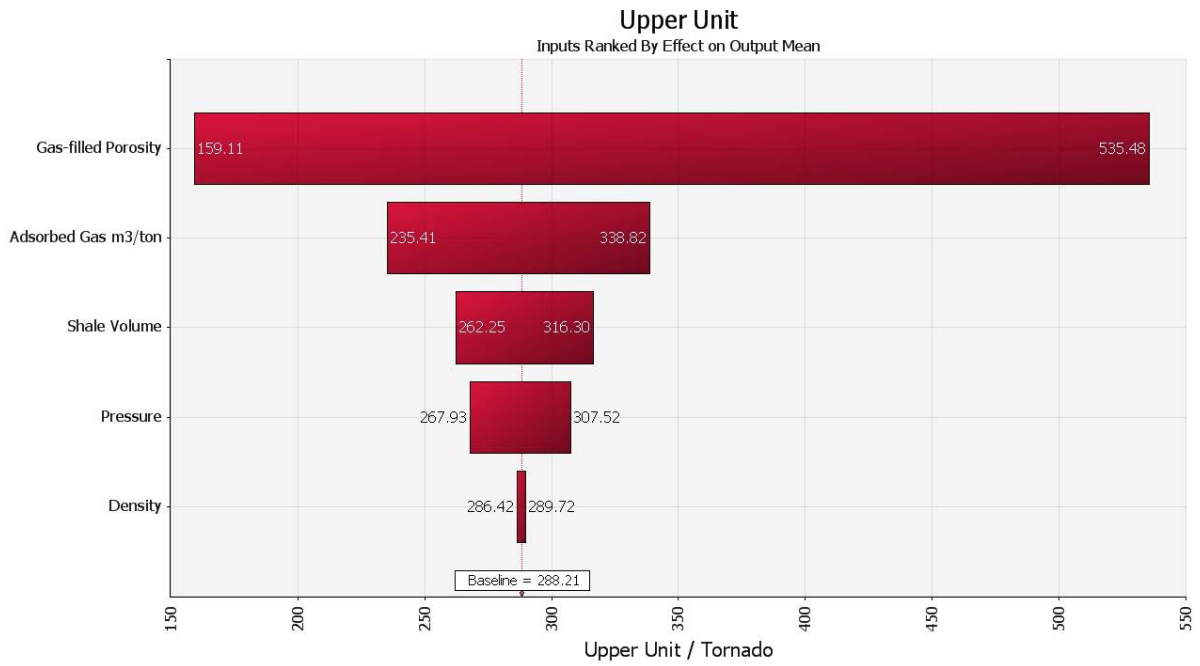
Figure 3. Tornado diagram representing the result of a Monte Carlo analysis for the in-place resource estimation of shale gas in the lower Bowland-Hodder unit.
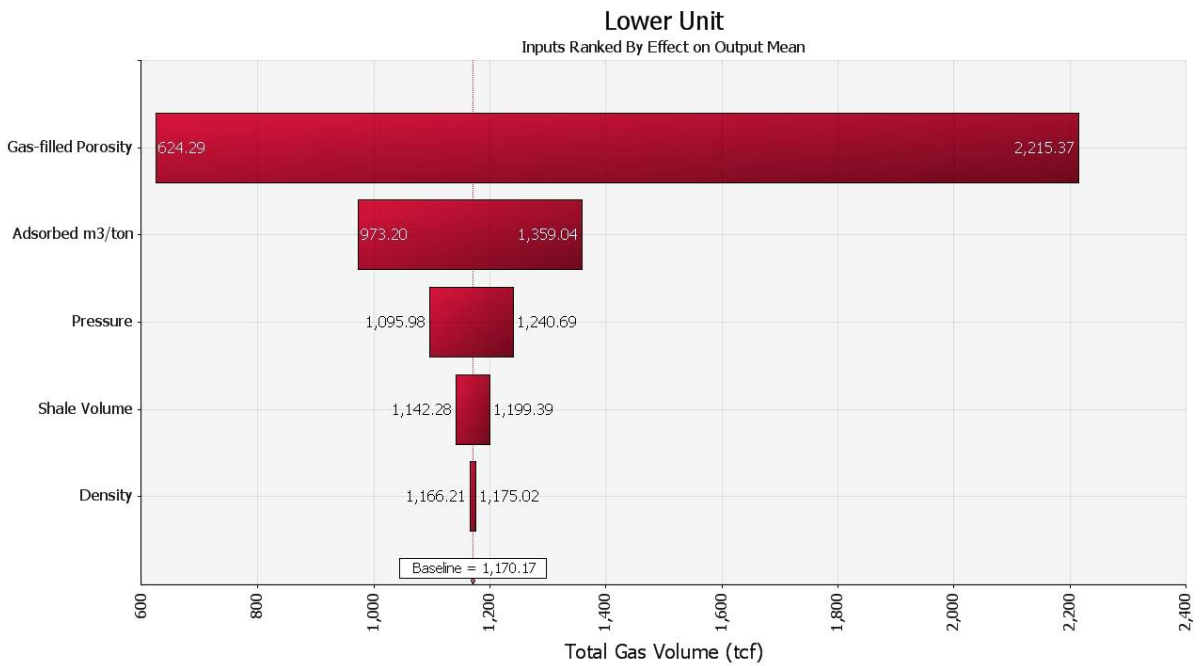
Figure 4. Tornado diagram representing the result of a Monte Carlo analysis for the in-place resource estimation of shale gas in the lower Bowland-Hodder unit.

Conclusion

This study estimates that the **total in-place gas resource** for the Bowland-Hodder (Carboniferous) shales across northern England is 822 – 1329 – 2281 tcf (23.3 – 37.6 – 64.6 tcm) (P90 – P50 – P10). It should be emphasised that this figure is an in-place resource estimate. The amount that could be recovered depends on factors outwith the scope of this report, and could very likely be a small percentage.

References

Curtis, J. B., 2002. Fractured shale gas systems: *AAPG Bulletin* 86(11): 1921–1938.

Jarvie, D. M., 2012. Shale resource systems for oil and gas: Part 1—Shale-gas resource systems, in J. A. Breyer (ed.). *Shale reservoirs—Giant resources for the 21st century. AAPG Memoir* 97: 69–87.

Lewis, R., Ingraham, D., Pearcy, M., Williamson, J., Sawyer, W. & Frantz, J. 2004. New evaluation techniques for gas shale reservoirs. Reservoir Symposium 2004. www.sipeshouston.com/presentations/pickens%20shale%20gas.pdf

TNO. 2009. *Inventory non-conventional gas*. TNO-034-UT-2009-00774/B.

BGR. 2012 Abschätzung des Erdgaspotenzials aus dichten Tongesteinen (Schiefergas) in Deutschland. http://www.bgr.bund.de/DE/Themen/Energie/Downloads/BGR_Schiefergaspotenzial_in_Deutschland_2012.pdf

I.J. Andrews, M.J. Sankey, A.L. Harvey & M. McCormac

Appendix B: Rock-Eval geochemical analysis of 109 samples from the Carboniferous of the Pennine Basin, including the Bowland-Hodder unit

Introduction

One hundred and nine core samples were collected from 16 selected wells within the Carboniferous Pennine Basin of central Britain (Figure 1, Table 1) and analysed using the BGS Rock-Eval machine. The spreadsheet of data derived from the Rock-Eval analysis (Appendix 1) records depths and the main parameters measured - S_1 (free hydrocarbons), S_2 (bound hydrocarbons), T_{max} (the temperature at which S_2 peaked), S_3 (carbon dioxide) and the total organic carbon (TOC).
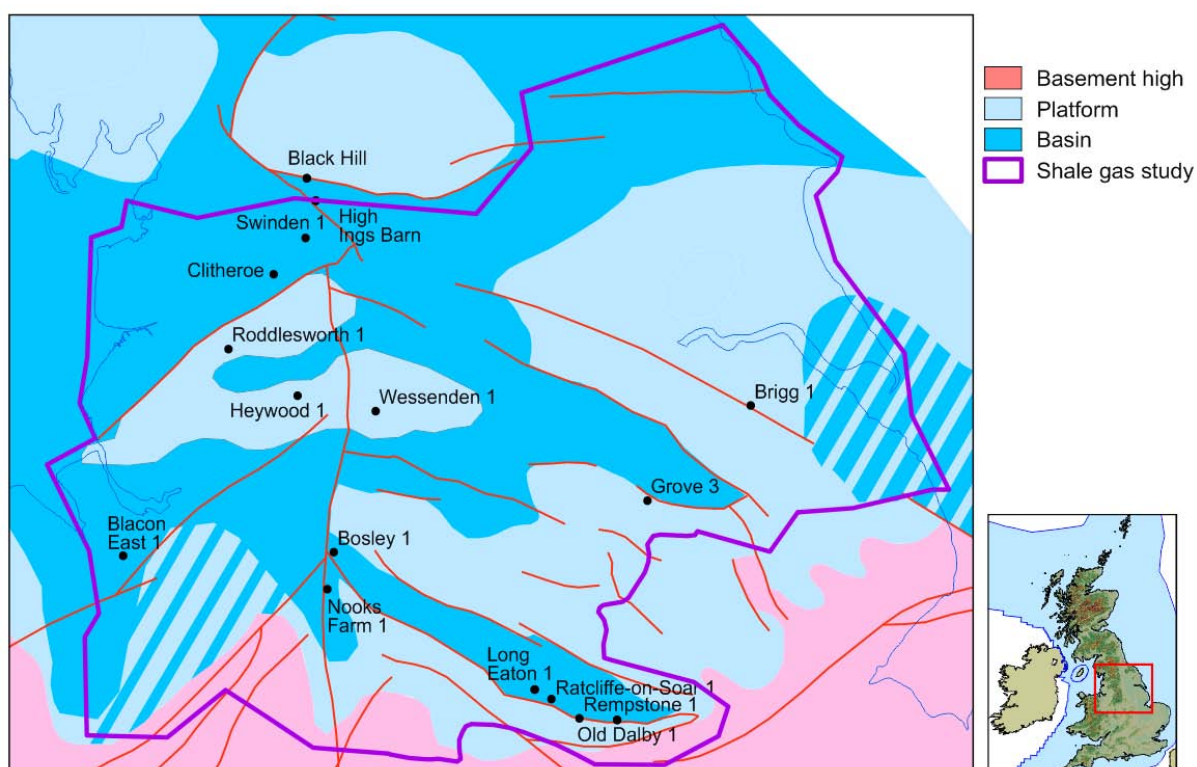
Figure 1. Map of central Britain showing the Early Carboniferous basins and the locations of the 16 sampled wells.

Well name	top sample (ft)	bottom sample (ft)	Chronostratigraphy	Lithostratigraphy	Unit (this report)
Black Hill	218.2	246.1	Namurian (Marsdenian?)	Millstone Grit	Millstone Grit
Blacon East 1	6122.0	6147.6	Visean (Brigantian)	Bowland Shale Fm	Upper BHU
	7423.0	7432.6	Visean (?Asbian)	Clwyd Limestone Group	?shelf limestone
Bosley 1	6568.9	6582.7	Chadian		Lower BHU?
Brigg 1	6328.4	6336.9	Visean	Carboniferous limestone	shelf limestone
Clitheroe	403.2	761.8	Visean	Hodder Mudstone	Lower BHU
Grove 3	7564.6	7594.0	Visean (Chadian)	Carboniferous limestone	shelf limestone
Heywood 1	5249.2	5260.2	Visean (Asbian-Brigantian)	Carboniferous limestone	shelf limestone
High Ings Barn	313.3	719.5	Visean	Carboniferous limestone	shelf limestone
Long Eaton 1	5871.0	5901.0	Visean (Arundian-Holkerian)	Long Eaton Fm	Lower BHU
Nooks Farm 1A	1401.0	1531.0	Visean (Asbian-Brigantian)	Onecote Sandstone	Lower BHU
Old Dalby 1	4562.3	4773.6	Visean (Asbian-Brigantian)	Widmerpool Fm	Lower BHU
Ratcliffe-on-Soar 1	891.4	949.8	Namurian (Arnsbergian)	Rempstone Fm	Millstone Grit
Rempstone 1	2181.8	2191.6	Namurian (Arnsbergian)	Upper Bowland Shale	Upper BHU
Roddlesworth 1	4226.0	4281.0	Visean (Asbian-Brigantian)	Carboniferous limestone	shelf limestone
Swinden 1	98.4	2065.3	Tournasian (Courceyan)	Carboniferous limestone	shelf limestone
Wessenden 1	3505.0	3513.0	Tournasian (Courceyan)	Carboniferous limestone	shelf limestone

Table 1. Wells analysed in this study, together with stratigraphic information. BHU = Bowland-Hodder unit, as used in the main shale gas assessment report.

In addition, the principal useful parameters derived from the data include Production Index (PI), present-day Hydrogen Index (HI_{pd}) and Oxygen Index (OI). PI is the sum of the S_1 and S_2 hydrocarbons. HI_{pd} is derived by the ratio of S_2 mg HC per gram of organic carbon and values above 350 are generally rated to be good source rocks (for conventional hydrocarbons, Tissot & Welte 1978, Fig. V.1.11). OI is the ratio of mg carbon dioxide per g organic carbon. HI and OI are plotted to be comparable with the van Krevelen diagram, showing the branching of the different kerogen types I (lacustrine, algal, oil prone), II (marine, oil prone), III (terrestrial, gas prone) and IV (oxidised or inertinite). From the work of Jarvie, in particular, it seems that these types cannot be fixed on such diagrams because there is a progressive change with increasing maturity (Jarvie *et al.* 2005). The immature Barnett Shale is Type II kerogen which has been converted to plot in the Type III field within the gas window fairway (Jarvie *et al.* 2005). Kerogen, of any type, once deeply buried or heated becomes gas prone and this explains the difference between conventional and unconventional plays. Carbon and hydrogen are lost during hydrocarbon generation. Gas is present in the source rock at lower maturities (R_o = 1.1% in the Newark East shale gas field (Texas), Smith *et al.* 2011) than in conventional gas fields (gas window R_o >1.3%) because it has not migrated. Overmaturity is a well-worn phrase in conventional exploration, effectively writing off some areas which deserve to be re-evaluated for unconventional hydrocarbons.

Total organic carbon (TOC)

Of the 16 wells, notably the Grove 3 and Brigg 1 samples were visually very light coloured, because they were from conventional reservoirs and give low TOC values (Figure 2). Samples from the other 14 wells had the appearance of dark grey and black shales containing probable organic matter. Rempstone 1, Ratcliffe-on-Soar 1 and Old Dalby 1, located in the Widmerpool Gulf, the southern sub-basin within the Pennine Basin, all had fairly consistent characters including consistently high TOC (Figure 2).

The Barnett Shale at crop has very high TOC (13.08%, Jarvie *et al.* 2005). During maturation organic matter is inevitably destroyed (Jarvie 2008). Jarvie *et al.* (2005) reported that 'artificially maturing' immature samples from one well reduced TOC by approximately 36% from its original value, whereas at peak oil maturity this had only been reduced by 18%. This could explain why the three Widmerpool Gulf wells had the highest TOC values and are immature (Figure 2).

Comparing the Pennine Basin samples with the Barnett Shale makes it clear that the former are slightly leaner (Figure 5).

Organic carbon content (average)

Well	% TOC (wt/wt)
Black Hill	2.1
Blacon East 1	2.0
Bosley 1	0.7
Brigg 1	0.2
Clitheroe	1.4
Grove 3	0.2
Heywood 1	0.6
High Ings Barn	1.5
Long Eaton 1	1.3
Nooks Farm 1A	1.4
Old Dalby 1	3.5
Ratcliffe-on-Soar 1	4.9
Rempstone 1	5.0
Roddlesworth 1	0.6
Swinden 1	1.7
Wessenden 1	0.3
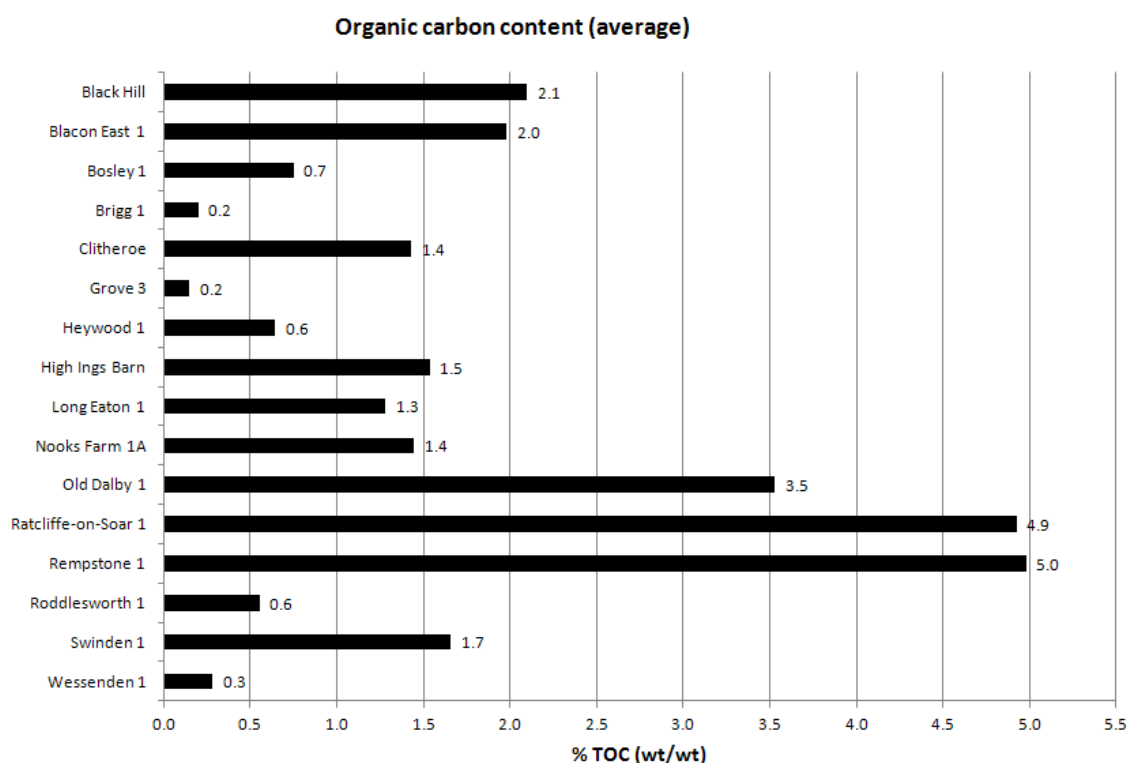
Figure 2. Average total organic carbon content of samples from the 16 selected wells.

Kerogen type

Kerogen types are identified by plotting on a modified van Krevelen diagram (Figure 3). Typical Type I (algal, lacustrine Green River Shale), Type II (oil prone Toarcian of Paris Basin) and Type III (gas prone Tertiary of Greenland) have been included. Some publications show the Type III curve emerging at about HI=100 (*e.g.* Tissot & Welte 1978, fig. V.1.12), nearer to the Greenland example (Figure 3, blue cross), which would seem preferable, so that the Paris Basin example plots in the Type II field. Some other publications have a Type IV kerogen (also near to HI=0) (Boyer *et al.* 2006). Type IV kerogens may have lost all generative potential at an early stage, perhaps as a result of oxidation or combustion.

Roche (2012, Fig. 7) showed Thistleton 1 samples as being Type III kerogens, mostly in the oil window, whereas Bowland outcrop samples plotted at immature or early oil window as Type II kerogens.

However, many Barnett Shale samples also plot near the base of modified van Krevelen diagrams and are considered to have been originally Type II kerogens, based on Barnett low maturity outcrops in the southern margin of the Fort Worth Basin *e.g.* at Lampasas (Jarvie *et al.* 2005). The samples in deeper parts of the basin are interpreted to have 'matured' to positions with very low HI (Figure 3). Similarly, the DECC samples differentiate into Widmerpool Gulf well samples, which plot in the Type II field, and the Craven Basin well samples that plot near the base of the graph. One interpretation is that they may have originated as the same Type II kerogens, but 'migrated' to the base of this diagram as they matured.
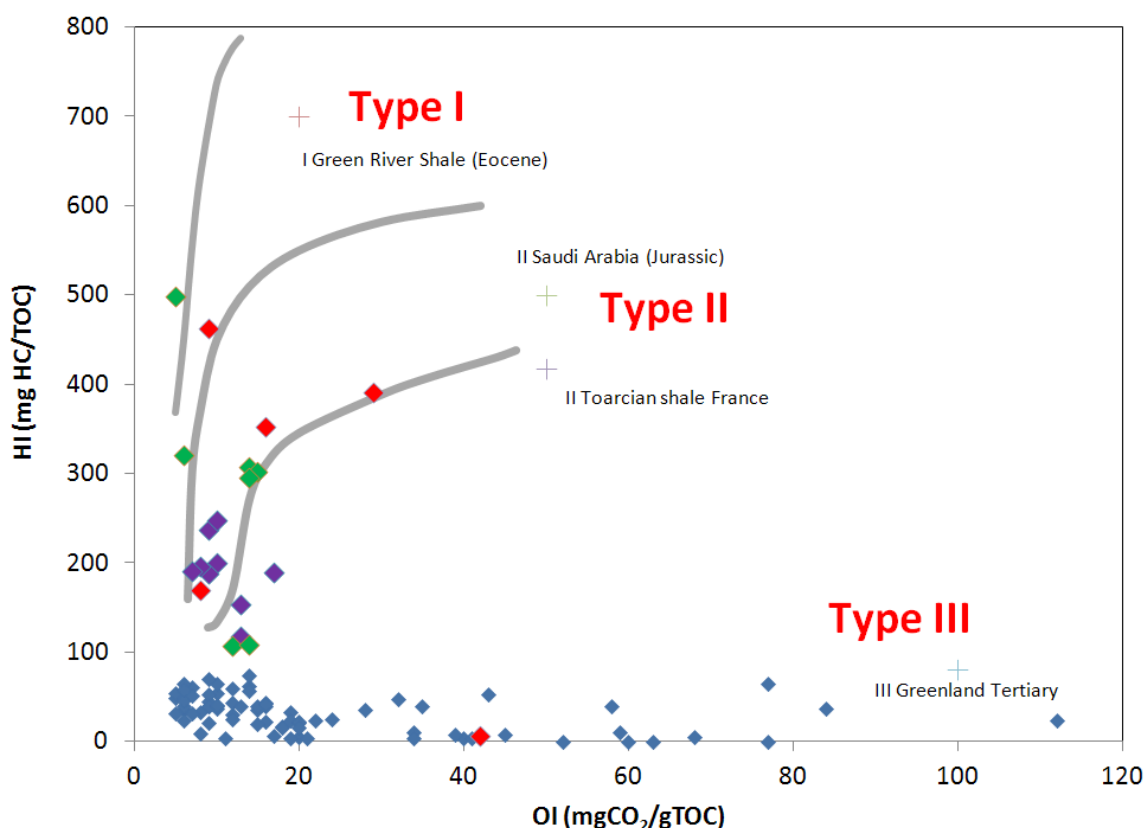
Figure 3. Modified van Krevelen diagram showing examples of Types I-III kerogens and relationship to the samples [Red = Rempstone 1; green = Ratcliffe-on-Soar 1; purple =Old Dalby 1; blue = remainder (see Fig. 1 for well locations)]

T_{max} (measured in degrees centigrade)

T_{max} is the Rock-Eval equivalent of vitrinite reflectance (R_o), similarly indicating the maturity of the sample. Conversion of T_{max} to vitrinite reflectance is by the following formula (Jarvie *et al.* 2005):

$$\text{Calculated } R_o \% = 0.018 \times T_{max} - 7.16$$

In the spreadsheet (Appendix 1), the various maturity windows have been indicated by the cell background colour. Immature samples have a background yellow, oil window samples are green, shale wet gas window samples are orange and shale dry gas samples are red.

Very low T_{max} is recorded for two samples. The Heywood sample (T_{max} = 352) and one Swinden sample (T_{max} = 331) are not shown on Figure 4. These two samples might be comparable with Barnett Shale and Bossier Shale Type III gas-prone sediments (Jarvie *et al.* 2007), but the rest of the Swinden 1 samples are within the dry gas window. T_{max} becomes more erratic at high maturity. The current samples conform quite closely to the pattern established for the Barnett Shale (Jarvie *et al.* 2005). The low Swinden T_{max} of 331 should perhaps be disregarded. Four samples at about 410-430 T_{max} might indicate both immaturity and low HI, possibly indicating non-prospective shale. These samples are from Heywood 1, Bosley 1 and Ratcliffe-on-Soar 1 (2) wells, although other samples from Bosley 1 and Ratcliffe-on-Soar 1 plot more uniformly with the Barnett Shale model.
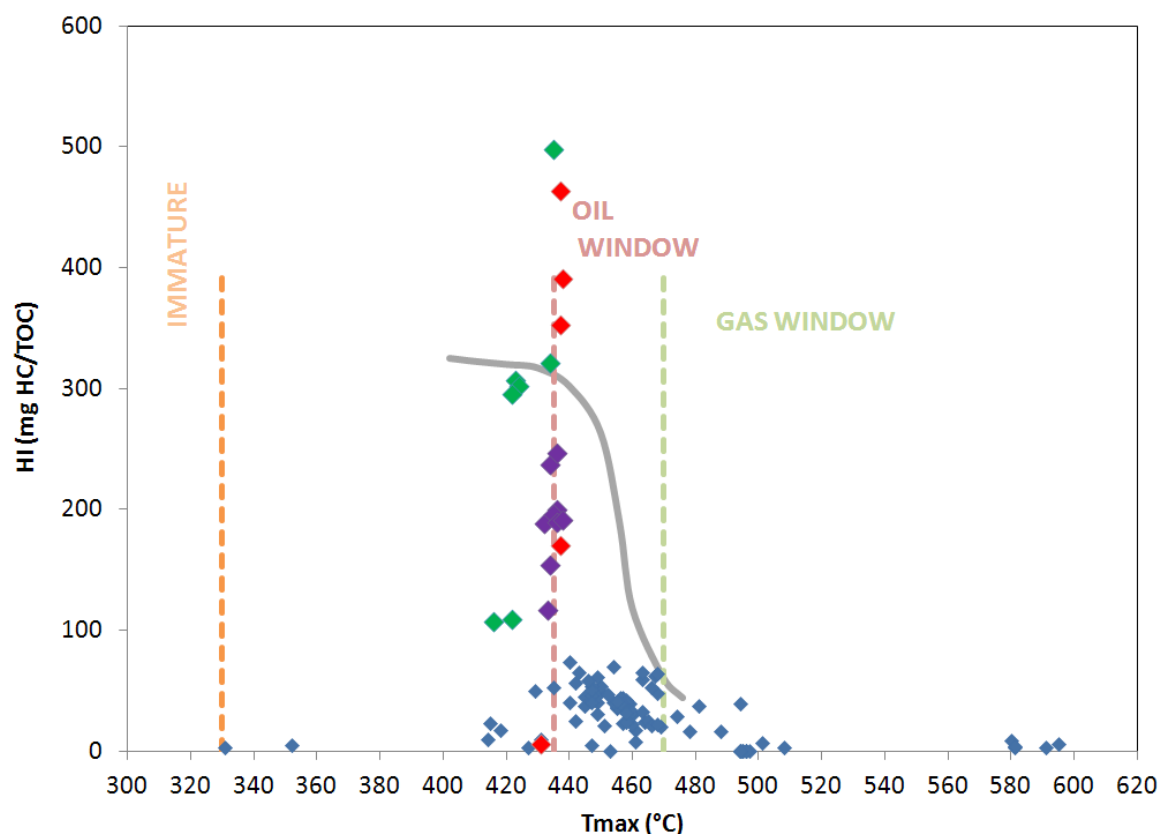
Figure 4. Plot of Hydrogen Index versus T_{max}. This is known as a modified Espitalie kerogen type and maturity plot.

Hydrogen Index

The HI of 500 to about 160 obtained from the Widmerpool Gulf samples from wells Rempstone 1, Ratcliffe-on-Soar 1 and Old Dalby 1 defines this group as Type II, comparable with the Mitcham well of the Barnett Shale kerogen (Figure 4). This is supported by other studies showing Type II (HI = 248.5) and some Type III (HI = 46.1) in the Pennine Basin (Ewbank *et al.* 1993). With increasing maturity the HI decreases, so that above T_{max} = 460 (at the onset of gas window maturity) the HI values of this study and the Barnett wells are mainly below 50 (Figure 4).

Remaining hydrocarbon potential (S₂)

Plotting S_2 against TOC, as done for the Barnett Shale (Jarvie & Lundell 1991, Jarvie *et al.* 2005), shows that a similar pattern occurs for the current Pennine Basin (DECC) data (Figure 5). The types of kerogen are shown, together with the organic lean area (TOC <1%) and the Barnett Shale maturation trend. This trend shows that during maturation, TOC declines (Mitcham well, Jarvie *et al.* 2005), incidentally creating porosity within the thermally more mature sections.
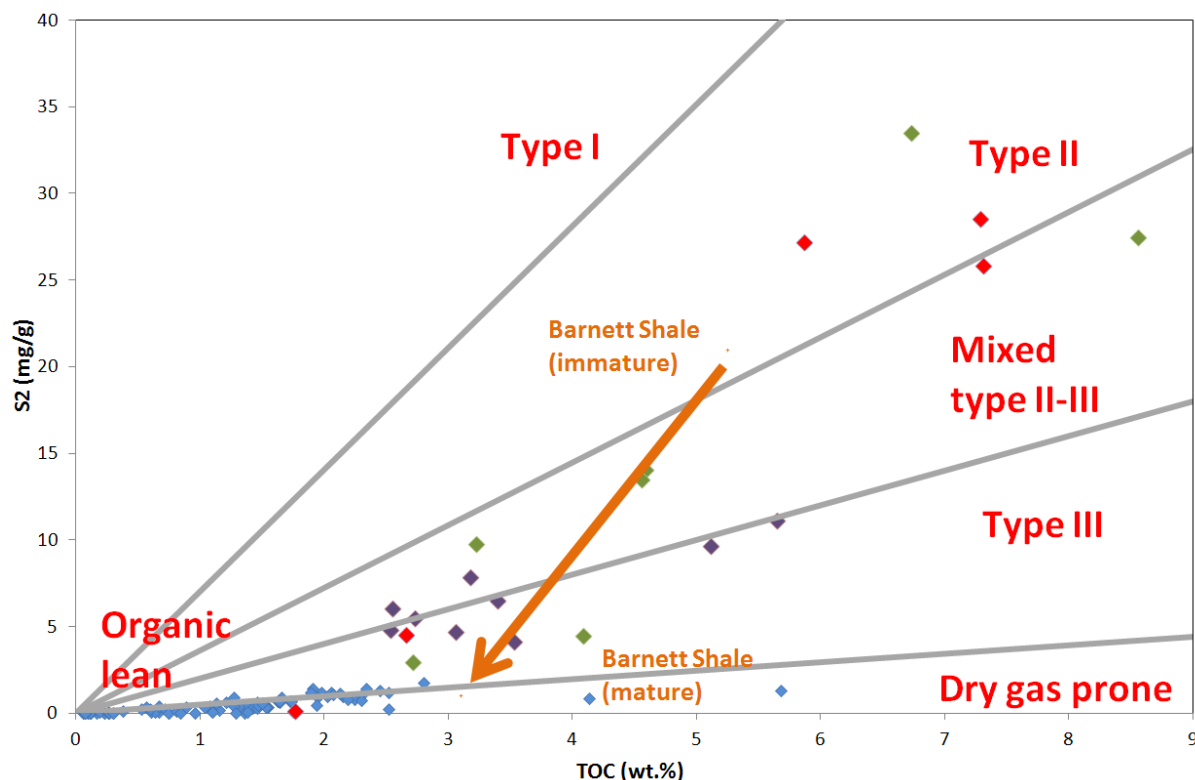
Figure 5. Remaining hydrocarbon potential (S_2) v TOC (cf. Jarvie & Lundell 1991). The orange arrow shows the Barnett Shale maturation trend (from Jarvie 2008). The current data, combining different sub-basins, collectively shows a gentler trend, resulting in residually lower TOC than the Barnett Shale. [Red = Rempstone 1; green = Ratcliff- on-Soar 1; purple =Old Dalby 1; blue = remainder]

Production index

The production index is the ratio of free hydrocarbons to the total free and bound hydrocarbons ($S_1/S_1 + S_2$). Values of 0.1 up to 0.4 define the oil window. Hence in the Widmerpool Gulf (Figure 6), Long Eaton 1, west of Nottingham, is more mature than Rempstone 1, Old Dalby 1 and Ratcliffe-on-Soar 1, which are south of Nottingham. Long Eaton 1 lies within the gas window at the levels of the samples, confirmed by its position on the van Krevelen diagram (Figure 3), whereas the others plot within the oil window.
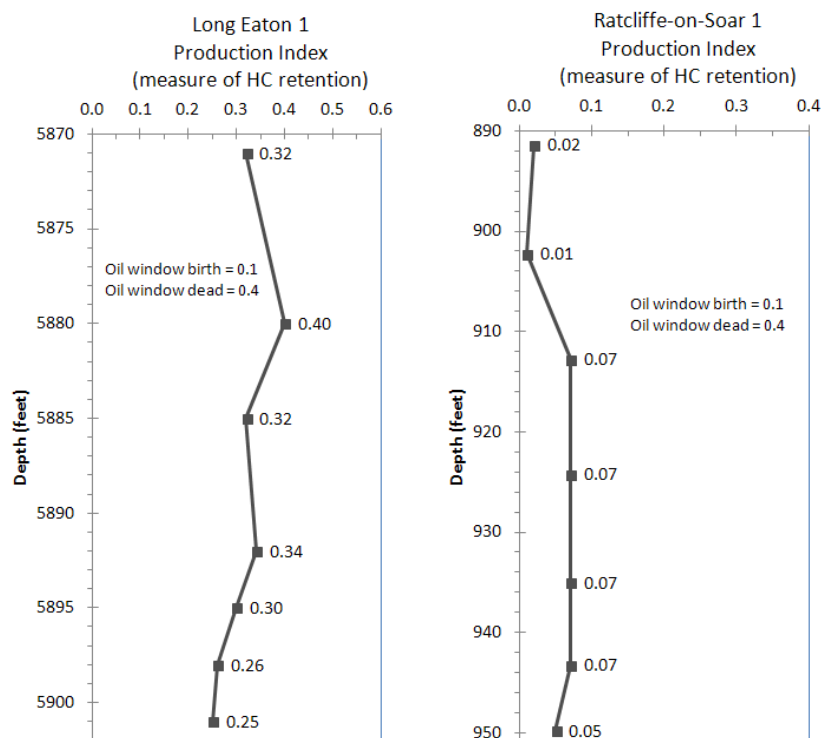
Figure 6. Widmerpool Gulf wells showing the onset of the conventional gas window maturity (Long Eaton 1) and the conventional oil window maturity (Ratcliffe-on-Soar 1).

Conclusions

For the Barnett Shale, Jarvie *et al.* (2005) concluded that although the shale currently plots in the gas window in the Type III kerogen part of the field in a modified van Krevelen diagram, the original kerogen had been Type II. This was based on outcrop data and data from immature wells. This important conclusion showed that during maturation the type of kerogen appears to change and the TOC decreases. An almost identical situation has been proven for the Craven Basin samples of this study with respect to the less-mature Widmerpool Gulf wells (with the notable exception of Long Eaton 1). The samples that do not fit the Barnett model are those which have a low T_{max} (*i.e.* are pre- or early oil window), but these also have a low hydrogen index. Apart from the Heywood well, these are wells with samples that otherwise plot within the Barnett model.

This geochemical evidence supports the comparison made by Smith *et al.* 2011 between the UK Upper Bowland Shale and the US Barnett Shale and the previous decision to compare the potential productivity of the UK Carboniferous Pennine Basin Upper Bowland Shale with the ongoing production from the Fort Worth Basin's Barnett Shale (DECC 2010). However, it should be emphasised that the Upper Bowland Shale is organically leaner than the Barnett Shale.

References

Boyer, C., Kieschnick, J., Suarez-Rivera, R., Lewis, R. E. & Waters, G. 2006. Producing gas from its source. *Oilfield Review* Autumn 2006: 36-49.

DECC. 2010. The unconventional hydrocarbon resources of Britain's onshore basins - shale gas. DECC Promote website, December 2010.
https://www.og.decc.gov.uk/UKpromote/onshore_paper/UK_onshore_shalegas.pdf

Ewbank, G., Manning, D. A. C. & Abbott, G. D. 1993. An organic geochemical study of bitumens and their potential source rocks from the South Pennine Orefield, central England. *Organic Geochemistry* 20(5): 579-598.

Jarvie, D. M., & Lundell, L.L. 1991. Hydrocarbon generation modelling of naturally and artificially matured Barnett Shale, Fort Worth Basin, Texas. Southwest Regional Geochemistry Meeting, September 8– 9, 1991, The Woodlands, Texas, 1991. www.humble-inc.com/Jarvie_Lundell_1991.pdf

Jarvie, D. M., Hill, R. J. & Pollastro, R. M. 2005. Assessment of the gas potential and yields from shales: the Barnett Shale model. In: Cardott, B. J. (Ed.) *Unconventional energy resources in the southern Midcontinent, 2004 Symposium*. Oklahoma Geological Survey Circular 110: 37-50.
http://wwgeochem.com/resources/Jarvie+et+al.+2005+OGS+Circ.+110+Barnett+paper.pdf

Jarvie, D. M., Hill, R. J., Ruble, T. E. & Pollastro, R. M. 2007. Unconventional shale gas systems: the Mississippian Barnett Shale of north-central Texas as one model for thermogenic shale gas assessment. *Bulletin of the American Association of Petroleum Geologists* 91(4): 475-499.

Jarvie, D. M. 2008. Geochemical comparison of shale-resource systems. Insight Shale Gas Summit, Dallas, Texas, 6-7 May 2008. http://wwgeochem.com/resources/Final+Jarvie+-+Insight+Dallas+May+2008.pdf

Roche, I. 2012. Lessons from history - unlocking a new UK shale oil play. *Society of Petroleum Engineers*, SPE 150933.

Smith, N., Turner, P. & Williams, G. 2011. UK data and analysis for shale gas prospectivity. In: Vining, B. A. & Pickering, S. C. (Eds) *Petroleum Geology: from mature basins to new frontiers – Proceedings of the 7th Petroleum Geology Conference*, Geological Society, London, 1087-1098.

Tissot, B.P. & Welte, D.H. 1978. *Petroleum Formation and Occurrence: A New Approach to Oil and Gas Exploration*. Springer-Verlag. 538pp.

N.J.P. Smith, C. Vane, V. Moss-Hayes & I.J. Andrews

Appendix A1. Selected output from the Rock-Eval analysis of 16 wells in central Britain. The various maturity windows are indicated by the cell background colour: yellow = immature, green = oil window, orange = shale wet gas window, red = shale dry gas.

Well	BGS sample number	Depth (m)	Depth (ft)	S_1 (mg/g)	S_2 (mg/g)	PI	T_{max} (°C)	S_3 (mg/g)	$S_{3'}$ (mg/g)	PC (%)	RC (%)	TOC (%)	HI	OICO	OI	pyroMINC (%)	oxiMINC (%)	MINC (%)
Black Hill	13003-0001	66.5	218.2	0.19	1.22	0.14	467	0.27	7	0.13	1.85	1.98	62	9	14	0.19	0.07	0.26
Black Hill	13003-0002	68.8	225.7	0.3	0.99	0.23	450	0.11	1.9	0.12	1.91	2.03	49	3	5	0.06	0.07	0.13
Black Hill	13003-0003	69.6	228.3	0.4	1.33	0.23	450	0.12	4.3	0.15	2.3	2.45	54	5	5	0.12	0.21	0.33
Black Hill	13003-0004	70.5	231.3	0.23	0.82	0.22	456	0.13	1.3	0.1	2.15	2.25	36	5	6	0.04	0.1	0.13
Black Hill	13003-0005	71.4	234.3	0.32	0.97	0.25	445	0.19	3	0.12	2.03	2.15	45	4	9	0.09	0.35	0.44
Black Hill	13003-0006	72.3	237.2	0.45	1.42	0.24	449	0.17	1.6	0.17	2.17	2.34	61	6	7	0.05	0.19	0.24
Black Hill	13003-0007	73.2	240.2	0.32	1.16	0.22	447	0.21	3.6	0.14	1.99	2.13	54	3	10	0.1	0.41	0.51
Black Hill	13003-0008	74.1	243.1	0.34	1.41	0.19	440	0.26	5.6	0.16	1.75	1.91	74	4	14	0.16	0.46	0.61
Black Hill	13003-0009	75.0	246.1	0.29	0.93	0.24	442	0.24	13	0.11	1.55	1.66	56	2	14	0.36	2.91	3.27
Blacon East	13003-0010		6122.0	0.03	0.11	0.21	461	0.12	3.70	0.02	0.63	0.65	17	5	18	0.10	0.17	0.27
Blacon East	13003-0011		6134.0	0.10	0.31	0.24	460	0.22	5.00	0.04	1.36	1.40	22	2	16	0.14	0.32	0.46
Blacon East	13003-0012		6139.0	0.28	0.85	0.25	451	0.38	14.20	0.11	4.03	4.14	21	3	9	0.39	2.66	3.05
Blacon East	13003-0013		6147.6	0.48	1.30	0.27	457	0.33	8.40	0.16	5.52	5.68	23	1	6	0.24	1.14	1.37
Blacon East	13003-0014		7423.0	0.01	0.19	0.06	488	0.21	7.20	0.03	1.13	1.16	16	3	18	0.20	7.86	8.06
Blacon East	13003-0015		7428.0	0.00	0.05	0.04	501	0.30	10.40	0.01	0.66	0.67	7	4	45	0.28	3.51	3.79
Blacon East	13003-0016		7432.6	0.00	0.00	0.60	496	0.26	3.80	0.01	0.16	0.17	0	24	153	0.10	9.18	9.28
Bosley	13003-0017	2002.2	6568.9	0.00	0.00	0.76	497	0.28	9.5	0.01	0.22	0.23	0	13	122	0.26	11.11	11.37
Bosley	13003-0018	2003.0	6571.5	0.01	0.11	0.08	431	0.37	10.6	0.02	1.07	1.09	10	3	34	0.29	6	6.3
Bosley	13003-0019	2003.7	6573.8	0.01	0.03	0.21	581	0.38	7.7	0.02	0.94	0.96	3	5	40	0.21	10.03	10.24
Bosley	13003-0020	2004.0	6574.8	0.00	0.00	0.29	495	0.39	4.5	0.01	0.09	0.1	0	50	390	0.12	11.28	11.41
Bosley	13003-0021	2005.8	6580.7	0.02	0.04	0.31	447	0.51	7.5	0.03	0.72	0.75	5	15	68	0.21	9.9	10.11
Bosley	13003-0022	2006.4	6582.7	0.01	0.04	0.22	591	0.46	11.2	0.02	1.34	1.36	3	7	34	0.31	5.44	5.75
Brigg 1	13003-0023	1928.9	6328.4	0.08	0.37	0.18	443	0.44	2.90	0.05	0.52	0.57	65	7	77	0.08	0.01	0.09
Brigg 1	13003-0024	1930.0	6332.0	0.00	0.00	0.00	453	0.13	1.70	0.01	0.06	0.07	0	57	186	0.05	12.16	12.20

Well	BGS sample number	Depth (m)	Depth (ft)	S_1 (mg/g)	S_2 (mg/g)	PI	T_{max} (°C)	S_3 (mg/g)	$S_{3'}$ (mg/g)	PC (%)	RC (%)	TOC (%)	HI	OICO	OI	pyroMINC (%)	oxiMINC (%)	MINC (%)
Brigg 1	13003-0025	1930.8	6334.6	0.01	0.01	0.52	418	0.14	4.20	0.01	0.05	0.06	17	50	233	0.11	11.75	11.87
Brigg 1	13003-0026	1931.5	6336.9	0.01	0.05	0.18	429	0.16	2.20	0.01	0.09	0.10	50	20	160	0.06	12.31	12.37
Clitheroe	13003-0027	122.9	403.2	0.65	1.21	0.35	463	0.24	6.40	0.17	1.89	2.06	59	5	12	0.18	4.77	4.95
Clitheroe	13003-0028	127.3	417.7	0.21	0.42	0.34	459	0.17	6.30	0.06	1.02	1.08	39	3	16	0.17	3.41	3.58
Clitheroe	13003-0029	215.05	705.5	0.15	0.25	0.37	455	0.20	8.60	0.04	0.68	0.72	35	10	28	0.23	6.19	6.43
Clitheroe	13003-0030	218.08	715.5	0.15	0.42	0.27	460	0.17	6.20	0.06	1.32	1.38	30	6	12	0.17	2.60	2.78
Clitheroe	13003-0031	222.99	731.6	0.50	1.02	0.33	457	0.27	7.60	0.14	2.16	2.30	44	5	12	0.21	4.32	4.53
Clitheroe	13003-0032	228.2	748.7	0.40	0.71	0.36	456	0.26	8.50	0.11	1.52	1.63	44	7	16	0.23	3.60	3.83
Clitheroe	13003-0033	232.2	761.8	0.14	0.20	0.41	458	0.19	7.60	0.04	0.81	0.85	24	8	22	0.21	6.81	7.02
Grove 3	13003-0034	2305.7	7564.6	0.01	0.00	0.97	496	0.23	9.00	0.01	0.09	0.10	0	10	230	0.25	13.07	13.32
Grove 3	13003-0035	2306.5	7567.3	0.00	0.00	0.00	495	0.32	11.60	0.01	0.11	0.12	0	17	267	0.32	12.92	13.24
Grove 3	13003-0036	2314.66	7594.0	0.00	0.00	0.00	495	0.39	17.00	0.01	0.22	0.23	0	9	170	0.46	12.72	13.19
Heywood	13003-0037	1600.0	5249.2	0.09	0.06	0.59	414	0.36	12.30	0.03	0.58	0.61	10	8	59	0.34	8.92	9.26
Heywood	13003-0038	1601.0	5252.6	0.04	0.06	0.40	352	0.22	8.30	0.02	1.08	1.10	5	5	20	0.23	1.71	1.94
Heywood	13003-0039	1602.4	5257.2	0.01	0.02	0.35	427	0.14	7.40	0.01	0.74	0.75	3	9	19	0.20	0.22	0.42
Heywood	13003-0040	1603.3	5260.2	0.00	0.00	0.96	496	0.25	4.80	0.01	0.10	0.11	0	45	227	0.13	9.94	10.07
High Ings	13003-0041	95.5	313.3	0.11	0.25	0.30	452	0.17	5.20	0.04	0.49	0.53	47	4	32	0.15	11.05	11.20
High Ings	13003-0042	98.0	321.5	0.07	0.37	0.16	455	0.16	7.70	0.05	0.99	1.04	36	6	15	0.21	3.62	3.84
High Ings	13003-0043	99.0	324.8	0.09	0.36	0.20	454	0.13	8.00	0.04	0.85	0.89	40	4	15	0.22	5.62	5.84
High Ings	13003-0044	100.0	328.1	0.13	0.62	0.18	458	0.24	8.30	0.07	1.39	1.46	42	2	16	0.23	2.21	2.44
High Ings	13003-0045	103.6	339.9	0.16	0.60	0.21	435	0.49	7.40	0.09	1.04	1.13	53	13	43	0.20	0.04	0.25
High Ings	13003-0046	105.0	344.5	0.24	1.22	0.17	463	0.18	9.80	0.13	1.76	1.89	65	5	10	0.27	4.85	5.12
High Ings	13003-0047	167.5	549.5	0.11	0.43	0.20	460	0.25	11.00	0.06	1.25	1.31	33	5	19	0.30	2.84	3.14
High Ings	13003-0048	169.0	554.5	0.08	0.42	0.16	463	0.10	4.50	0.05	1.22	1.27	33	6	8	0.12	1.31	1.44
High Ings	13003-0049	217.0	711.9	0.21	1.21	0.15	468	0.16	9.00	0.13	2.39	2.52	48	4	6	0.25	5.18	5.43
High Ings	13003-0050	219.0	718.5	0.29	1.10	0.21	466	0.18	9.90	0.13	1.94	2.07	53	4	9	0.27	7.06	7.33
High	13003-0051	219.3	719.5	0.34	1.78	0.16	468	0.18	9.00	0.19	2.61	2.80	64	4	6	0.25	7.36	7.62

Well	BGS sample number	Depth (m)	Depth (ft)	S_1 (mg/g)	S_2 (mg/g)	PI	T_{max} (°C)	S_3 (mg/g)	$S_{3'}$ (mg/g)	PC (%)	RC (%)	TOC (%)	HI	OICO	OI	pyroMINC (%)	oxiMINC (%)	MINC (%)
Ings+A87																		
Long Eaton	13003-0052		5871	0.18	0.37	0.32	464	0.30	7.20	0.06	1.49	1.55	24	3	19	0.20	0.68	0.88
Long Eaton	13003-0053		5880	0.03	0.05	0.40	461	0.25	6.40	0.01	0.63	0.64	8	5	39	0.17	0.12	0.30
Long Eaton	13003-0054		5885	0.13	0.28	0.32	469	0.22	5.80	0.04	1.38	1.42	20	1	15	0.16	0.28	0.44
Long Eaton	13003-0055		5892	0.19	0.38	0.34	465	0.37	8.50	0.06	1.48	1.54	25	5	24	0.23	1.91	2.14
Long Eaton	13003-0056		5895	0.12	0.30	0.30	466	0.29	6.70	0.05	1.41	1.46	21	4	20	0.18	0.62	0.81
Long Eaton	13003-0057		5898	0.12	0.34	0.26	468	0.30	7.20	0.05	1.48	1.53	22	1	20	0.20	0.67	0.87
Long Eaton	13003-0058		5901	0.04	0.13	0.25	478	0.16	4.40	0.02	0.79	0.81	16	4	20	0.12	0.03	0.15
Nooks Farm	13003-0059		1401	0.08	0.24	0.25	440	0.21	4.30	0.04	0.56	0.60	40	10	35	0.12	0.57	0.68
Nooks Farm	13003-0060		1410	0.28	0.70	0.29	449	0.10	1.20	0.09	1.64	1.73	40	2	6	0.04	0.00	0.04
Nooks Farm	13003-0061		1417	0.23	0.89	0.21	454	0.12	2.20	0.10	1.17	1.27	70	2	9	0.06	0.00	0.06
Nooks Farm	13003-0062		1418	0.35	0.89	0.28	447	0.12	1.20	0.11	1.84	1.95	46	6	6	0.03	0.00	0.04
Nooks Farm	13003-0063		1429	0.25	0.62	0.29	447	0.08	0.90	0.08	1.13	1.21	51	6	7	0.03	0.00	0.03
Nooks Farm	13003-0064		1432	0.32	0.39	0.45	446	0.04	0.60	0.07	0.60	0.67	58	3	6	0.02	0.00	0.02
Nooks Farm	13003-0065		1450	0.30	0.81	0.27	445	0.21	1.90	0.11	2.08	2.19	37	3	10	0.06	0.02	0.08
Nooks Farm	13003-0066		1519	0.23	0.48	0.33	442	0.24	1.90	0.08	1.86	1.94	25	9	12	0.05	0.03	0.08
Nooks Farm	13003-0067		1531	0.19	0.45	0.29	449	0.08	0.80	0.06	1.41	1.47	31	3	5	0.03	0.03	0.05
Old Dalby	13003-0068	1390.6	4562.3	0.91	5.46	0.14	436	0.27	6.70	0.55	2.18	2.73	200	1	10	0.19	2.67	2.86
Old Dalby	13003-0069	1394.3	4574.5	0.97	4.13	0.19	433	0.47	7.80	0.46	3.07	3.53	117	6	13	0.22	0.28	0.50
Old Dalby	13003-0070	1398.5	4588.3	0.80	4.70	0.15	434	0.41	6.00	0.48	2.58	3.06	154	5	13	0.17	0.19	0.36
Old Dalby	13003-0071	1404.6	4608.3	1.79	9.63	0.16	432	0.45	9.60	0.98	4.14	5.12	188	4	9	0.27	1.10	1.38
Old Dalby	13003-0072	1437.5	4716.2	1.61	11.10	0.13	435	0.43	5.50	1.09	4.56	5.65	196	4	8	0.16	0.21	0.37
Old Dalby	13003-0073	1442.5	4732.6	1.12	6.05	0.16	434	0.24	9.30	0.61	1.94	2.55	237	1	9	0.26	7.46	7.72
Old Dalby	13003-0074	1447.8	4750.0	0.80	4.79	0.14	436	0.42	9.50	0.49	2.05	2.54	189	5	17	0.27	1.08	1.35
Old Dalby	13003-0075	1450.8	4759.8	0.93	6.48	0.13	438	0.24	3.10	0.64	2.76	3.40	191	4	7	0.09	0.04	0.13
Old Dalby	13003-0076	1455.0	4773.6	1.45	7.84	0.16	436	0.33	9.70	0.79	2.39	3.18	247	1	10	0.28	4.86	5.14
Ratcliffe on	13003-0077	271.7	891.4	0.51	27.44	0.02	434	0.53	1.90	2.38	6.18	8.56	321	6	6	0.08	0.02	0.10

Well	BGS sample number	Depth (m)	Depth (ft)	S_1 (mg/g)	S_2 (mg/g)	PI	T_{max} (°C)	S_3 (mg/g)	$S_{3'}$ (mg/g)	PC (%)	RC (%)	TOC (%)	HI	OICO	OI	pyroMINC (%)	oxiMINC (%)	MINC (%)
Soar																		
Ratcliffe on Soar	13003-0078	275.0	902.2	0.50	33.51	0.01	435	0.34	1.60	2.86	3.87	6.73	498	6	5	0.06	0.03	0.09
Ratcliffe on Soar	13003-0079	278.2	912.7	1.09	14.07	0.07	423	0.62	11.20	1.31	3.28	4.59	307	7	14	0.33	0.33	0.65
Ratcliffe on Soar	13003-0080	281.7	924.2	0.76	9.74	0.07	424	0.50	9.40	0.91	2.32	3.23	302	6	15	0.27	1.26	1.53
Ratcliffe on Soar	13003-0081	285.0	935.0	0.96	13.47	0.07	422	0.62	9.40	1.25	3.31	4.56	295	7	14	0.27	0.55	0.83
Ratcliffe on Soar	13003-0082	287.5	943.2	0.21	2.92	0.07	416	0.33	3.70	0.30	2.42	2.72	107	14	12	0.11	0.01	0.12
Ratcliffe on Soar	13003-0083	289.5	949.8	0.25	4.44	0.05	422	0.56	12.60	0.43	3.66	4.09	109	11	14	0.35	0.25	0.60
Rempstone	13003-0084	665.0	2181.8	0.86	4.52	0.16	437	0.20	0.50	0.47	2.19	2.66	170	4	8	0.02	0.00	0.03
Rempstone	13003-0085	665.3	2182.7	1.67	25.80	0.06	437	1.15	5.80	2.35	4.96	7.31	353	5	16	0.18	0.01	0.19
Rempstone	13003-0086	666.0	2185.0	1.58	28.53	0.05	438	2.11	25.30	2.59	4.70	7.29	391	6	29	0.70	0.01	0.71
Rempstone	13003-0087	667.0	2188.3	0.92	27.18	0.03	437	0.50	1.50	2.37	3.50	5.87	463	6	9	0.05	0.01	0.06
Rempstone	13003-0088	668.0	2191.6	0.10	0.10	0.50	431	0.74	12.30	0.05	1.72	1.77	6	10	42	0.34	7.30	7.64
Roddlesworth	13003-0089		4226	0.09	0.06	0.62	508	0.72	12.10	0.04	1.71	1.75	3	9	41	0.33	7.38	7.71
Roddlesworth	13003-0090		4239	0.15	0.07	0.69	481	0.16	5.20	0.03	0.16	0.19	37	5	84	0.14	11.07	11.21
Roddlesworth	13003-0091		4250	0.01	0.00	0.99	494	0.12	2.60	0.00	0.07	0.07	0	29	171	0.07	12.07	12.14
Roddlesworth	13003-0092		4256	0.12	0.06	0.66	415	0.29	9.20	0.03	0.23	0.26	23	19	112	0.25	10.51	10.76
Roddlesworth	13003-0093		4268	0.00	0.00	0.67	494	0.09	2.00	0.00	0.07	0.07	0	14	129	0.05	12.44	12.49
Roddlesworth	13003-0094		4277	0.30	0.15	0.66	494	0.22	8.00	0.05	0.33	0.38	39	5	58	0.22	9.73	9.96
Roddlesworth	13003-0095		4281	0.02	0.02	0.48	474	0.15	1.90	0.01	0.06	0.07	29	43	214	0.05	11.88	11.94
Swinden 1	13003-0096	30.0	98.4	0.28	0.66	0.30	447	0.22	8.80	0.09	1.55	1.64	40	8	13	0.24	4.58	4.83
Swinden 1	13003-0097	33.0	108.3	0.27	0.70	0.28	458	0.16	7.90	0.09	1.64	1.73	40	8	9	0.22	3.10	3.32
Swinden 1	13003-0098	38.5	126.3	0.25	0.67	0.27	457	0.16	7.10	0.09	1.65	1.74	39	8	9	0.20	3.13	3.32
Swinden 1	13003-0099	40.5	132.9	0.27	0.58	0.32	456	0.15	8.00	0.08	1.42	1.50	39	8	10	0.22	3.11	3.33
Swinden 1	13003-0100	44.7	146.7	0.24	0.67	0.27	455	0.17	8.50	0.09	1.55	1.64	41	5	10	0.23	1.92	2.16
Swinden 1	13003-0101	48.8	160.1	0.25	0.74	0.25	458	0.16	7.60	0.09	2.21	2.30	32	6	7	0.21	2.70	2.91

Well	BGS sample number	Depth (m)	Depth (ft)	S_1 (mg/g)	S_2 (mg/g)	PI	T_{max} (°C)	S_3 (mg/g)	$S_{3'}$ (mg/g)	PC (%)	RC (%)	TOC (%)	HI	OICO	OI	pyroMINC (%)	oxiMINC (%)	MINC (%)
Swinden 1	13003-0102	621.2	2038.1	0.04	0.23	0.15	580	0.20	7.70	0.03	2.49	2.52	9	4	8	0.21	4.28	4.50
Swinden 1	13003-0103	623.0	2044.0	0.03	0.03	0.46	581	0.18	8.70	0.01	0.83	0.84	4	5	21	0.24	7.35	7.58
Swinden 1	13003-0104	626.8	2056.4	0.03	0.04	0.44	331	0.14	10.60	0.01	1.28	1.29	3	5	11	0.29	3.96	4.25
Swinden 1	13003-0105	629.5	2065.3	0.04	0.08	0.31	595	0.23	8.90	0.02	1.36	1.38	6	4	17	0.24	6.24	6.48
Wessenden 1	13003-0106		3505	0.01	0.00	0.98	494	0.19	11.40	0.01	0.29	0.30	0	20	63	0.31	2.45	2.76
Wessenden 1	13003-0107		3510	0.02	0.00	1.00	494	0.20	10.80	0.01	0.25	0.26	0	15	77	0.29	4.53	4.83
Wessenden 1	13003-0108		3512	0.01	0.00	1.00	494	0.14	7.40	0.01	0.26	0.27	0	19	52	0.20	4.09	4.29
Wessenden 1	13003-0109		3513	0.01	0.00	1.00	494	0.18	3.00	0.01	0.29	0.30	0	10	60	0.08	0.46	0.54

Appendix C: Stratigraphic data from key wells penetrating the Bowland-Hodder shales in central Britain

Non-released wells are in red. **BGS boreholes are in bold italics.** Note that all depths of subsea, not downhole relative to KB. Conf. = confidential

Well abbrev-iation	Well name	Year spudded	KB elevation (ft above MSL)	GL elevation (ft above MSL) (or DTM)	Base Permian (ft below MSL) (or outcrop)	Top Bowland-Hodder unit (ft below MSL)	Base Bowland-Hodder unit (ft below MSL)	Bowland-Hodder unit thickness (ft)	Net shale upper unit (ft)
ALP	Alport 1	1939	930	(928)	(Nam)	-910	1630+	>2540	?1000
ASK	Askern 1	1957	25.4	(25)	1033	4595	4787.6+	>193	87
BECH	Becconsall 1	2011	27	(19)	conf.	conf.	conf.	conf.	conf.
BLE	Blacon East 1	1981	47	32	1318	4214	7387+	>3173	819
BOS	Bosley 1	1986	1332.4	1308.7	(Nam)	-223.5	4994	5217.5	408
BOT	Bothamsall 1	1957	117.3	(125)	860	3682.7	4566.7+	>884	412
BOU	Boulsworth 1	1963	1408	1385	(Nam)	1752	3448	1696	98
BRA	Bramley Moor 1	1987	725	714	(West)	2376	3208+	>662	527
CAL	Calow 1	1957	420	(413)	(West)	1860	3299+	>1439	475
CLO	Cloughton 1	1986	573	(542)	5969	8535	9527+	>992	317
CRA	Crayke 1	1964	161	(156)	2653	3479	4339+	>860	?
CRO	Croxteth 1	1953	84	(79)	1579	3216	4132+	>916	419
DUF	*Duffield*	1966	202	(216)	(Nam)	-71	3251+	>3322	764
DUG	Duggleby 1	1990	673	650	4869	8393	9351+	>958	324
EAK	Eakring 146	1944	342	(341)	942	1988	4728	2740	?185
EDA	Edale 1	1937	c.850	(845)	(Nam)	-850	-93+	>757	?
EGM	Egmanton 68	1980	126	112.9	1515	3676	6041.9	2365.9	?10
ELL	Ellenthorpe 1	1945	60	(46)	1181	1181	3538+	>2357	?
ERB	Erbistock 1	1986	208	184	(West)	3793	5986+	>2193	236
FLE	Fletcher Bank 1	1958	857	(837)	(Nam)	3400	4658+	>1258	288
FOR1	Formby 1	1940	18	(20)	5862	7122	7662+	>540	73
FOR4	Formby 4	1949	36	(32)	2742	3144	3844+	>700	210
GAI	Gainsborough 2	1959	104.3	(87)	2380	5816	6154.7+	>338.7	0
GRA	Grange Hill 1	2011	73	47.5	conf.	conf.	conf.	conf.	conf.
GRO	Grove 3	1981	210.4	192	1766	4909	7253	2344	90
GUN	Gun Hill 1	1938	1157	1142	(Nam)	-862	2008	2870	510
HAN	Hanbury 1	1990	467	452	1148	2382	3949	1567	110
HATM	Hatfield Moors 3	1983	29	12	1341	5471	5971+	>500	No logs
HAT	Hathern 1	1954	161	(157)	300	657	1602	945	93
HEA	Heath 1	1919	516	(519)	(West)	3034	3484+	>450	?390
HES	Hesketh 1	1990	41	27	2126	2126	4202+	>2076	798
HEY	Heywood 1	1984	393.8	377.7	(West)	4147.9	4917.9+	>770	180
HIG	High Hutton 1	1987	171	151	3908	6854	8829+	>1975	562
HOL	Holme Chapel 1	1974	891	871	(West)	3964	5566	1602	52
ILK	Ilkeston 1	1985	222.37	208.6	(West)	2335.7	3386.7+	>1051	960
INC	Ince Marshes 1	2011	47.2	33	conf.	conf.	conf.	conf.	conf.
IRO	Ironville 5	1984	303.5	290.4	(West)	1439	3452.5	2013.5	95
KIN	Kinoulton 1	1985	147.4	130.9	932	3742.6	4741+	>998.4	369
KRM	Kirby Misperton 1	1985	118	98	5221	6415	11013	4598	868
KRS	Kirk Smeaton 1	1985	123.7	107.6	2.3	4715.5	5243.7	528.2	381
LONC	Long Clawson 1	1943	178	(178)	1222	4022	4527+	>505	85
LONE	Long Eaton 1	1988	129.7	113	382	382	8410	8028	0 (eroded)
MIL	Milton Green 1	1965	63	52.4	(West)	3801	4858	1057	505

Well abbreviation	Well name	Year spudded	KB elevation (ft above MSL)	GL elevation (ft above MSL) (or DTM)	Base Permian (ft below MSL) (or outcrop)	Top Bowland-Hodder unit (ft below MSL)	Base Bowland-Hodder unit (ft below MSL)	Bowland-Hodder unit thickness (ft)	Net shale upper unit (ft)
NOO	Nooks Farm 1	1982	997	980	(Nam)	-517	2623+	>3140	824
NORM	Normanby 1	1985	63.7	43.8	2642	6884	7347.7+	>463.7	308
OLD	Old Dalby 1	1988	323	305.8	1128	3587	4532+	>945	268
PRH	Preese Hall 1	2010	25.5	16.7	conf.	conf.	conf.	conf.	conf.
RAN	Ranton 1	1980	407	394	1913	4209	5428	1219	?0
RAT	Ratcliffe-on-Soar 1	1986	124.8	108.1	696	1015.6	5913.2+	>4895	198
REM	Rempstone 1	1985	273.9	259.8	620.1	1912.1	3437	1524.9	297
ROD	Roddlesworth 1	1987	774	754	(Nam)	3369	7332	3963	44
ROO	*Roosecote*	1970	121.4	(127)	397.4	1615	2501.6+	>886.6	420
SCA	Scaftworth 2	1982	45.6	27.2	1062	6814.2	7585.6+	>771.4	474
SES	Sessay 1	1988	95	80	1225	2164	5405+	>3241	331
SOU	South Leverton 1	1960	37.3	(29)	1913.7	4802.7	5087.7+	>285	124
STR	Strelley 1	1986	436.8	422.1	-376	2412.6	4320.4+	>1907.8	205
SWI	Swinden 1	1978	462.6	456	(Tourn)	-	-	>2310[1]	-
THI	Thistleton 1	1987	75	15	2964	4019	6945+	>2926	2096
THO	Tholthorpe 1	1965	80.4	(75)	1489.6	2609.6	2969.6+	>360	?
TOR	Torksey 4	1975	47.2	34.3	2323	5598.8	6019.8+	>421	279
WEE	Weeton 1	1984	166.8	141.7	(Nam)	909	4886	3977	246
WES	Wessenden 1	1987	1631.5	1620	(Nam)	-131	368	499	117
WHM	Whitmoor 1	1966	1024	(1018)	(Nam)	2096	3426	1330	140
WID	Widmerpool 1	1945	266	(261)	754	2234	5934+	>3700	?3700

NB These data present the interpretation used in this study.

[1] >2310 ft of pre Bowland-Hodder unit shales.

Other wells

Well abbreviation	Well name	Well abbreviation	Well name
ALD	Aldfield 1	MAL1	Malton 1
APL	Apley 1	MAL4	Malton 4
BARD	Bardney 1	MAR	Marishes 1
BART	Barton 1	NET1	Nettleham 1
BEC	Beckering 1	NET2	Nettleham 2 (B2)
BIS	Biscathorpe 1	NEW	Newton Mulgrave 1
BIT	Bittern's Wood 1	NORG	North Greetwell 1
BLW	Blacon West 1	NOR	Northwood 1
BRAF	Brafferton 1	PIC	Pickering 1
BRI	Brigg 1	PLU	Plungar 8A
BRM	Broomfleet 1	PRE	Prees 1
BRO	Broughton B1	RAL	Ralph Cross 1
BUT	Butterwick 1	ROB	Robin Hood's Bay 1
CHE	Cherry Willingham 1	ROS	Rosedale 1
CLE	Cleveland Hills 1	RUD	Rudston 1
COL	Cold Hanworth 1	SAL	Saltfleetby 3
DUN	Dunholme 1	SCAL	Scaling 1
EGT	Egton High Moor 1	SCU	Scupholme 1
ELS	Elswick 1	SEA	Seal Sands
ESK12	Eskdale 12	SPA	Spaldington 1

Well abbreviation	Well name	Well abbreviation	Well name
FOR	Fordon 1	STA	Stainton 1
FOR5	Formby F5	TET	Tetney Lock 1
GLA	Glanford 1	WEL	Welton 1
HAR	Harlsey 1	WELW	Welton West 1
HEAF	Heath Farm 1	WHEL	Wheldrake 1
HEM	Hemswell 1	WHE	Whenby 1
HUN	Hunmanby 1	WHI	Whitwell on the Hill 1
KED	Keddington 1Z		
KEL	Kelstern 1		
KIR	Kirkleatham 1		
KNU	Knutsford 1		
LAN	Langtoft 1		
LOC2	Lockton 3		
LOCE	Lockton East 1		

Appendix E: Thermal modelling of the Pennine Basin, central Britain

Summary

This report describes a thermal modelling study covering boreholes across the Pennine Basin, central Britain, from the East Irish Sea Basin, across the Bowland Basin, through the Cheshire Basin and the Widmerpool Trough to the Gainsborough Trough. It forms part of a wider study to assess the extent of the region's shale gas resource.

The regional structural history of the area includes Early Carboniferous rifting that resulted in a period of fault-controlled deposition followed by a Late Carboniferous phase of regional subsidence. This is reflected by widespread marine deposition during the Visean, with shallowing marine conditions during deposition of the Millstone Grit Group during the Namurian and shallow marine/paralic delta top deposition of Coal Measures and Warwickshire Group during the Westphalian. Subsequent regional uplift and erosion occurred during the Variscan Orogeny. Sediments were then deposited on this erosional surface during renewed subsidence during the Permian – Cretaceous, though deposition was interrupted by a short hiatus or period of erosion during the Triassic (Hardegsen event). Following the Variscan Orogeny, subsidence resulted in the deposition of Permian and Triassic sediments in shallow marine/deltaic/lacustrine/sabkha environments. Based on evidence from the closest outcrops, deposition during the Jurassic and Cretaceous is likely to reflect a deepening marine environment. Finally, uplift and erosion removed sediments for almost all the basins in this study during the Palaeocene – recent times.

Generally, the present-day heat flow figures calculated from available boreholes are quite modest (50 – 54 mWm^{-2}), however, in the past, during rifting, this would be expected to have been higher, indeed the models in the depocentres of these basins imply heat flows as high as 78 mWm^{-2} during Early Carboniferous rifting and 65 mWm^{-2} during Cretaceous uplift.

The strata penetrated by each borehole were entered into a 1-D model. The eroded thicknesses of Carboniferous strata for the 1-D models were estimated from surrounding boreholes and published sources in order to estimate the model layers needed to represent these eroded sediments. These varied from a few hundred metres to over 1000 m of sediment removed during Variscan uplift and erosion. Some Permian – Triassic deposits were present in the boreholes used in this study; where these sediments had been removed, the eroded Permian – Cretaceous strata thickness was estimated from surrounding boreholes and published sources. These estimated eroded thicknesses were then used to match the modelled maturity to available vitrinite reflectance (VR) data. Where data were sparse, models from nearby boreholes were used to supplement the modelled heat flow.

Finally, these 1-D models were combined to generate three 2-D model sections, these are not as sophisticated as the 1-D models as simplification is required in order to allow the model to run, however, they give a useful overview of the boreholes in context of the depositional basins which contain them. For the 2-D sections, it was assumed that the strata layers have a uniform lithology across each section, the constitution of which was based on the 1-D models.

1. Introduction

BasinMod[TM] (Platte River Software, Inc.) was used to model the maturity of sediments in selected boreholes in the Pennine Basin. The final 1-D models may be used alongside geological assessments of the basin to consider the geological history of the Pennine Basin from the Carboniferous to the present day.

The approach taken was to model the boreholes individually using BasinMod[TM] 1-D as these models allow entry of detailed lithology and modelling of the heat flow to achieve the best fit to the vitrinite reflectance (VR) data. These 1-D models were then used to model the burial history and maturity along a 2-D profile between boreholes using interpreted seismic data to complete the section.

The VR data, 1-D and 2-D models give an understanding of the maturity of the basin and indicate which strata have reached sufficient maturity for any organic material which is present to generate oil or gas.

2. Modelling

This report describes the results of 1-D thermal models in the Pennine Basin. BasinMod[TM] (Platte River Associates, Inc.) was used to model the maturity of sediments in selected boreholes then these boreholes were integrated into three 2-D sections. The report considers the region area through the Carboniferous to the present day, concentrating on the Bowland Shale where maturity data are available.

The boreholes to be modelled were chosen based on availability of data (Table 1) and the location of the boreholes such that the models would contribute to understanding the thermal maturity of these basins (Figure 1).

The 1-D models and 2-D model presented here were produced using Platte River Associates Software BasinMod 1-D version 7.61 and BasinMod 2-D version 4.61. Borehole stratigraphy and rock properties were used to model compaction and temperature through burial over geological time. The modelled maturity and vitrinite reflectance maturity (VR) data were then compared graphically and used to refine the model until the best fit to the available data was achieved. Plots of the maturity, temperature vs. depth and vs. time were produced. The oil and gas windows were changed from the BasinMod defaults after discussion with I. Andrews, BGS.

BasinMod 1-D calculates heat flow curves based on the finite rifting model of Jarvis & McKenzie (1980). This assumes that in an extensional environment there is rapid initial subsidence due to crustal thinning associated with a thermal anomaly i.e., high heat flow. Unlike McKenzie's earlier model, this one recognises that continental basin formation by extension takes a finite time. When crustal stretching ceases, heat is lost by vertical conduction and the slow decay of the heat flow leads to further subsidence due to thermal contraction. For modelling heat flow in basins with limited extension (stretching factor $\beta \leq 2$), the Jarvis & McKenzie (1980) model assumes that the thermal anomaly develops and decays within about 60 Ma.

In order to match the model to the recorded vitrinite data, estimates of the palaeo-heat flow and eroded sediments thicknesses are required. The thickness of sediment removed is estimated based on surrounding sediments and the VR data. The palaeo-heat flow is estimated based on known rifting events and the slope of the scattered VR point data. Boreholes with more complete VR data were used to supplement models where there were fewer VR data available.

Minor modifications were made to the Jarvis & McKenzie palaeo-heat flow curves to improve the fit of the model to the data. The modelled maturity was calibrated graphically against the maturity data for the borehole. The eroded sediment thickness was estimated using vitrinite reflectance (VR) and apatite fission track analysis (AFTA) where available. Palaeozoic stratigraphical ages were taken from the BGS online stratigraphical tables (Powell 2009 pers. comm., Gradstein *et al.* 2004 and ICS 2006). Lithology mixes to best approximate the stratigraphy were constructed from borehole records held by BGS in the National Geological Records Centre (NGRC), and published data. Permo-Triassic deposits are not well preserved at all sites across this region. Finally, estimates of water depth, surface palaeo-temperature and palaeo-sea level were included. The vitrinite reflectance data were then used for final calibration to produce a best-fit, geologically reasonable model.

The 2-D models were generated by combining results from the calibrated 1-D models. Seismic data was used to interpret the horizons between these wells and these profiles were then used to generate 2-D section models of basin maturity. Only faults that cut more than one horizon affect calculated model results. For simplicity the 2-D model the lithologies were assumed to be uniform across the basin. Initially the model was constructed using only the current sediment thickness. The model was 'coupled', (i.e. the lines separating model layers were joined correctly such that the correct rock properties were contained within the appropriate model layers) and successfully run. This initial model was then modified to include the Variscan Unconformity and erosional surface. A simplified heat flow based on those developed for the 1-D models was used, with a high heat flow in the Carboniferous decreasing to present day levels. The broken lines above the Variscan Unconformity and current land surface indicate the modelled eroded sediment thicknesses above the Variscan unconformity and present day surface (see figure for more detail). It should be noted that the 2-D model cannot model the eroded thickness of Carboniferous sediment where the Variscan Unconformity itself has been eroded, instead, the eroded sediment thickness is then added to the layers removed by recent erosion, which slightly degrades the fit of the VR data compared to the more satisfactory fit of the 1-D models. The Sclater & Christie (1980) or exponential method of compaction was chosen. This method was developed from wells on the North Sea Central Graben, which may show some overpressuring; correcting for this tends to result in undercompaction, which may have affected the fit of the model.

In general, the models fit the data well and are geologically reasonable. Using the more sophisticated and detailed 1-D models to produce a 2-D cross section was a successful approach. There is still potential to refine the 2-D model, for example, by varying lithologies across the basin.

3. Boreholes modelled

The boreholes modelled for this report are given in Table 1. Logs and stratigraphic data are available in the BGS NGRC and archives. Vitrinite reflectance data were taken from published papers, confidential reports, PhD theses or new BGS analytical results (Smith *et al.* 2012).

Table 1: Boreholes modelled

WELL NAME	NUMBER	DRILLED DEPTH (m)	EASTING	NORTHING	COMMENTS (TD – total depth, VR – number of vitrinite reflectance data)
Irish Sea	110/2b-10	2540.51	03°44' 34°589' W	53°50' 38°157'	Released well 16VR (confidential report) TD in Millstone Grit (Namurian C Yeadonian – Marsdenian)
Thistleton 1	SD33NE17	2139.69	339760	437000	Released well 16VR (Smith *et al.* 2012) TD in Bowland Shale (Brigantian – Pendleian)
Hesketh 1	SD42NW6	1295.4	343001	425197	Released well 3VR (Smith *et al.* 2012) TD in Lower Bowland Shale (Brigantian)
Upholland 1	SD50SW20	1523.39	350440	402900	Released well 14 VR (Pearson & Russell, 2000) TD in Sabden Shale (Arnsbergian – Kinderscoutian)
Ince Marshes 1		1570	346211	376439	Confidential well 18 VR (courtesy of IGas Energy Plc.) TD in Craven Group
Blacon East 1	SJ36NE23	2265.88	337890	366860	Released well 7 VR (Smith *et al.* 2012) TD in Carboniferous limestone (Visean)
Knutsford 1	SJ77NW4	3045.7	370269	377851	Released well 4 VR (Pearson & Russell, 2000), 5 AFTA (Lewis *et al.* 1992) TD in Westphalian Coal Measures
Gun Hill 1	SJ96SE18	904	397230	361820	Released well 12 VR (confidential report) TD in Carboniferous Limestone
Long Eaton 1	SK43SE161	2752.34	446400	331660	Released well 8 VR (confidential report) TD in Craven Group (Chadian)
Ilkeston 1	SK44NE47	1103.5	447537	345172	Released well 3 VR (confidential report) TD in Millstone Grit (Arnsbergian)
Grove 3	SK78SE30	2933.0	476155	381373	Released well 3 VR (Smith *et al.* 2012) TD in Early Palaeozoic phyllites with Visean (Courceyan) overlying
Gainsborough 2	SK89SW2	1907.74	481774	390785	Released well 39 VR (confidential report) TD in Upper Bowland Shale (with basic igneous extrusive rock as lowest layer)
Kirk Smeaton 1	SE51NW40	1636.0	451142	416097	Released well 30 VR (confidential report) TD in Craven Group (Brigantian)
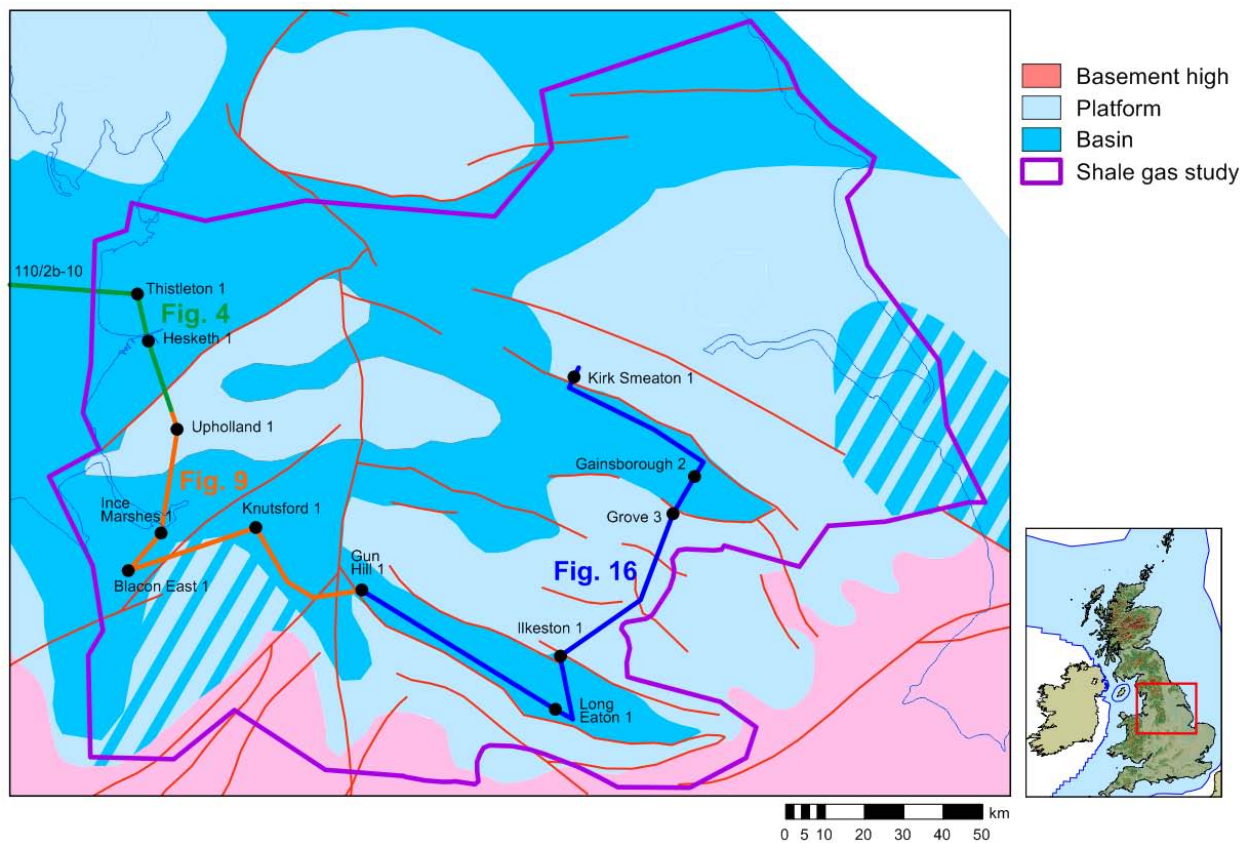
Figure 1. Location of the study area, wells and lines of section

4.   East Irish Sea – Craven Basin section

4.1 East Irish Sea geology

The oldest deposits penetrated by the boreholes in this study are of Namurian age. Seismic interpretation extends the 2-D model in this basin to the top of the Chadian in the Bowland-Hodder unit. The East Irish Sea Basin succession comprises Lower Bowland Shale deposited in a deep marine environment in the early Carboniferous (Rowley & White 1998). Rifting and regional extension during the Visean resulted in multiple faults showing syn-depositional deposition of thick marine sediments. Rifting ceased in the late Visean and thermal subsidence occurred through Namurian and Westphalian times and deposition of sediments in paralic and shallow marine environments. This was followed by uplift and erosion during the Variscan Orogeny. A second phase of east-west rifting began during Permian times, resulting in syn-tectonic deposition of thick Permian and early Triassic sediments in a fluvial basin environment followed by marine sediments in the late Triassic. This rifting may have continued to the Late Jurassic. Deposition in deeper marine waters continued through to the Late Cretaceous (Rowley & White 1998). This period of rifting and deposition was again followed by uplift and erosion, most likely due to magmatic underplating.

4.1.1 Well 110/02b-10

This offshore borehole penetrates Namurian to Quaternary sediments and has 16 vitrinite reflectance measurements.

An estimated 800 m of sediment was removed during the Variscan Orogeny and around 1200 m during the later erosional period during the Cretaceous uplift. This figure is in agreement with the estimated thickness of eroded Carboniferous strata in Rowley & White (1998).

A satisfactory fit to the data was achieved. The comparison of model maturity and maturity data is shown in Figure 2c. The heat flow model (Figure 2b) is fairly well constrained by the slope of the VR data curve (Figure 2c). Heat flow appears to have reached 73 mWm^{-2} during the late Carboniferous, resulting in temperatures of around 80ºC in the deepest Westphalian A strata during Carboniferous burial and 140ºC during deep Cretaceous burial. This model implies that the Westphalian A coals achieved a depth of burial of around 3.7 km during the Cretaceous, reaching higher temperatures than during the Carboniferous. A change in the gradient of the line is observed at the Variscan Unconformity. The model indicates that the Carboniferous Coal Measures reached the oil generation window during the Triassic and the gas generation window during the Cretaceous.

4.2 Craven Basin geology

During the Devonian, Old Red Sandstone was deposited in a continental environment. In the early Visean, a marine transgression resulted in deposition of shallow marine sediments and water depths increased to deeper marine in the late Visean as the basin subsided as an asymmetrical southward-tilted graben along the Pendle Fault. The Bowland Shale was deposited in the final stages of Visean sedimentation starting in the Asbian. In the early Namurian, these seas shallowed until during the late Namurian – early Westphalian sediments are of coastal/alluvial/lacustrine/nearshore origin. The Namurian sediments show cyclical deposition and can be correlated across the basin using marine bands. The Millstone Grit Group was deposited in a deltaic environment, sourced from the north. Over 3 km of Devonian – Courceyan sediments are recorded in the basin and over 2.5 km of Visean sediments (Aitkenhead *et al.* 2002). Although the younger rocks have been eroded in the Craven Basin, it was assumed that the younger sediments were also deposited as they are present close to this basin in the region west of the Pennines. The Westphalian Coal Measures were deposited as cyclothems in swampy environment followed by the alluvial/lacustrine Warwickshire Group in the Pennine region.

Sills and dykes in this region are recorded to have ages of 296 ±15 and 302 ±20 Ma.

Carboniferous deposition was followed by uplift and erosion during the Variscan Orogeny. Following this uplift, the basin subsided and Permian and Triassic sediments were deposited in a major rift system. The Craven Basin (previously Bowland Basin or West Lancashire Basin) was contiguous with the East Irish Sea Basin and Cheshire Basin during the Carboniferous and Permian-Triassic (Rowley & White 1998) during regional subsidence and subsequent uplift. Preserved Permo-Triassic sediments are 1 km thick and locally over 2 km thick. As the top of these sediments are eroded, the thickness of these sediments was initially greater. The Triassic Hardegsen unconformity is believed to be present across this basin (Aitkenhead *et al.* 2002).

The current heat flow in this basin is around 50 mWm^{-2} based on observations in the boreholes at Thornton Cleveley and Weeton Camp (Downing & Gray 1986), so it was assumed the present day heat flow in Thistleton 1 and Hesketh 1 is the same.
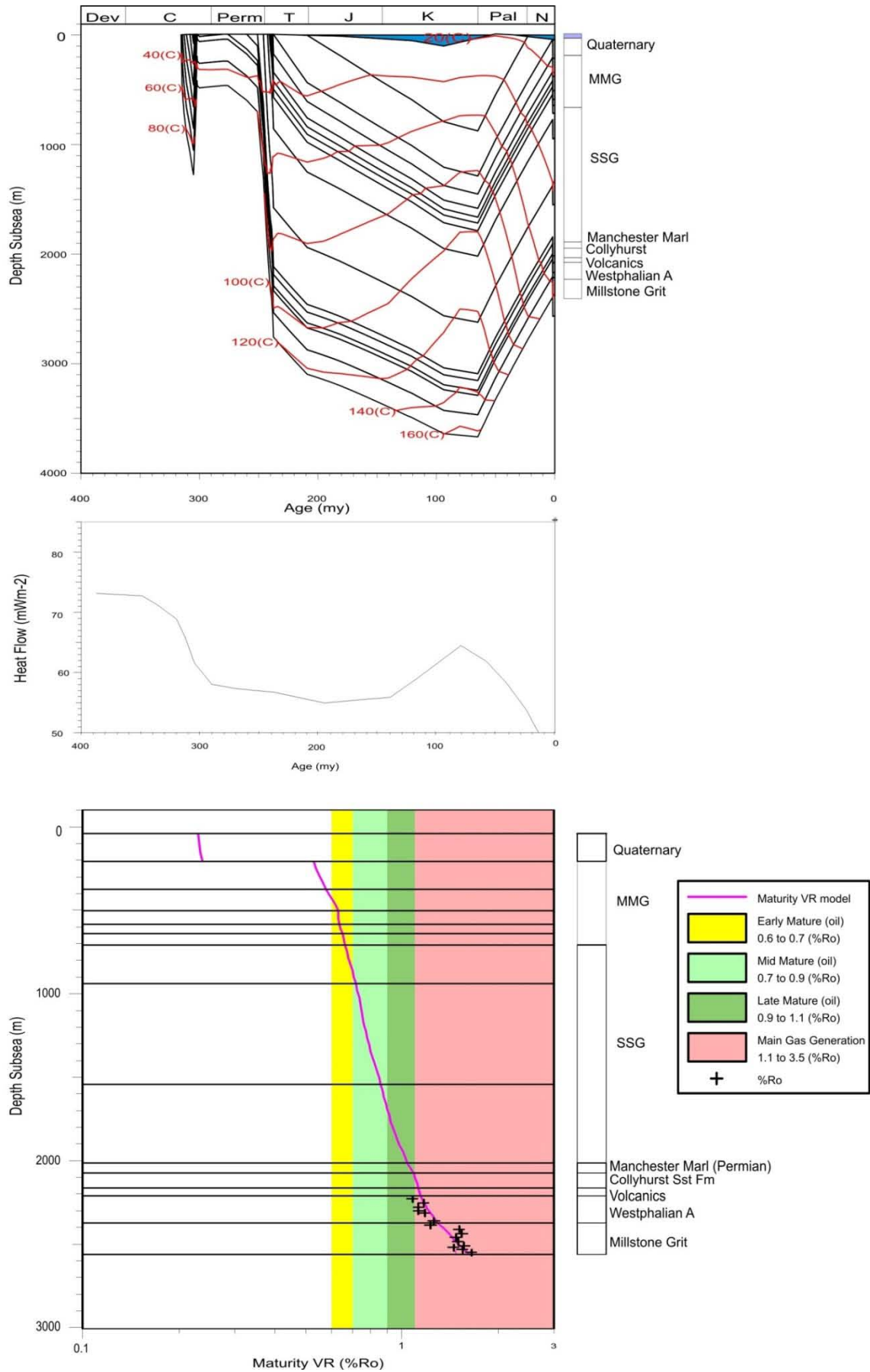
Figure 2. 110/2b-10 model, 2a (top) shows the depositional history and isotherms (isotherms are at 20°C intervals), the blue polygons at the top represent water depth, 2b (centre) shows the modelled palaeo-heat flow and 2c (bottom) compares the modelled VR maturity and VR data.

4.2.1 Thistleton 1

The 16 vitrinite data for Thistleton 1 have quite a broad scatter (Figure 3), the relatively gentle slope implies a low heat flow, but given the scatter of the data, and the heat flow models for the nearby Hesketh 1 and 110/2b-10, the palaeo-heat flow may actually have been higher and the thickness of eroded sediment, lower. However, despite uncertainty in the model, the VR data do indicate that the Bowland Shale reached the oil generation window in this borehole.

The lower part of the Pendleian is offset from the upper part by faulting as shown by the offset of VR data (also A. Carr pers. comm.). Unfortunately, this cannot be modelled without affecting the rest of the model or falsely giving the oldest sediments in this basin a greater age in order to allow sufficient time for these sediments to mature and model the deeper burial of these sediments. It should be noted that due to this, the model indicates that the Bowland Shale only reaches the oil window in this borehole, though the sediments below the fault do reach the gas window (Figure 3c).

The high VR values suggest great quantities of sediment were deposited in the Carboniferous and eroded during the Variscan Orogeny. Near Manchester, over 2.5 km of Coal Measures and Warwickshire Group sediments are recorded. In this model, an additional 3 km of Carboniferous sediments were included in order to fit the data (Figure 3a). This additional thickness may partly be a result of the lower heat flow modelled at this location.

Permian and Triassic sediments are preserved onshore with 600 m of Permian sediments and over 200 m of Triassic Sherwood Sandstone and Mercia Mudstone sediments. The model fits the data when these layers are included as eroded sediments along with a further 3.1 km of deposition during the late Permian to Cretaceous, which was then eroded during the final period of uplift. There is more uncertainty on this final amount of deposition as the model is less sensitive to this layer, however, in order to fit these data, a significant amount of sediment must have been deposited during this period of time.
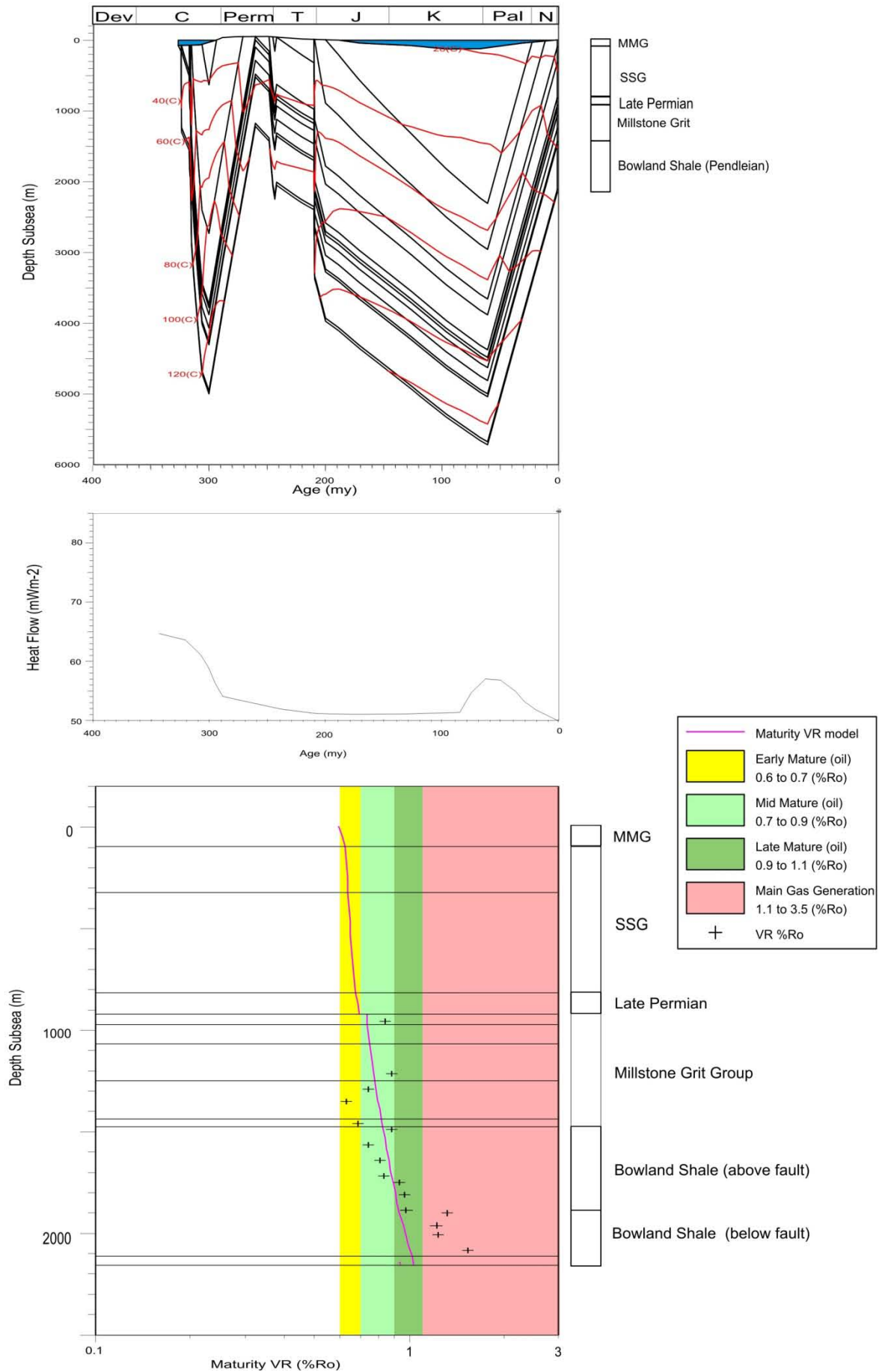
Figure 3. Thistleton model, 3a (top) shows the depositional history, 3b (centre) shows the modelled palaeo-heat flow and 3c (bottom) shows the modelled VR maturity and VR data.

4.2.2 Hesketh 1

As only 3 VR data points are available for this borehole (Figure 4), this model relies heavily on the nearby Thistleton 1 borehole model. The heat flow is subject to the same cautionary note that it may have been higher during Carboniferous rifting and that the thickness of deposited sediment may therefore have been overestimated. However, despite uncertainty in the model, the VR data do indicate that the Bowland Shale reached the oil generation window in this borehole.

In this case, it was estimated that 1500 m of Namurian and 2500 m of Westphalian – Stephanian sediments were deposited during the Carboniferous then eroded from the basin during the Variscan Orogeny. The Bowland Shale reached model temperatures of 120°C and depths of burial of almost 5 km, pushing these sediments into the oil generation window. Following uplift and erosion during the Variscan Orogeny, around 660 m of Permo-Triassic sediments are penetrated by the borehole. The model includes a further 3.9 km of Triassic – Cretaceous sediments which again increased the model temperatures of the Bowland Shales to 120°C and around 5 km depth of burial. These sediments were then removed by the latest uplift and erosion to the present day.

The heat flow for this model was based on the Thistleton model as there are only three VR data points and so the slope of the model is not well constrained outside of this small window.

The model indicates that the Bowland Shale Formation reached the oil generation window during the Carboniferous.

4.2.3 2-D section

Figure 5 and Figure 6 show the 2-D model which was generated using the 1-D models as a basis. Figure 5 shows the current sediment thicknesses across the basin as interpreted from seismic data. These are shown as coloured polygons, dashed lines show missing thicknesses of strata. A reasonable fit to the maturity data was achieved (Figure 6 and Figure 8) and this section shows the great thickness of eroded sediment implied by the models in order to achieve the maturity recorded by the VR data for the Hesketh and Thistleton boreholes in the Bowland Basin. It should be noted that as the lithologies used for the 2-D section are averaged for each formation and as such, the models are less detailed that the 1-D versions, the thickness of sediments over Hesketh and Thistleton is less than shown for the 1D models for this 2-D section. This highlights the need for a combined approach – using the 1-D models to assess the wells in detail and the 2-D model for a basin overview.

The present day gas window is shown in Figure 7. This indicates that most of the Bowland-Hodder unit is currently in the gas generation window (VR 1.1 – 3.5%). It should be noted that the deepest part of the Irish Sea Basin is uncontrolled by VR data and so the maturity model here is unconstrained. This area appears to have undergone rapid syn-depositional faulting so the maturity may in fact be underestimated here since eroded sediment thicknesses were estimated based on nearby boreholes but no VR data were available for this project in order to verify the model in this sub-basin.
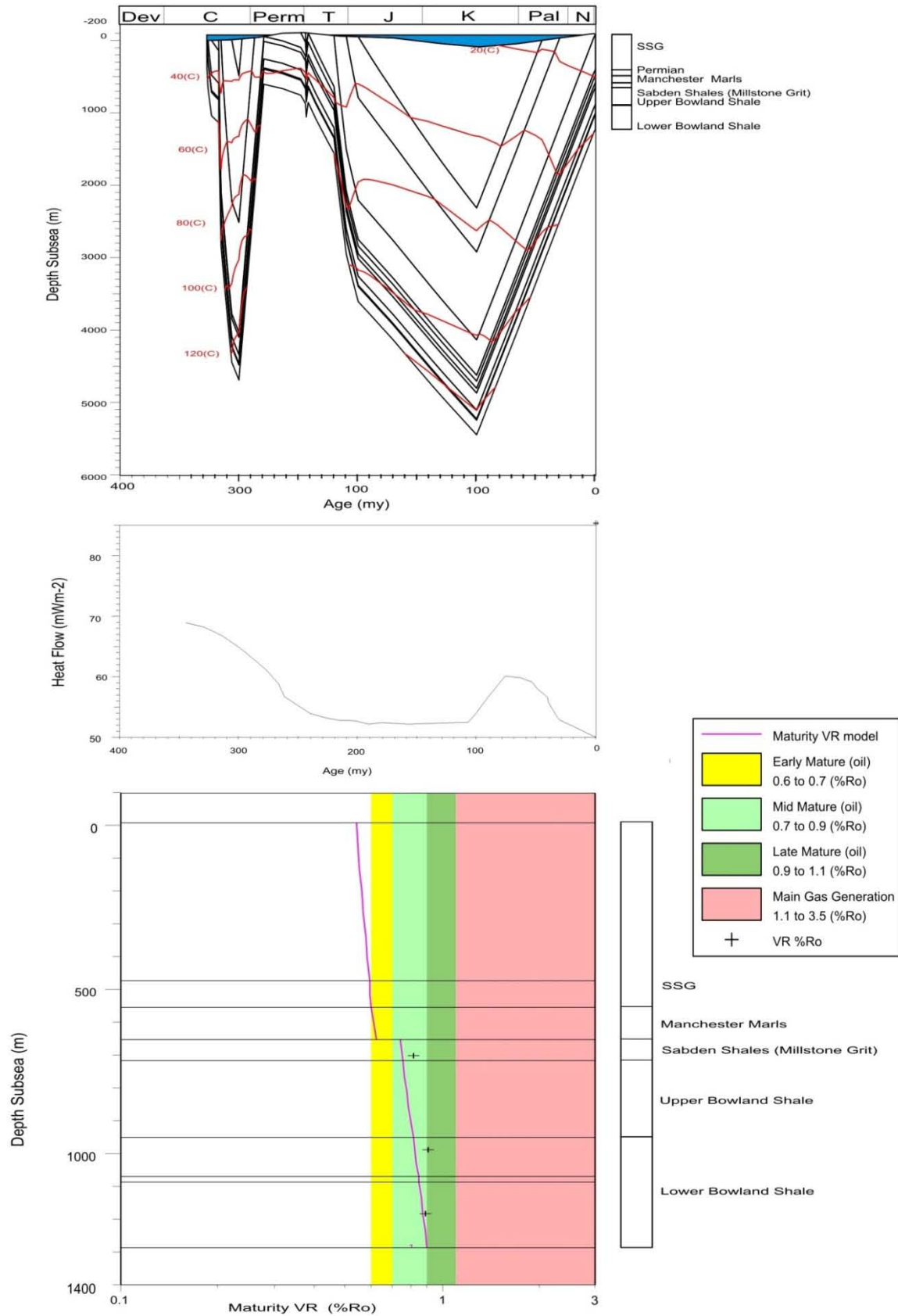
Figure 4. Hesketh model, 4a (top) shows the depositional history, 4b (centre) shows the modelled palaeo-heat flow and 4c (bottom) shows the modelled VR maturity and VR data.
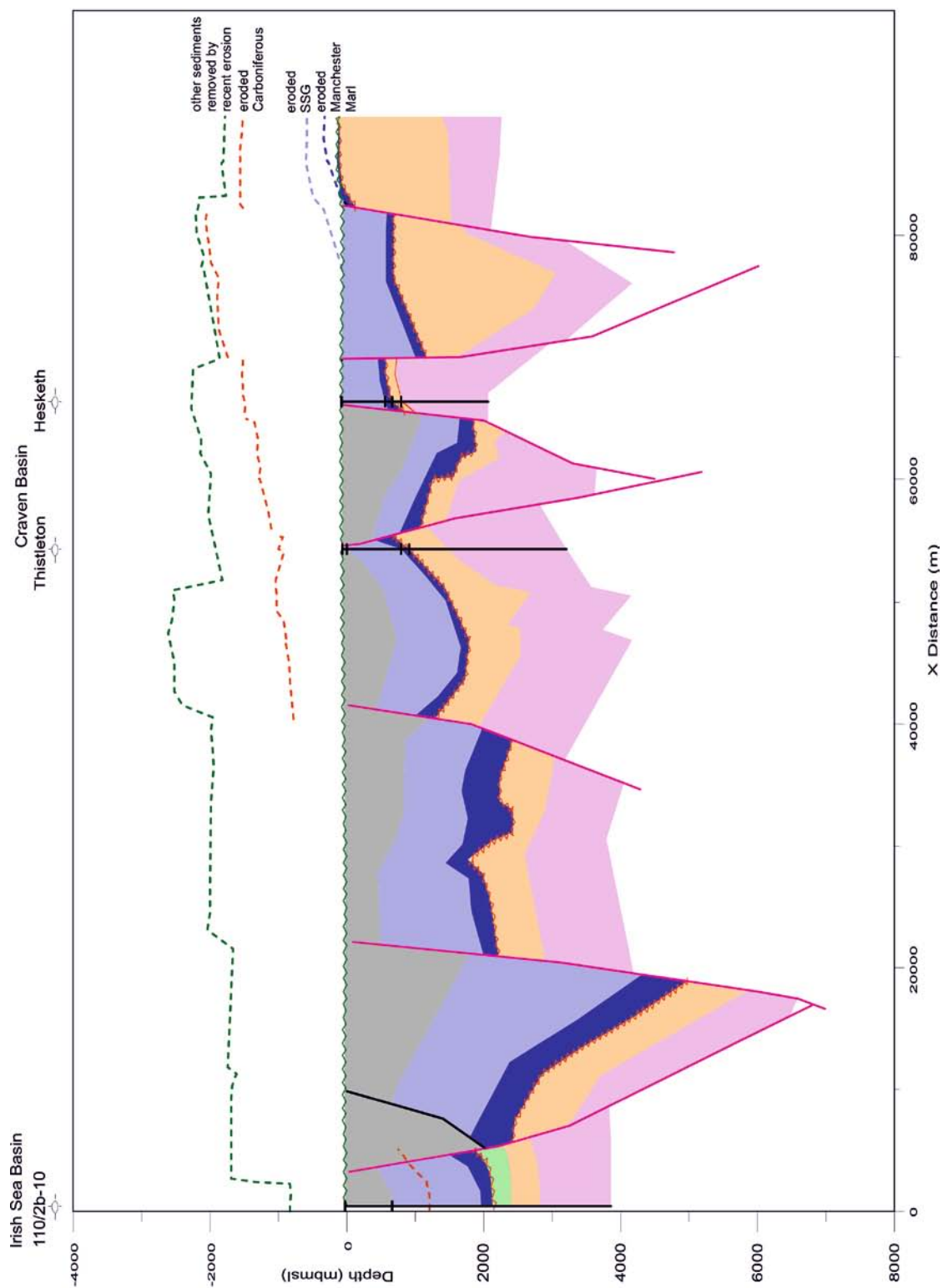
Figure 5. East Irish Sea/Craven Basin 2-D model. Grey is Mercia Mudstone Group, violet is Sherwood Sandstone Group, Dark blue is Manchester Marl, pale green is Westphalian, orange is Millstone Grit, pink is the Bowland-Hodder unit. The dark green unconformity is the current land surface, the red unconformity is the Variscan Unconformity. Dashed lines show eroded thicknesses of strata (the thickness between the unconformity/underlying eroded layer and the dashed line represents the eroded thickness). The bottom of the model is Top Chadian.
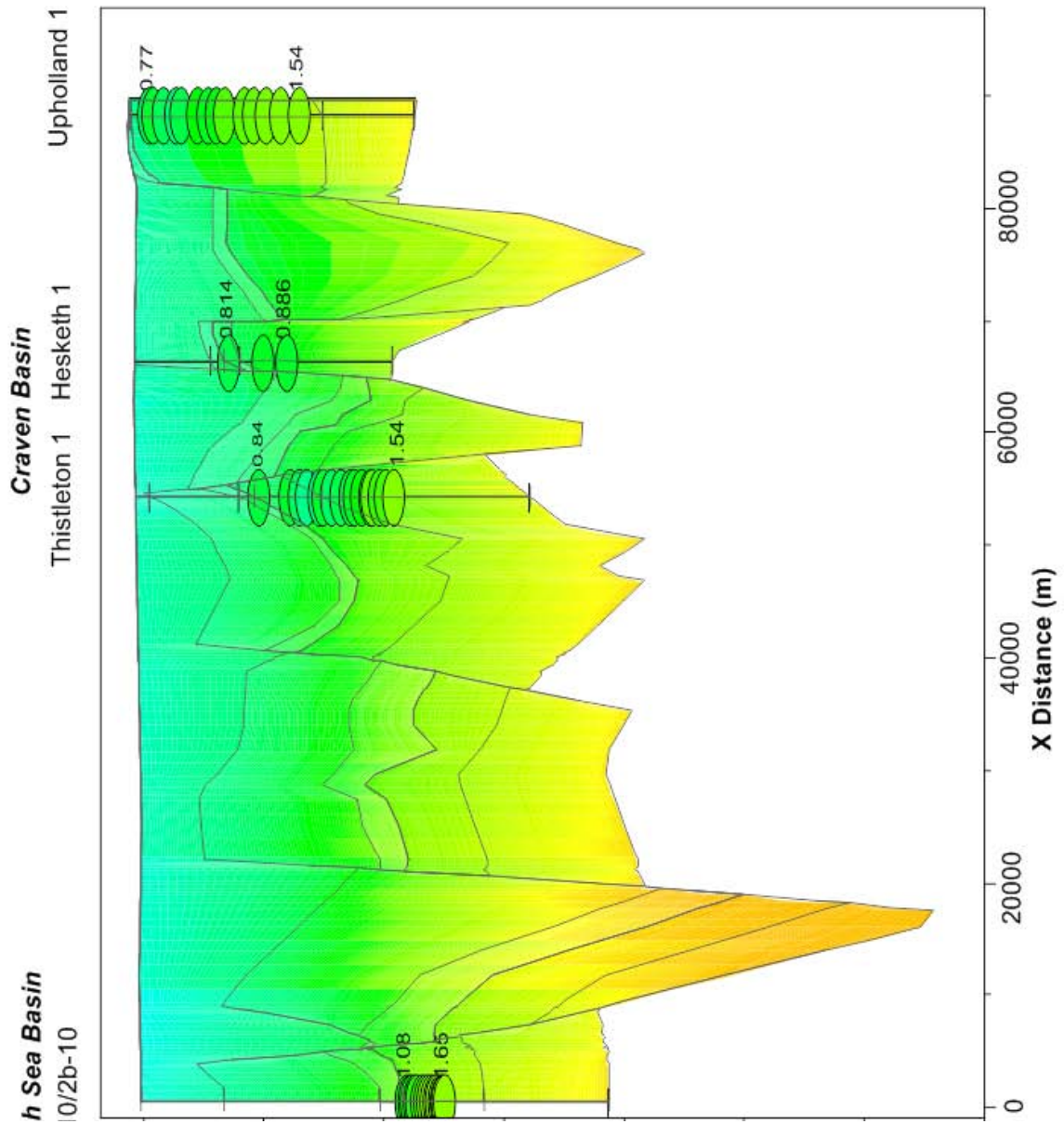
Figure 6. Irish Sea and Craven Basin maturity based on the model is indicated by colour across the whole basin, for comparison, the ovals show the measured VR data at the wells.
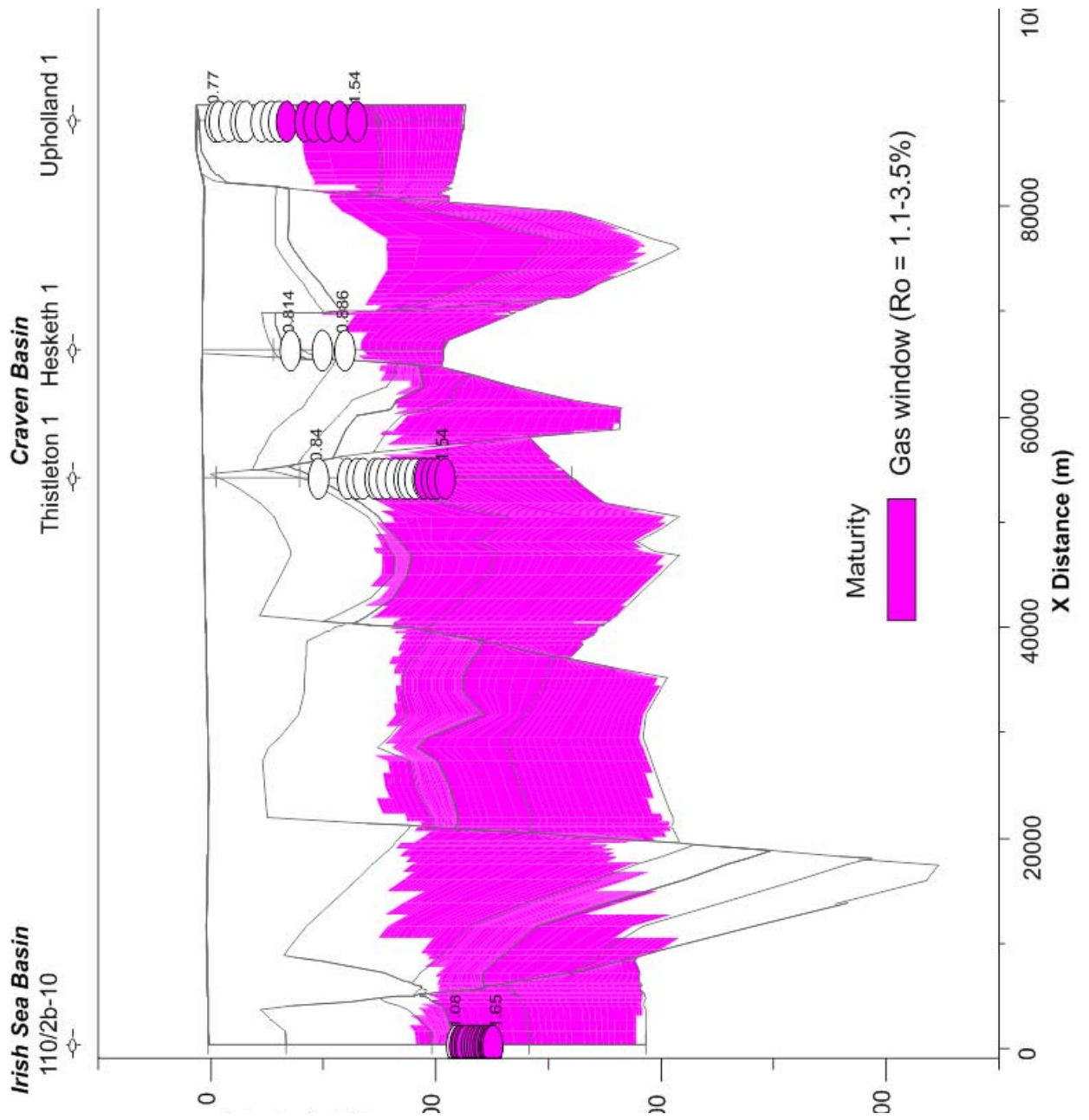
Figure 7. Present day gas window in the Irish Sea and Craven Basin 2-D model
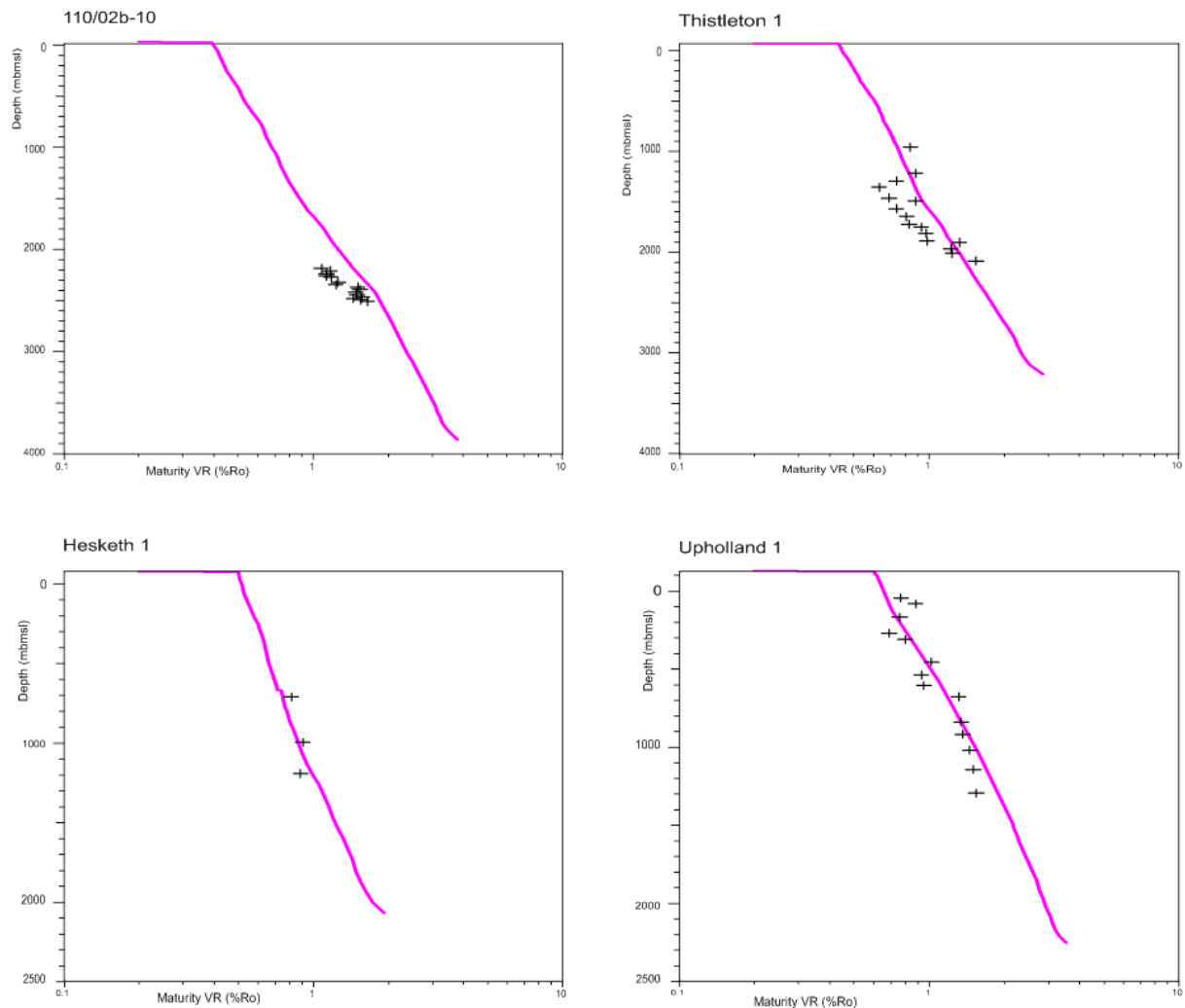
Figure 8. Maturity at well locations across the Irish Sea – Craven Basin 2-D section. The pink line shows model maturity, black crosses show VR data

5.   Cheshire Basin section

5.1 Cheshire Basin geology

During most the Devonian, the Cheshire Basin was a region of erosion. Crustal extension began in the late Devonian and continued through the Visean. During the Early Visean, shallow marine deposition occurred in the north of the Cheshire Basin. Subsidence continued into the Late Visean, during which the whole Cheshire Basin region underwent marine deposition with a deeper marine environment prevailing in the north of the region. This was followed by uplift during early Namurian times when the south of the Cheshire Basin became emergent though the north of the basin remained an area of shallow marine deposition until the late Namurian when a more coastal/deltaic environment prevailed (Aitkenhead *et al.* 2002).

The Cheshire Basin is a half-graben formed as one of a series of sedimentary basins during Permo-Triassic rifting. The Permo-Triassic infill of this basin may have been up to four or five kilometres thick prior to geologically recent erosion. The basin is flanked to the east and west by Carboniferous and older rocks. The succession in this region displays widespread uplift and erosion resulting from the Variscan Orogeny (Plant *et al.* 1999).

5.1.1 Upholland 1

The palaeo-heat flow from a previously modelled borehole (Keele 1) was used as a basis for the heat flow for Upholland 1 as the vitrinite reflectance dataset is more complete (Vincent & Merriman 2002). Pearson & Russell (2000) provided VR data for Westphalian A to Pendleian age strata from the Upholland borehole. Stratigraphical data from Plant *et al.* (1999) were used to model the eroded stratigraphy. The VR data were then used to calibrate the model and the heat flow history was assumed to follow a similar pattern to that at Keele 1. Coal Measures in the Westphalian are algal-rich, which may have caused suppression of the VR values and therefore account for the slight difference between the model maturity curve and maturity data points in the Carboniferous coals of Upholland 1 (Figure 9c).

The Upholland 1-D model indicates approximately 800 m of sediment was removed during the Variscan uplift and 50 m during the Hardegsen event (Figure 9a), which agrees with thicknesses estimated in Plant *et al.* (1999). Permo-Triassic cover was calculated to be around 900 m, with a further 500 m deposited during the Jurassic and Cretaceous. The heat flow and temperatures reached are slightly lower than in the centre of the Cheshire Basin; this model shows heat flow of up to 73mWm^{-2} during the early Carboniferous, with temperatures of around 120°C in the Westphalian A coals, and slightly lower temperatures achieved on reaching a depth of about 2 km during the Cretaceous (Figure 9a and b). These results are fairly well constrained by the VR data. Figure 9c indicates that the Coal Measures reached the oil generation window.

5.1.2 Ince Marshes 1

Ince Marshes 1 lies between Knutsford 1 and Blacon East 1 in terms of proximity to the depocentre of the Cheshire Basin. It penetrates the Upper Bowland Shale (Figure 10a). The model achieved a reasonable fit to the data with an estimated 190 m additional Carboniferous strata added then eroded during the Variscan Orogeny and over 1 km of Permian – Triassic strata and 500 m of Jurassic to Cretaceous strata added then eroded during the Hardegsen and Palaeocene – Recent erosion. Model heat flow is shown in Figure 10b. Based on this model, the Upper Bowland Shale reached temperatures over 100°C during Carboniferous burial, and 120°C during deeper Cretaceous burial (Figure 10a), following a similar pattern to Knutsford 1. According to the model, both the Coal Measures and the Upper Bowland Shale reached the oil generation window (Figure 10c) from the Carboniferous onwards.
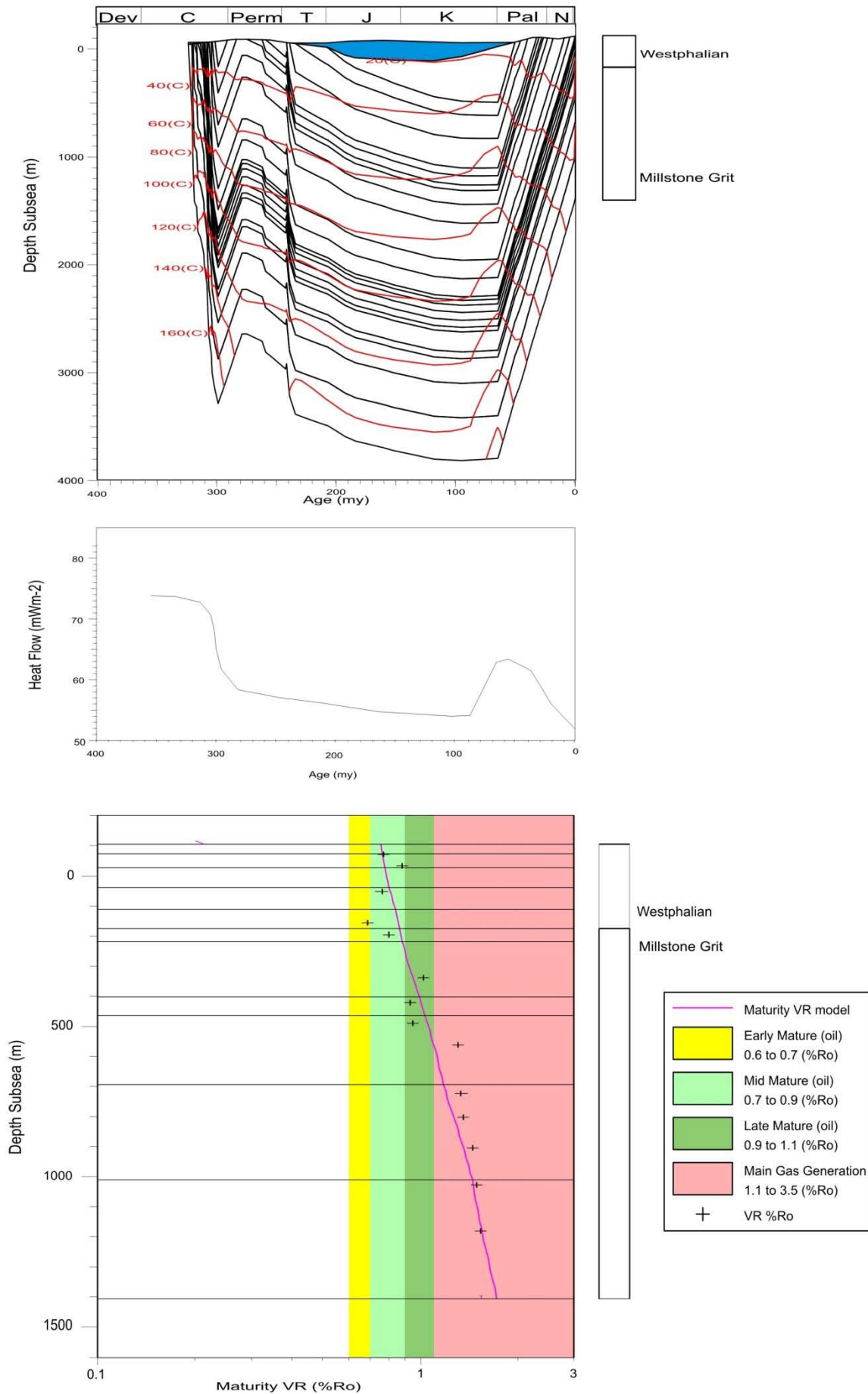
Figure 9. Upholland 1 model, 9a (top) shows the depositional history, 9b (centre) shows the modelled palaeo-heat flow and 9c (bottom) shows the modelled VR maturity and VR data.
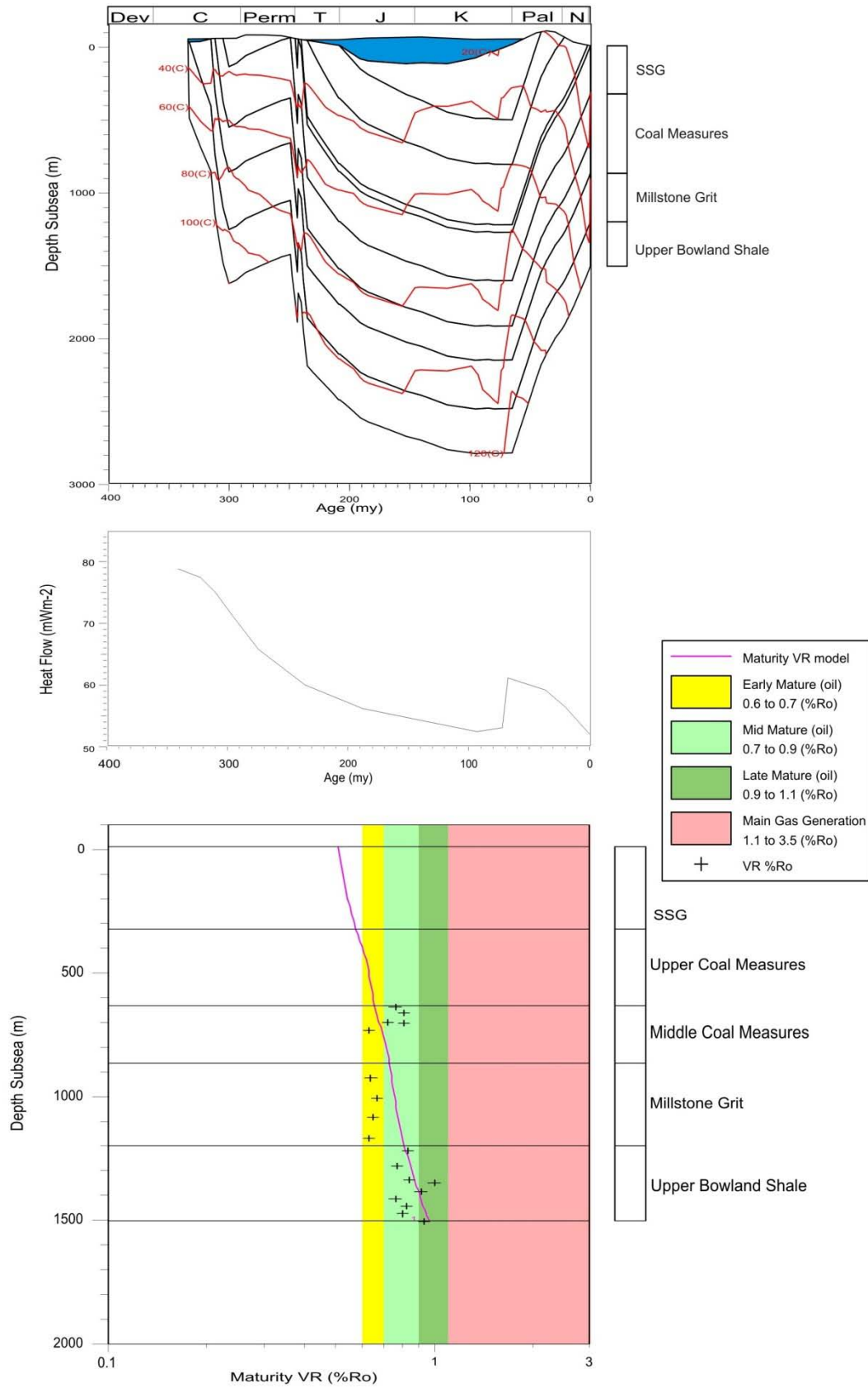
Figure 10. Ince Marshes 1 model, 10a (top) shows the depositional history, 10b (centre) shows the modelled palaeo-heat flow and 10c (bottom) shows the modelled VR maturity and VR data.

5.1.3 Knutsford 1

Limited vitrinite reflectance data are available in Pearson & Russell (2000) for the Knutsford 1 borehole. Porosity data from Plant *et al.* (1999) was also used. Borehole temperature data is also available in Burley *et al.* (1984). Lewis *et al.* (1992) provided AFTA data from the Westphalian, Permian and Triassic. Following the findings in Plant *et al.* (1999), fluid circulation in the basin was included in the model, using the '2-D fluid flow' and 'delta heat' options in BasinMod. '2-D fluid flow' assumes fluid flows through the borehole and surrounding area rather than a closed system with fluid circulation contained within the borehole. It was assumed that most circulation occurred in the porous Permo-Triassic sandstones during the Palaeogene. Borehole data were taken from records held in the NGRC at BGS Keyworth, and the eroded stratigraphy was estimated using information in Plant *et al.* (1999). These data were then used to develop a best-fit model.

The Knutsford 1-D model (Figure 11a) shows a different burial history from that of Keele 1 and Upholland 1, with highest temperatures achieved during the Cretaceous. The model implies removal of approximately 500 m of Carboniferous sediment during Variscan uplift, with deposition recommencing with the Sherwood Sandstone (Figure 11a). An estimated 50 m of overburden was also removed during the Hardegsen event. The model palaeo-heat flow peaked at 78 mWm^{-2} during the late Carboniferous (Figure 11b), with the Westphalian C coals reaching temperatures of around 60°C during the Westphalian and 160°C during Cretaceous/Palaeogene burial. Model calculations imply that late Cretaceous burial beneath 2.8 km of Permo-Triassic strata, with a further 1 km of Jurassic and Cretaceous strata, resulted in these coals experiencing burial of around 4 km and temperatures of 140°C. Figure 11c indicates that the Coal Measures reached the oil generation window during the Triassic and the gas generation window during the Cretaceous.

5.1.4 Blacon East 1

Blacon East 1 is located away from the main Cheshire Basin depocentre and Permo-Triassic sediment thicknesses are therefore thinner than at Knutsford 1. Eroded sediment thicknesses were estimated using Plant *et al.* (1999).

Limited VR data were available for Blacon East 1. The model implies removal of c.600 m of Carboniferous sediment during Variscan uplift, with deposition recommencing with the Sherwood Sandstone (Figure 12a). An estimated 50 m of overburden was also removed during the Hardegsen event. The model palaeo-heat flow peaked at 78 mWm^{-2} during the late Carboniferous (Figure 12b), with the deepest Bowland Shale sediments achieving temperatures of 160°C. Model calculations imply that late Cretaceous burial beneath 220 m of Permo-Triassic strata, with a further 200 m of Triassic, Jurassic and Cretaceous strata, resulted in these coals experiencing burial of around 1.5 km and temperatures of 140°C. Figure 12c indicates that the Bowland Shale reached the gas generation window during the Carboniferous.
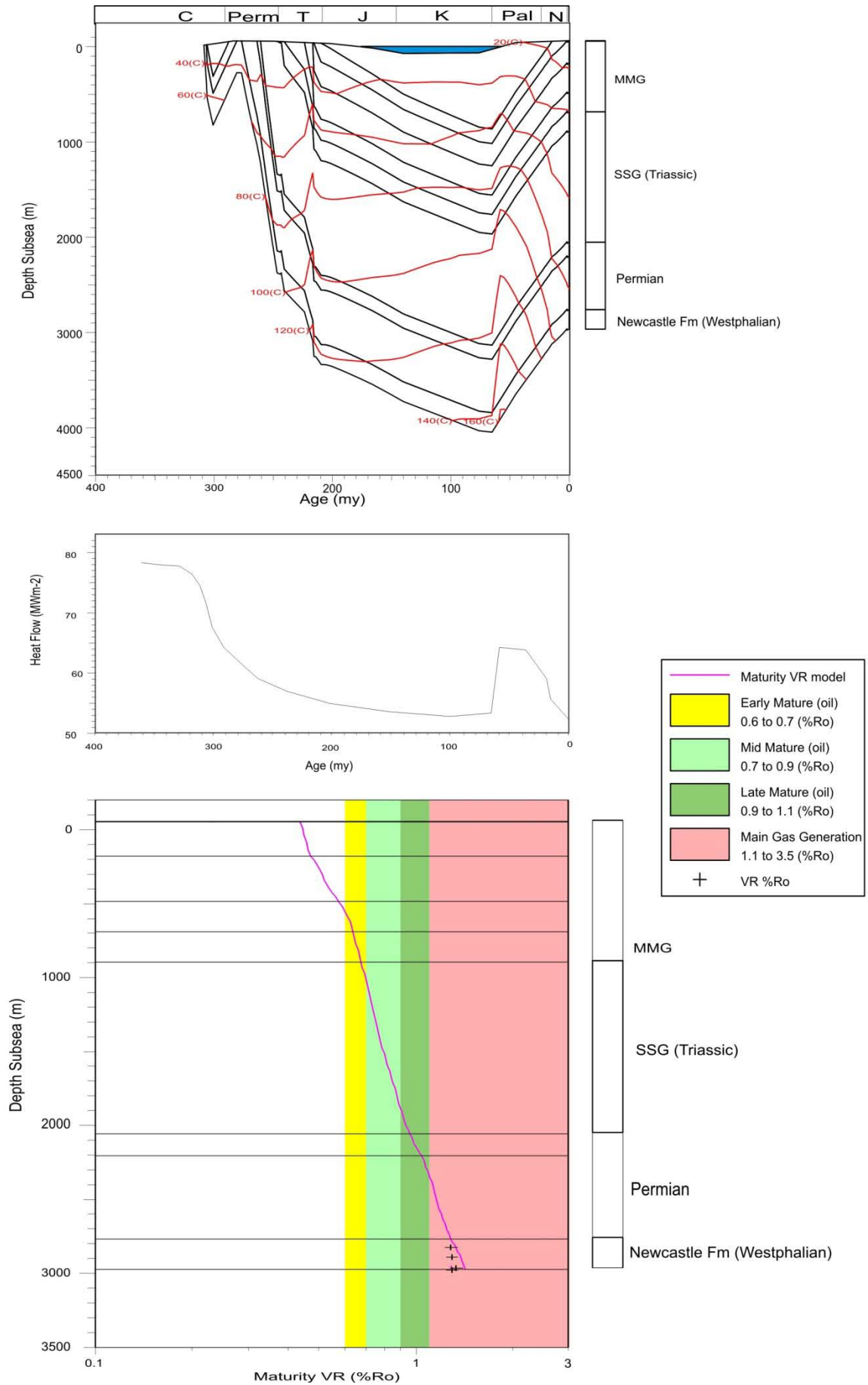
Figure 11. Knutford model, 11a (top) shows the depositional history, 11b (centre) shows the modelled palaeo-heat flow and 11c (bottom) shows the modelled VR maturity and VR data.
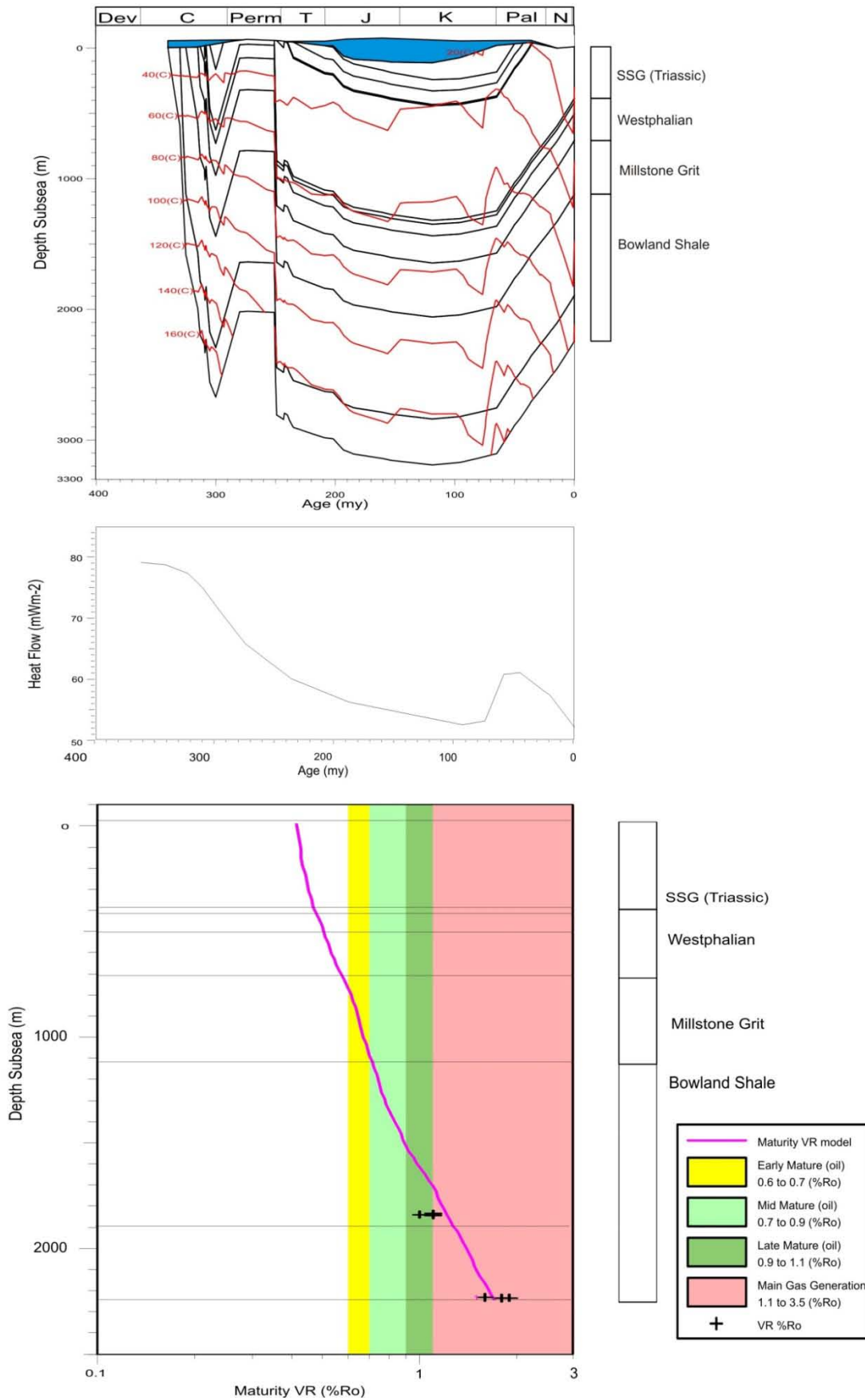
Figure 12. Blacon East 1 model, 12a (top) shows the depositional history, 12b (centre) shows the modelled palaeo-heat flow and 12c (bottom) shows the modelled VR maturity and VR data.
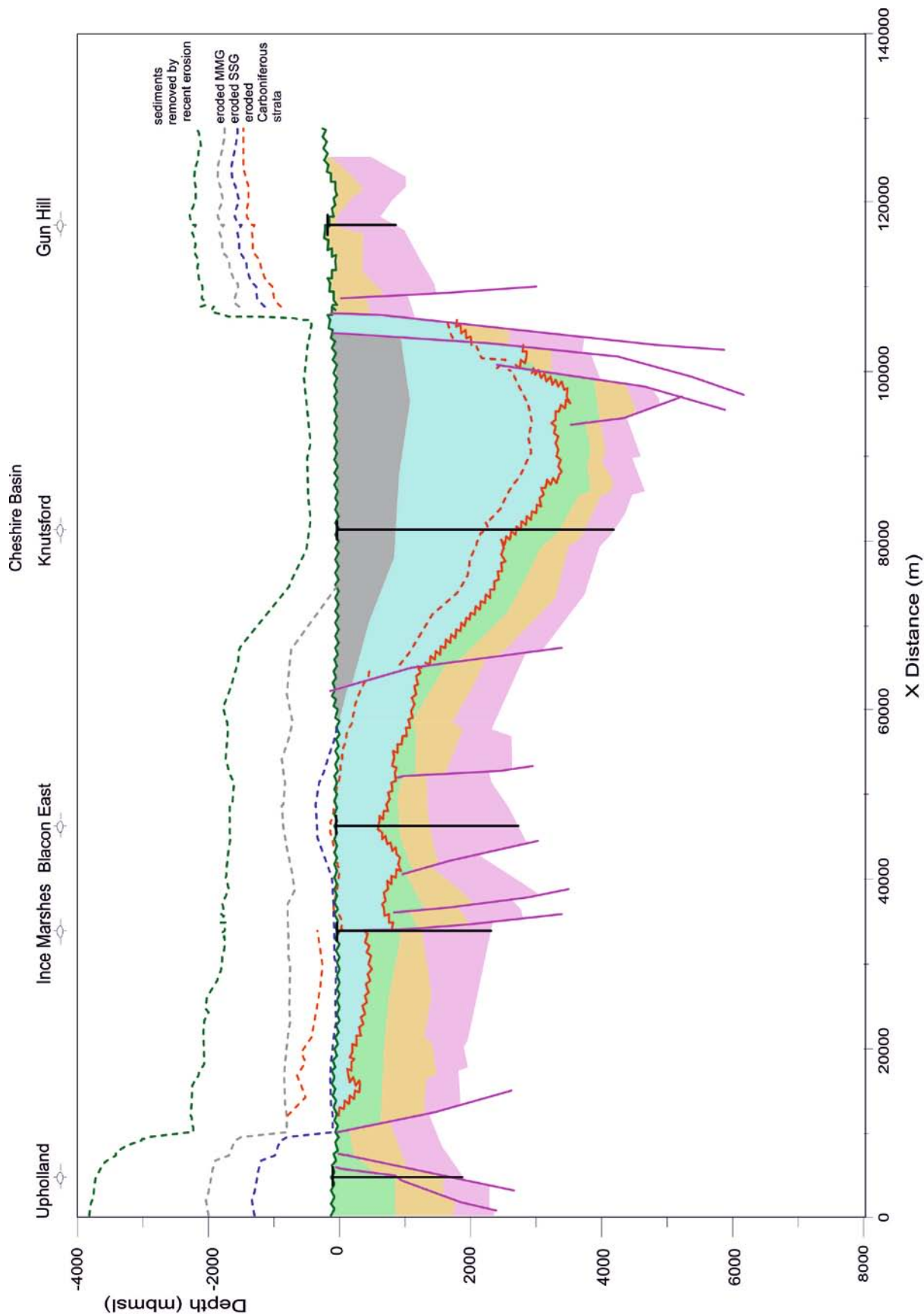
Figure 13. Cheshire Basin 2-D model. Grey is Mercia Mudstone Group, blue is Sherwood Sandstone Group and Permian, green is Westphalian, orange is Millstone Grit, pink is the Bowland-Hodder unit. The green unconformity is the current land surface, the red unconformity is the Variscan Unconformity. Dashed lines show eroded thicknesses of strata (the thickness between the unconformity/underlying eroded layer and the dashed line represents the eroded thickness). The base of the model is top Chadian.
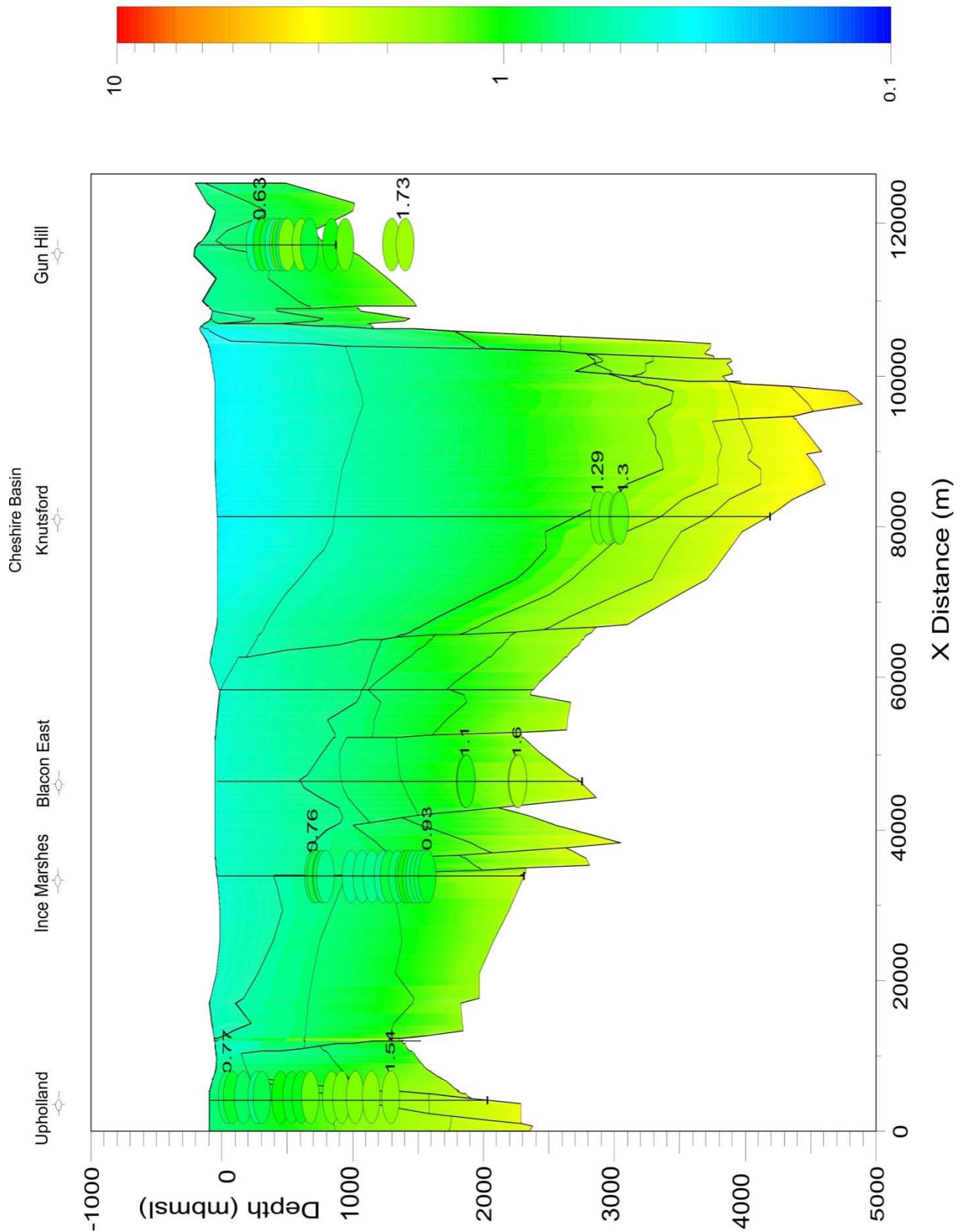
Figure 14. Maturity based on the model is indicated by colour across the whole basin, for comparison, the ovals show the VR data at the wells.
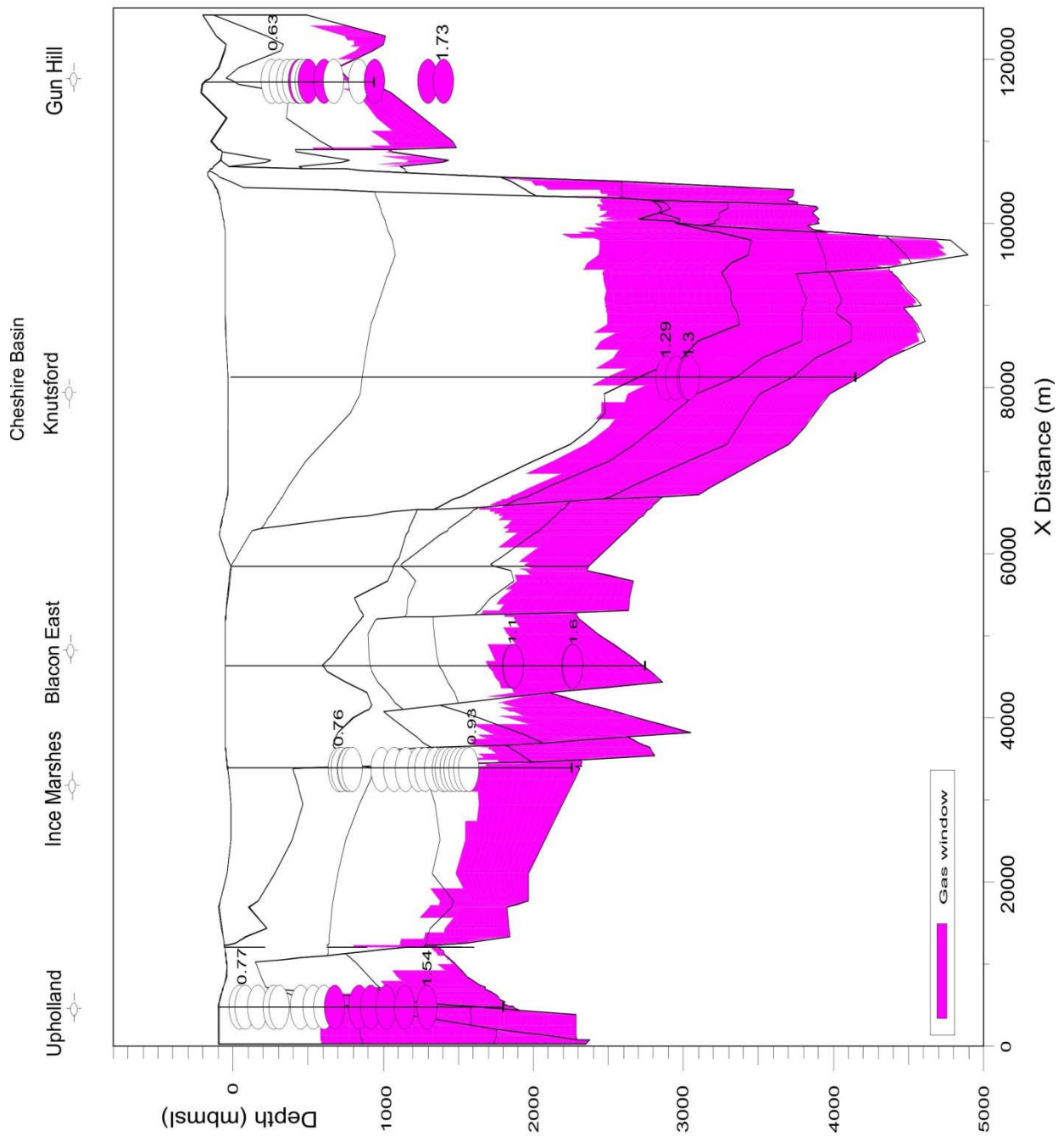
Figure 15. Present day gas window for the Cheshire Basin 2-D section
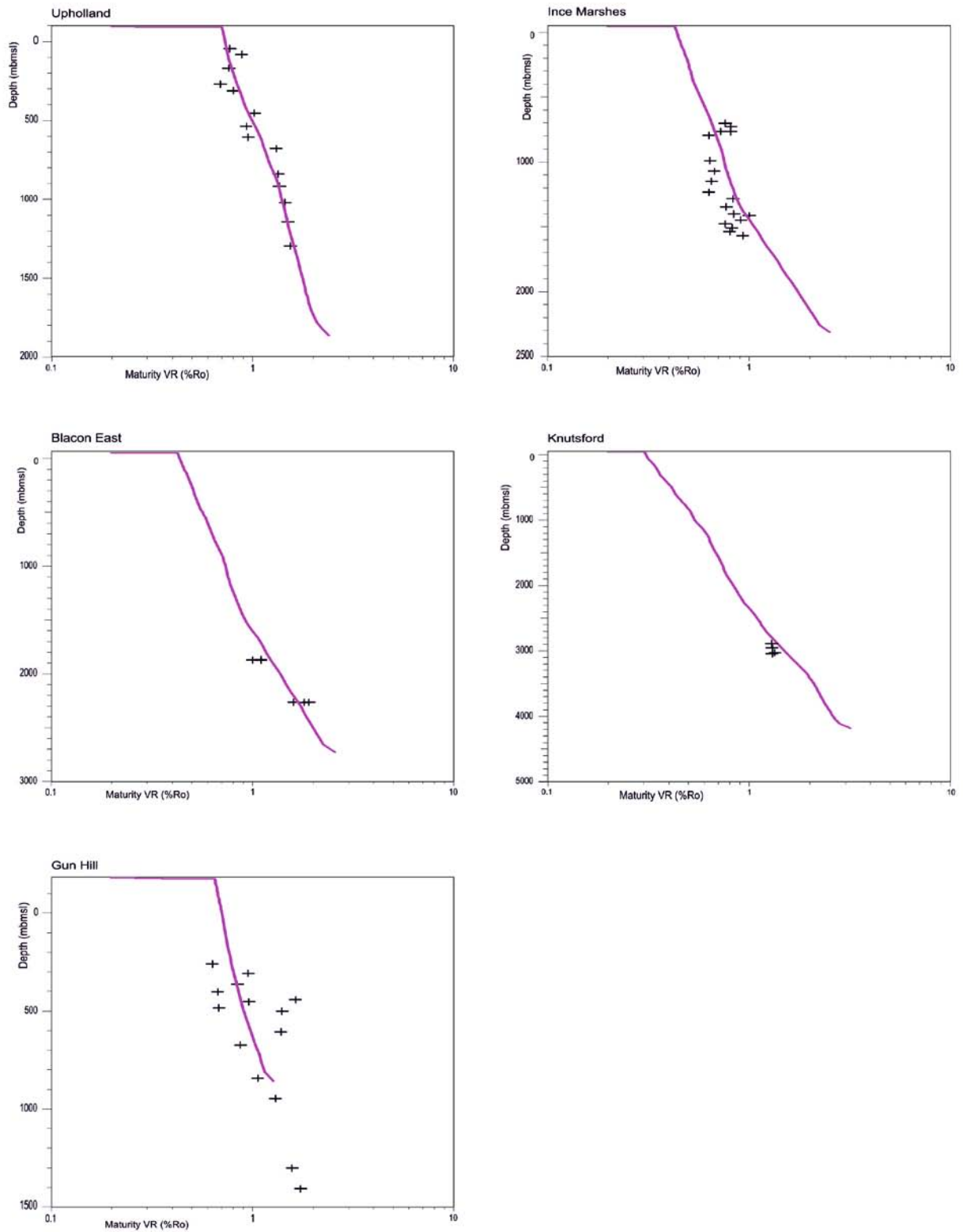
Figure 16. Maturity from the Cheshire Basin 2-D model at the borehole locations across the basin. The pink line shows the model maturity, the black crosses show the VR data

5.1.5 2-D section

Figure *13* and Figure 14 show the 2-D model which was generated for the Cheshire Basin section using the 1-D models as a basis.

Figure 13 shows the current sediment thicknesses across the basin as interpreted from seismic data. A good match to the data was obtained (Figure 14 and Figure 16) given the limitations on entering eroded thicknesses as described in section 2; i.e. that the eroded Carboniferous thickness has been added to the eroded thickness of sediment removed by the latest erosion and the time for the start of this combined erosion was given as the end Carboniferous (Figure *13*). The model indicates that much of the Bowland-Hodder unit of Arundian to Pendleian age is in the gas generation window

6.   Widmerpool Gulf – Gainsborough Trough

6.1 Widmerpool Gulf geology

The Bowland Shale is thick in this region, with over 2 km predicted by seismic interpretation (Pharaoh *et al.* 2011). In North Staffordshire, the Millstone Grit shows rhythmic deposition in a deltaic environment and has a recorded thickness of around 1055 m in boreholes in the Widmerpool Gulf. Deposition began in the Marsdenian in South Staffordshire and Widmerpool Gulf became a depocentre for Millstone Grit during the Marsdenian. To the north of the region, the Millstone Grit was more argillaceous. Westphalian Lower and Middle Coal Measures have a recorded thickness of up to 1220 m in North Staffordshire, with Westphalian A sediments being particularly well developed. The oldest Lower Coal Measures are found in the northern part of the region. North Staffordshire coalfields show the maximum development of Upper Coal Measures and Warwickshire Group, including around 335 m Upper Coal Measures and 1320 – 1412 m Warwickshire Group sediments (Hains & Horton 1969).

In this region, the total estimated thickness of the Sherwood Sandstone Group (SSG) varies widely and reaches a maximum thickness in the Cheshire Basin of around 2621 m (Plant *et al.* 1999). Between 30 – 152 m of overlying Mercia Mudstone Group (MMG) has been recorded and around 15 m of Rhaetic sediments occur near East Leake. Jurassic sediments 352 – 527 m thick have been recorded in boreholes and outcrops in this region (Nottinghamshire and the Midlands; Hains & Horton 1969).

In Derbyshire, there are volcanic rocks of Brigantian age and Tertiary intrusions are recorded in Cheshire and Shropshire (Hains & Horton 1969).
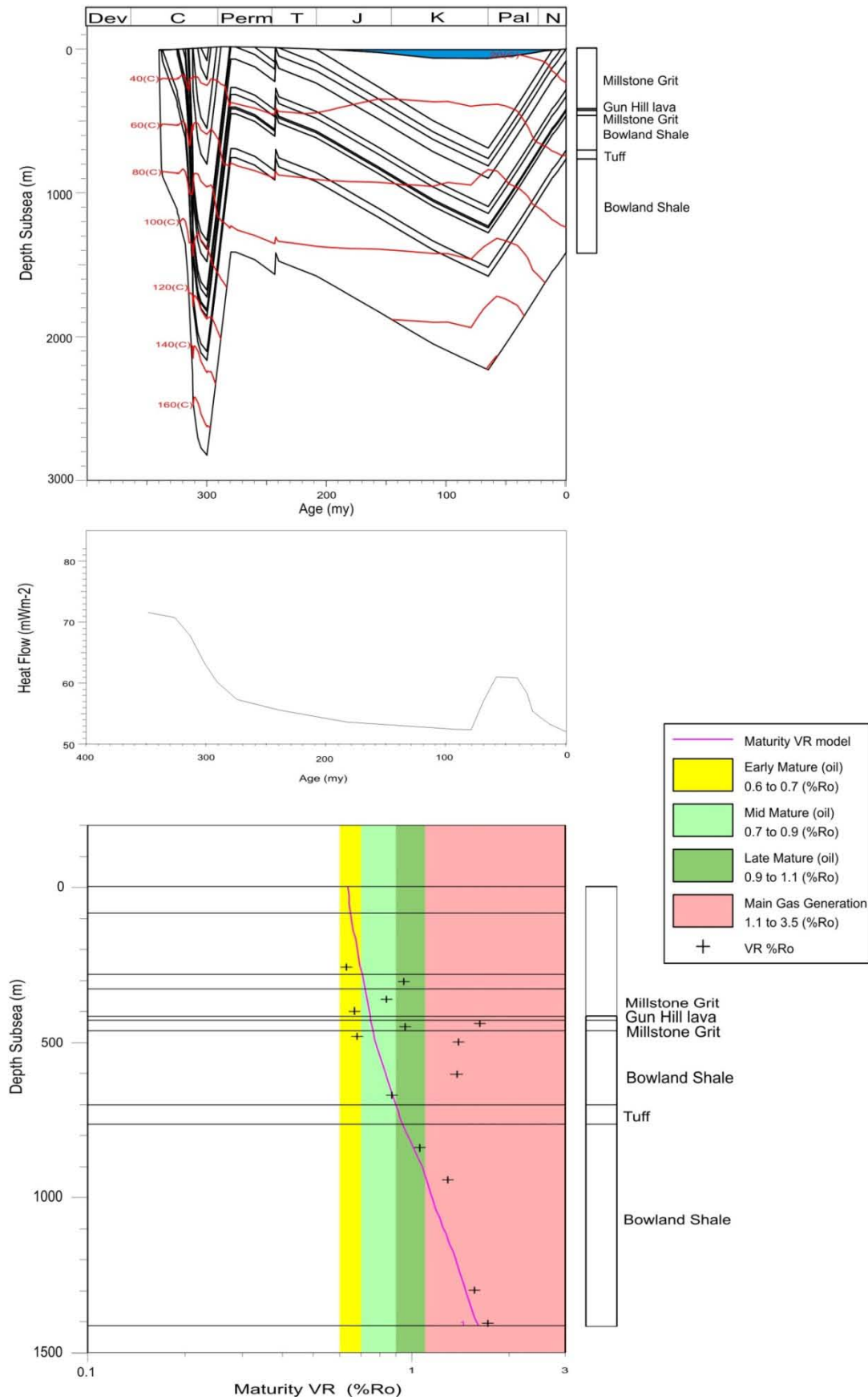
Figure 17. Gun Hill model, 17a (top) shows the depositional history, 17b (centre) shows the modelled palaeo-heat flow and 17c (bottom) shows the modelled VR maturity and VR data.

6.1.1 Gun Hill 1

The Gun Hill 1 borehole shows rapid deposition of thick Carboniferous sequences, with the oldest Bowland Shale reaching temperatures of 160°C (Figure 17a). The model implies removal of approximately 1320 m of Carboniferous sediment during Variscan uplift. The model palaeo-heat flow peaked at 70 mWm^{-2} during the late Carboniferous (Figure 17b). Model calculations imply that late Cretaceous burial beneath 180 m of Permo-Triassic strata, with a further 600 m of Jurassic and Cretaceous strata resulted in temperatures of 120°C in the Bowland Shale.

The VR data indicate that the Bowland Shale reached the gas generation window. Erosion occurred during the Triassic (Hardegsen) and Palaeocene - Recent times exposing Millstone Grit at the surface. The model indicates that the Bowland Shale reached the gas generation window during the Carboniferous (Figure 17c).

The fit of the model to the data may also be influenced by the Gun Hill lava, as the additional heat would have affected the VR readings of layers immediately underneath. In Figure 17c, a high VR reading is recorded immediately underneath the lava flow.

6.1.2 Long Eaton 1

The Long Eaton 1 borehole shows Triassic sediments deposited unconformably on the Widmerpool and Long Eaton Formations of Asbian to Chadian age (Craven Group). These sediments reached maximum depths of burial of around 3 km (Figure 18a) according to the model. The model was constructed with an estimated additional 890 m of Carboniferous sediments removed during erosion associated with the Variscan Orogeny. This was followed by deposition of around 170 m of Permo-Triassic and 340 m of Jurassic – Cretaceous. As there are very few VR data, the heat flow profile from nearby Gun Hill 1 was used as a basis for this model. The model implies that the deepest Craven Group sediments reached the gas generation window and achieved temperatures of up to 200°C during Carboniferous burial.

Given the lack of VR data for this borehole (8 VR data within a very narrow depth range, see Figure 18c) and the fact that this borehole is located in the depocentre of the Widmerpool Gulf, it seems likely that these eroded sediment thicknesses are rather underestimated and confidence in the results of this 1-D model is low.

6.1.3 Ilkeston 1

The Ilkeston 1 borehole penetrates sediments of Westphalian A and Namurian (Yeadonian – Arnsbergian) age (Figure 19a). The model implies that an estimated 600 m of Carboniferous strata were removed during Variscan uplift and erosion. This was followed by deposition of Permo-Triassic sediments, with a modelled thickness of 540 m and Jurassic – Cretaceous sediments with a modelled thickness of 510 m. Limited VR data were available for Ilkeston 1 and the heat flow from Gun Hill 1 formed the basis for this model. The model implies the deepest Bowland Shale sediments achieved temperatures of 120°C during Carboniferous burial (Figure 19a). Figure 19c indicates that the Bowland Shale reached the early oil generation window during the Carboniferous.

Very few VR data are available, so this model should be used with caution; however, the depth of burial seems reasonable for the location (near to the margin of the Widmerpool Trough). It should also be noted that the VR readings are taken from sediments below a fault shown on the borehole log and the data may not give an accurate indication of maturity for this borehole if the rocks have been significantly displaced in depth.
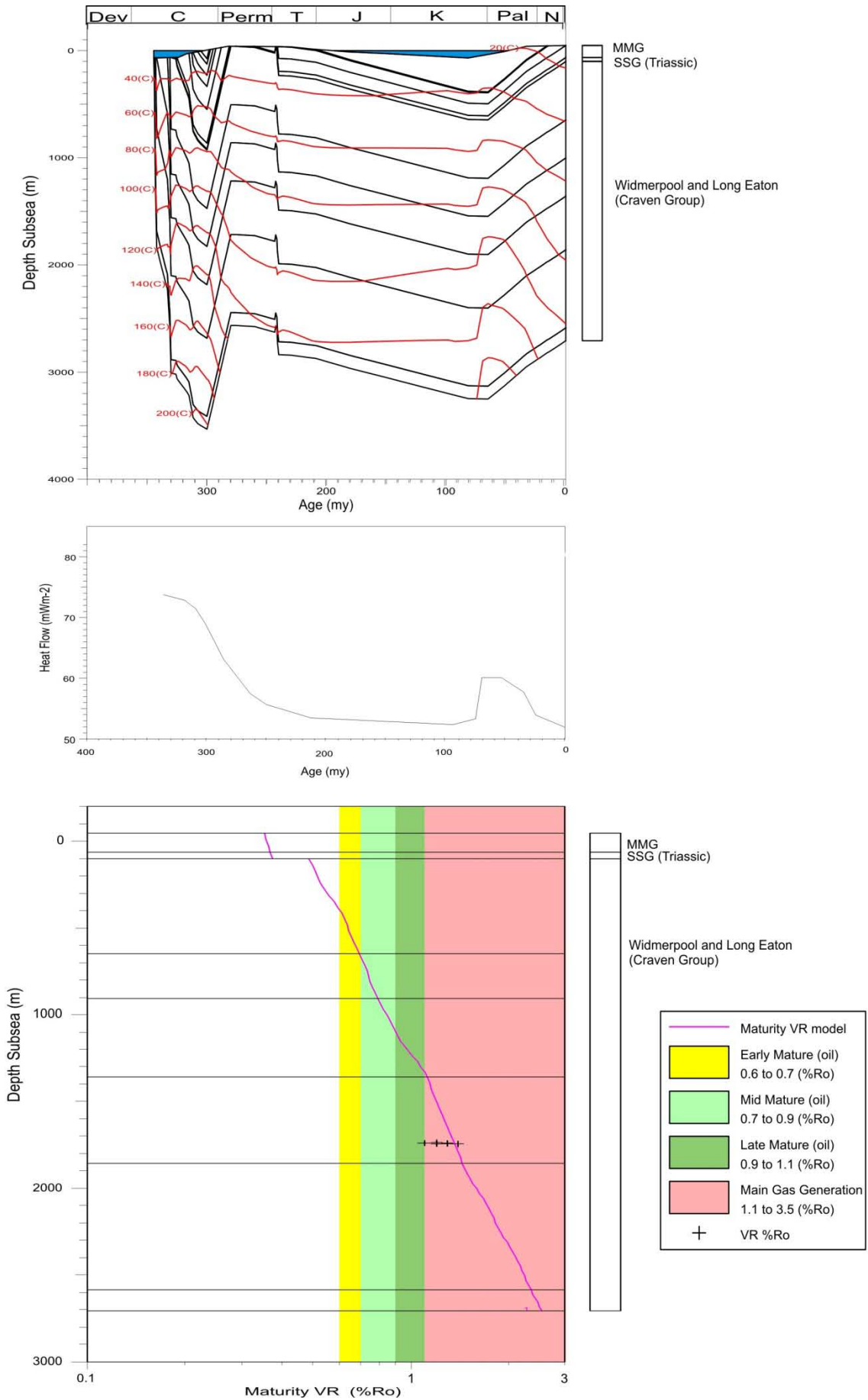
Figure 18. Long Eaton model, 18a (top) shows the depositional history, 18b (centre) shows the modelled palaeo-heat flow and 18c (bottom) shows the modelled VR maturity and VR data.
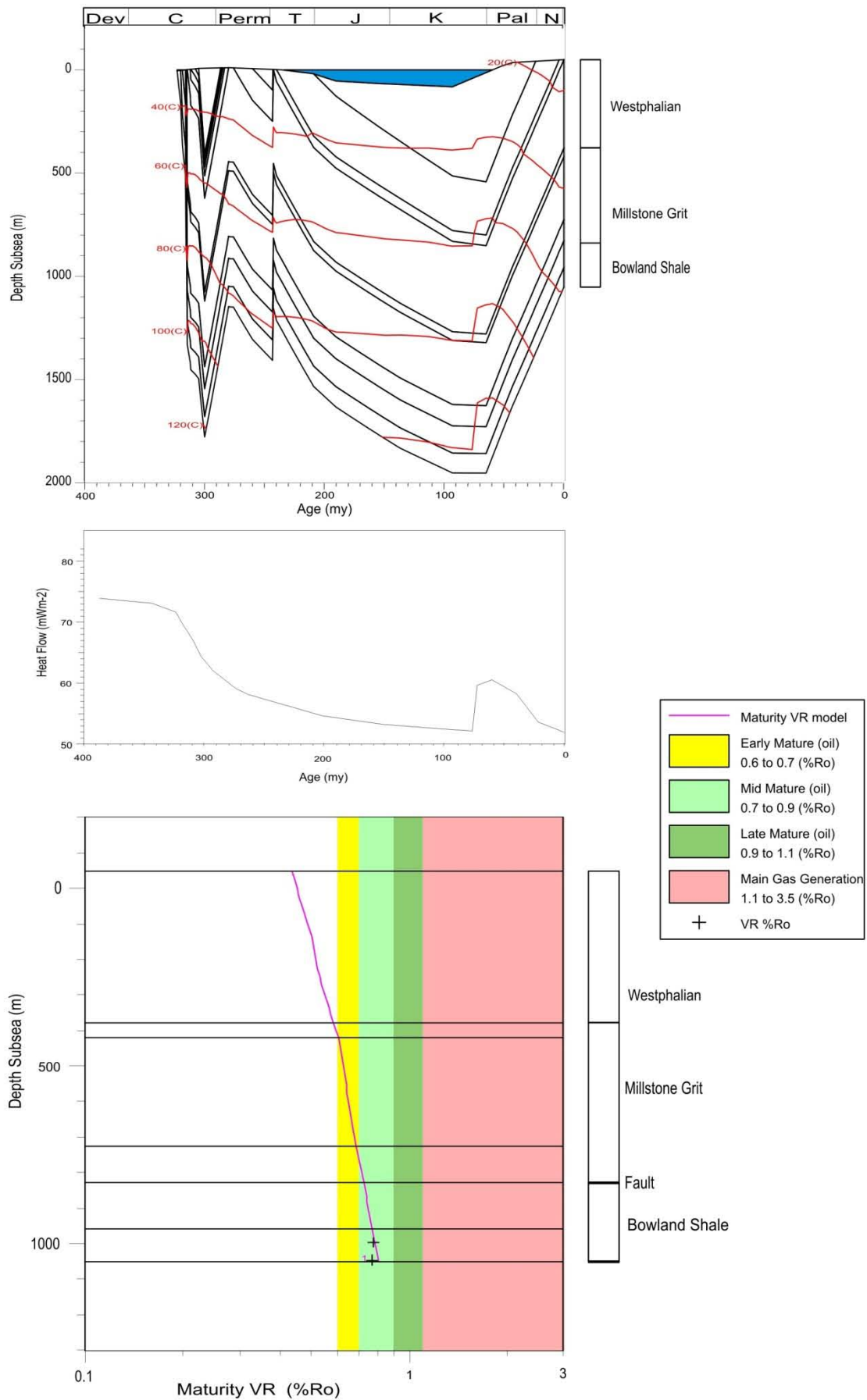
Figure 19. Ilkeston model, 19a (top) shows the depositional history, 19b (centre) shows the modelled palaeo-heat flow and 19c (bottom) shows the modelled VR maturity and VR data.

6.2 Gainsborough Trough geology

The Bowland Shale was deposited in shallowing marine condition, with deep marine conditions during the early Visean and shallow marine conditions during the late Visean. This was followed by deposition of shallow marine/deltaic sediments during the Namurian and Westphalian. Following uplift during the Variscan Orogeny, this region again subsided through the Permian to become fully marine during the Jurassic and Cretaceous. Recent uplift has exposed Permian and Carboniferous rocks in this region.

Recorded thicknesses of Coal Measures are up to 2200 m and the Warwickshire Group reaches thicknesses of up to 140 m east of the Pennine High. Permian sediments in this region are around 88 – 158 m thick, Triassic Sherwood Sandstone Group sediments are around 400 m thick and Mercia Mudstone Group sediments are up to 190 m thick (Aitkenhead *et al.* 2002).

Volcanic activity occurred to the south during latest Namurian times.

The Grove 3 borehole has a heat flow of 54 mWm^{-2} (Downing & Gray 1986), however, other boreholes in this trough such as Ranby 1 and Scaftworth B2 have higher present day heat flows (75 to 83 mWm^{-2}) (Downing & Gray 1986).

Overall, the VR data for the Gainsborough Trough are not as satisfactory as for the other regions modelled for this report. There are very limited data for Grove 3 and the data for Gainsborough 2 and Kirk Smeaton 1 show a broad scatter. Thus confidence in the models is lower than for models previously described. However, it should be noted that a significant number of the VR data for Kirk Smeaton 1 and the VR data for Grove 3 are all in the gas generation window.

6.2.1 Grove 3

Grove 3 penetrates sediments of Permo-Triassic age resting unconformably on sediments of Westphalian C age (Figure 20a). The oldest sediments are Bowland Shales of Courceyan age and the well terminated in Early Palaeozoic phyllites. The model implies deposition and subsequent removal of 900 m of Carboniferous sediment. The deepest Bowland Shale sediments reached temperatures of over 180°C during Carboniferous burial and again during Cretaceous burial. Over 350 m of Permian sediments are recorded in the borehole. An estimated eroded thickness of 1200 m of Permian – Cretaceous sediments was also included in the model. The oldest Bowland Shale in the borehole reached the gas generation window during the Carboniferous.

It should be noted that only 1 VR data point was available, so confidence in this model is low and much of the heat flow model was based on Gainsborough 2 and Kirk Smeaton 1 which have more complete VR datasets (Figure 20c).
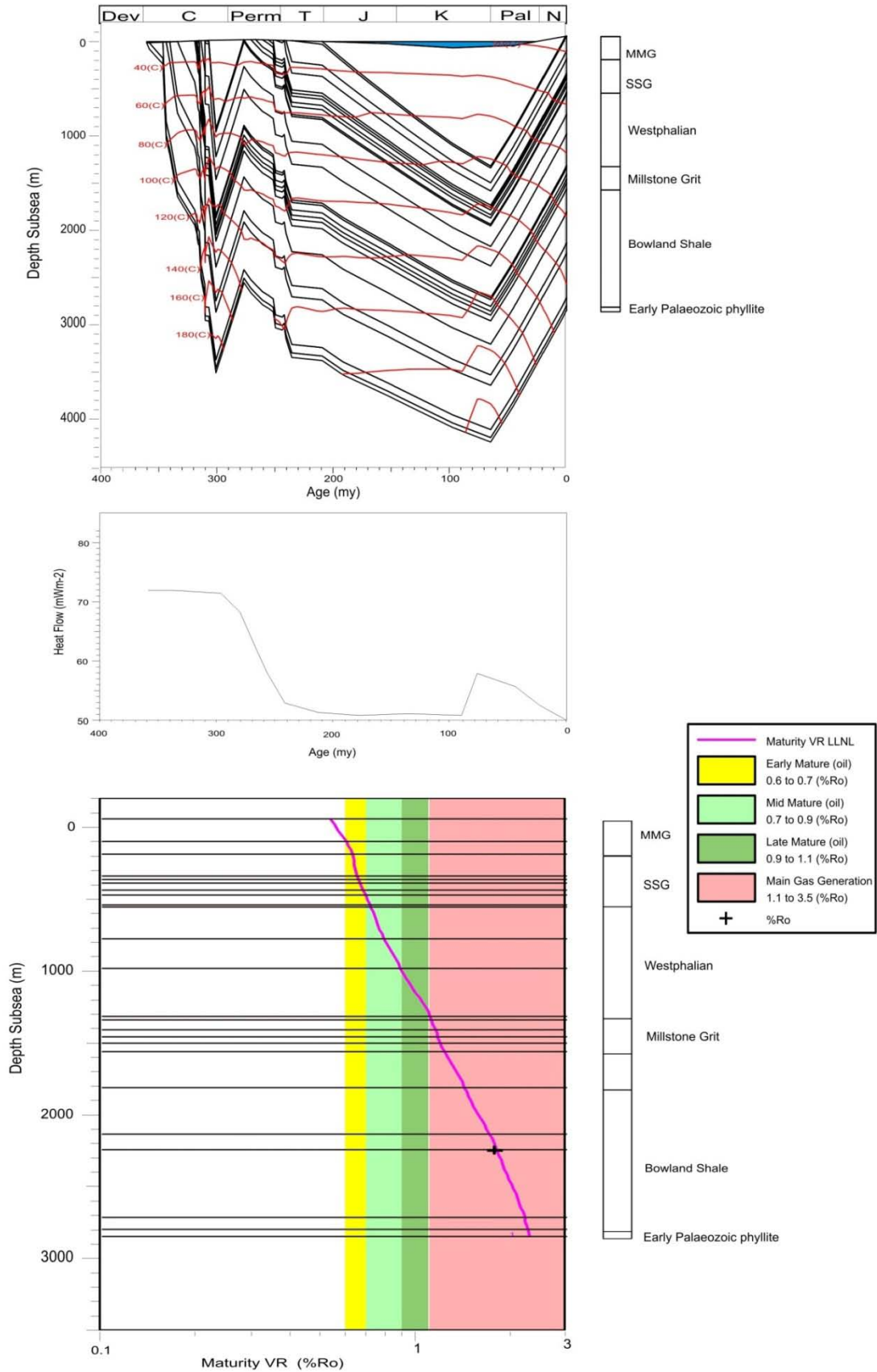
Figure 20. Grove 3 model, 20a (top) shows the depositional history, 20b (centre) shows the modelled palaeo-heat flow and 20c (bottom) shows the modelled VR maturity and VR data.
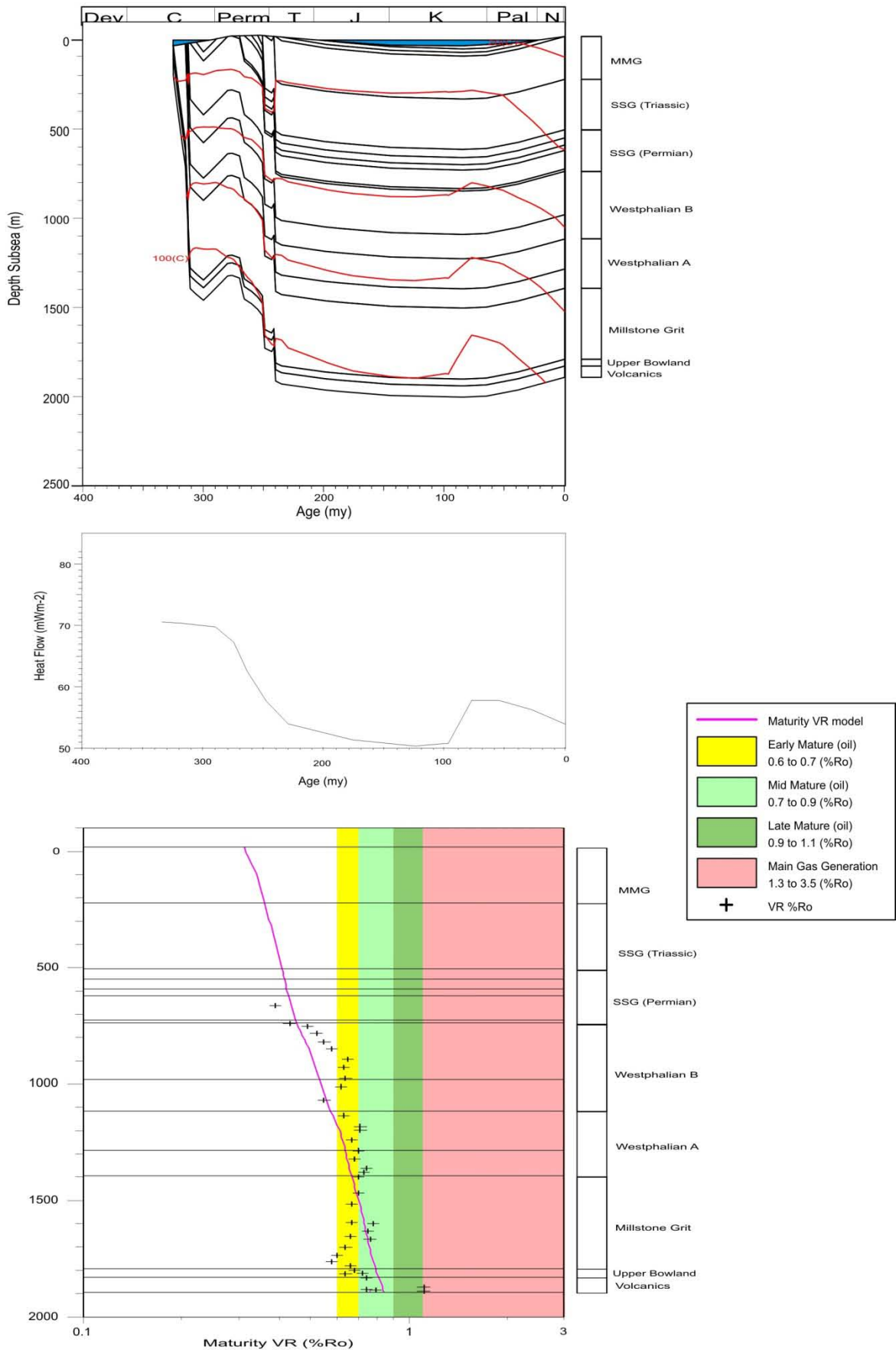
Figure 21. Gainsborough 2 model, 21a (top) shows the depositional history, 21b (centre) shows the modelled palaeo-heat flow and 21c (bottom) shows the modelled VR maturity and VR data.

6.2.2 Gainsborough 2

The Gainsborough 2 borehole penetrates through Permian sediments to the Upper Bowland Shale (Figure 21a). Thirty nine VR data were available and the model fit is reasonable, though there is a broad scatter on the data.

The model heat flow is quite low, having a heat flow of around 70 mWm^{-2} during the late Carboniferous (Figure 21b). The deepest Bowland Shale sediments reached temperatures of over 100°C (Figure 21a). The Upper Bowland Shale reached the oil generation window during Carboniferous burial. An estimated 110 m of Carboniferous sediment was removed during uplift during the Variscan Orogeny. Deposition during the Permian – Cretaceous was quite thin in comparison with other wells in this area; only 515 m is proven in the borehole and a modelled additional 85 m of Permian – Cretaceous sediments eroded by the Hardegsen and Palaeocene – Recent erosion were included in the model. Both the low heat flow and thin sediment deposition seem unusual given the location is not particularly close to the Gainsborough Trough margins. The fit of the 1-D model clearly shows the compromise made here between palaeo-heat flow and eroded sediment thicknesses; if a greater palaeo-heat flow had been modelled to better match the gradient, then the estimated thicknesses of eroded sediment would have been even smaller.

6.2.3 Kirk Smeaton 1

Kirk Smeaton 1 lies on a northern basin bounding fault on the Gainsborough Trough. The modelled heat flow is quite low having a heat flow of around 65 mWm^{-2} during the late Carboniferous. The model indicates that the Lower Bowland Shale reached temperatures of 120°C during Carboniferous burial and 140ºC during Cretaceous burial (Figure 22a). An estimated 1 km of sediment was removed during the Variscan Orogeny. A small remnant of Permian Collyhurst Sandstone is present in the borehole. The removed thicknesses of the Permo-Triassic and Jurassic – Cretaceous layers were 450 m and 800 m respectively. The model fit is reasonable (Figure 22c) and the low heat flow and thin sediments are typical of boreholes closer to the basin margin than the basin depocentre. The fit of the 1-D model clearly shows the compromise made here between palaeo-heat flow and eroded sediment thicknesses; if a greater palaeo-heat flow had been modelled to better match the gradient, then the estimated thicknesses of eroded sediment would have been even smaller.

6.2.4 2-D section

Figure 23 and Figure 24 show the 2-D model which was generated using the 1-D models as a basis. Figure 23 shows the current sediment thicknesses across the basin as interpreted from seismic data. A good fit to the VR data was achieved (Figure 24 and Figure 26). This section clearly shows the impact of the modelled eroded sediments on the maturity of the basins. The deepest parts of the basin have gone through the gas window and are now over-mature (Figure 25). Note that the reverse fault near Eakring has been included as a normal fault in order to model the sediments as BasinMod 2-D cannot include repeated layers in vertical section (Figure 23). Also, where the Variscan erosional surface has been removed, most the eroded thickness of Carboniferous sediments has been added to the thickness removed by the most recent erosion.
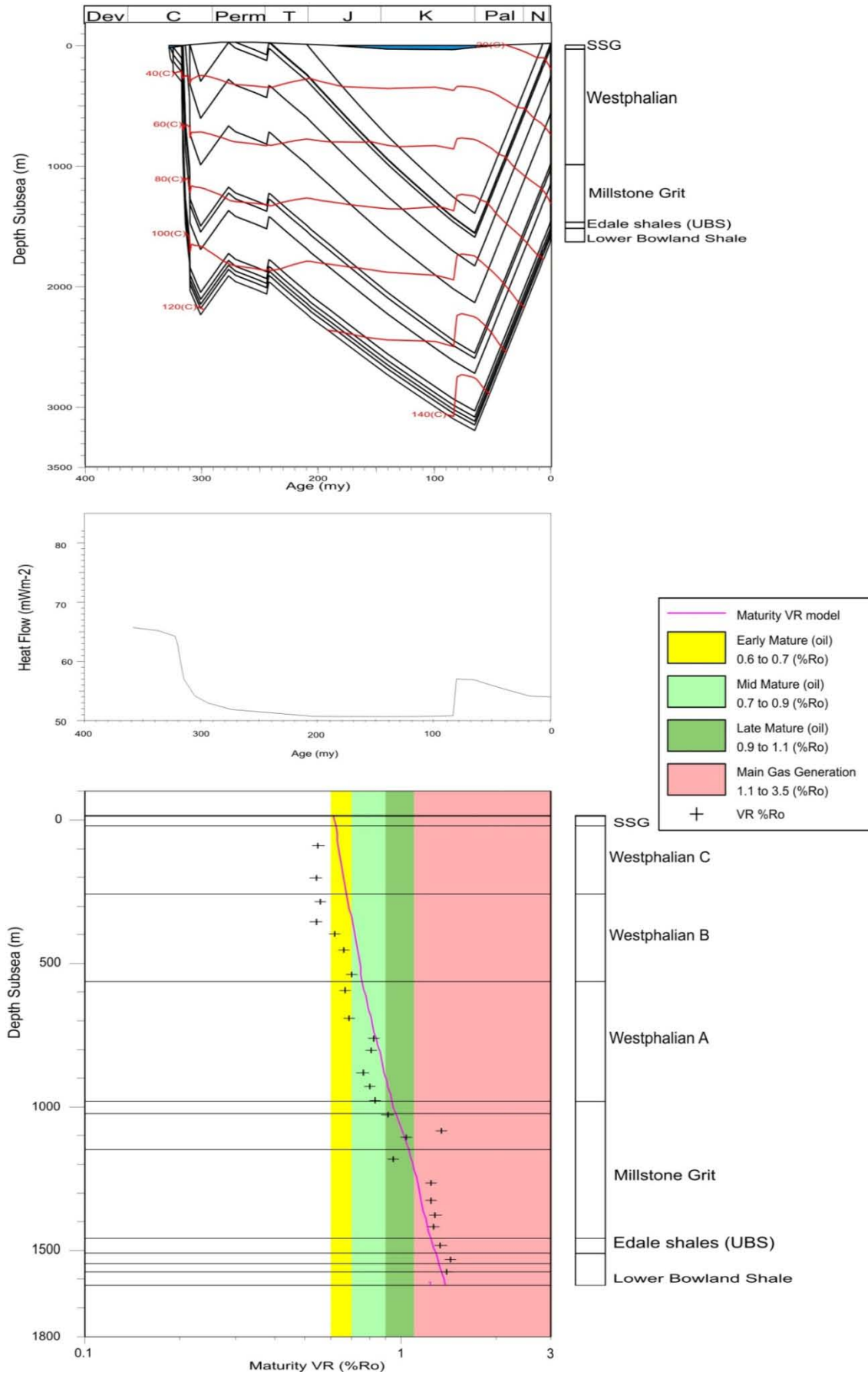
Figure 22. Kirk Smeaton model, 22a (top) shows the depositional history, 22b (centre) shows the modelled palaeo-heat flow and 22c (bottom) shows the modelled VR maturity and VR data.
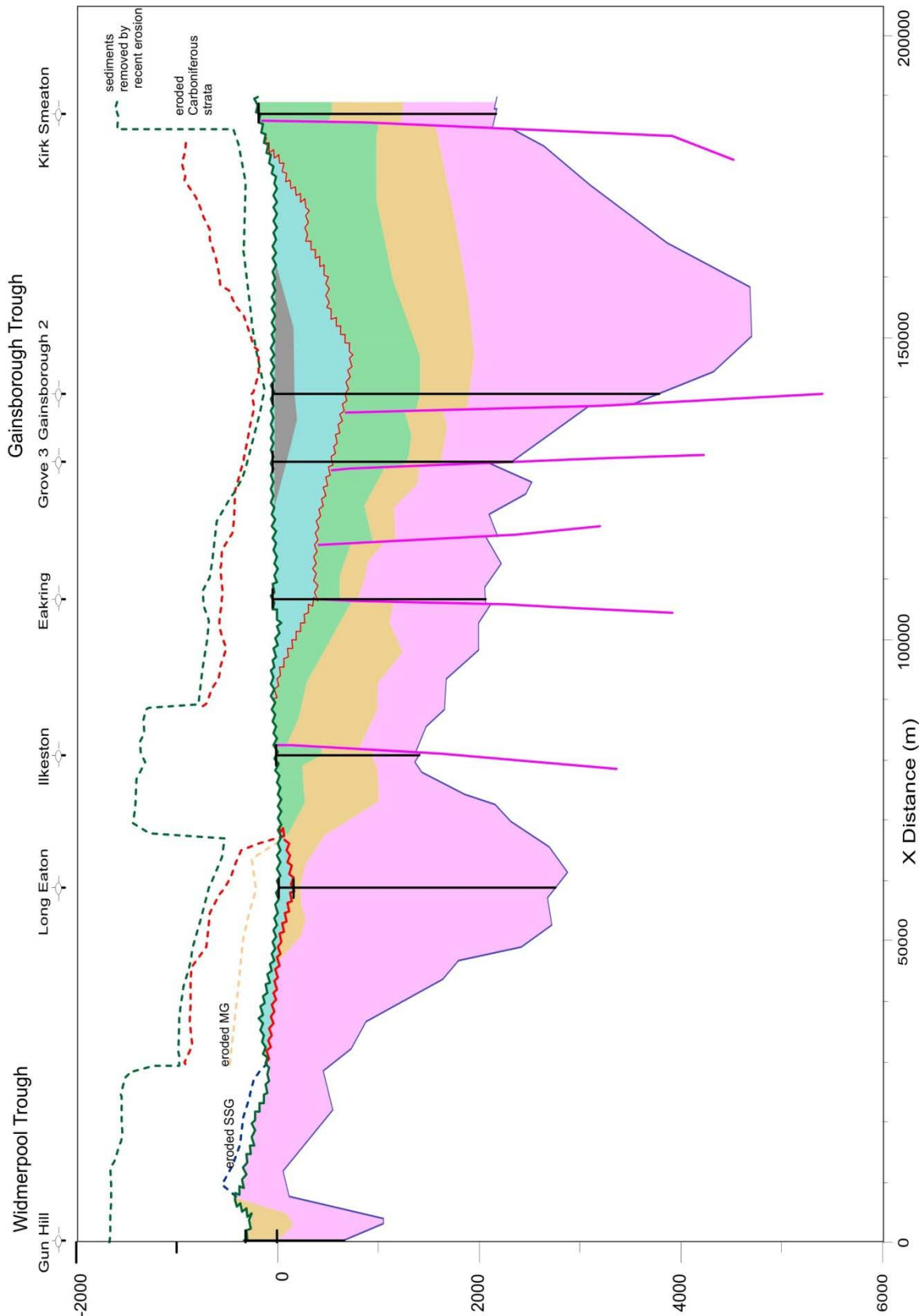
Figure 23. 2-D section across the Widmerpool Gulf and Gainsborough Trough. Grey is MMG, blue is SSG and Permian, green is Westphalian, orange is Millstone Grit, pink is the Bowland-Hodder unit. The green unconformity is the current land surface, the red unconformity is the Variscan Unconformity. Dashed lines show eroded thicknesses of strata (the thickness between the unconformity/underlying eroded layer and the dashed line represents the eroded thickness). The bottom of the model is Top Chadian.
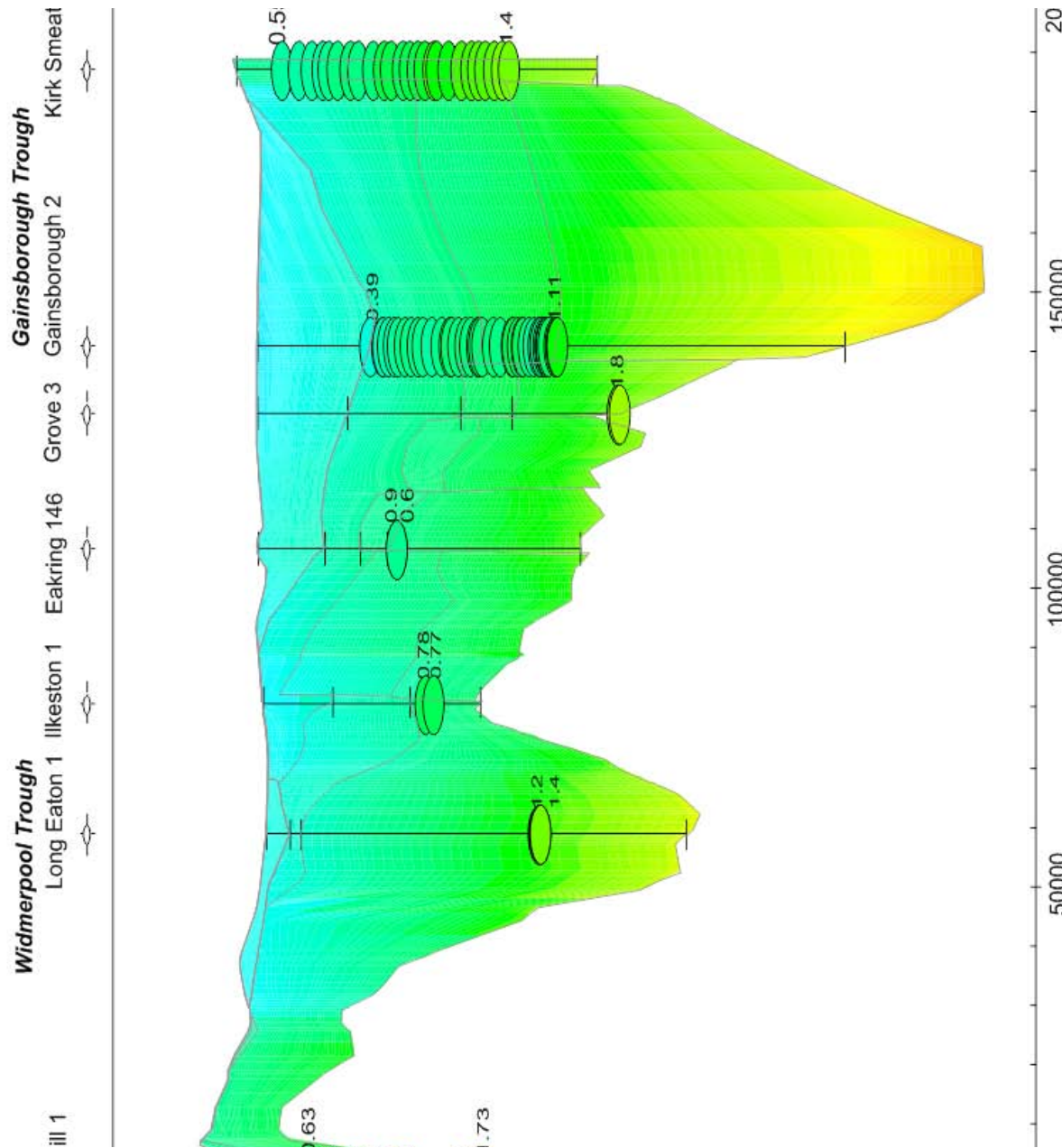
Figure 24. Maturity for the Widmerpool Trough – Gainsborough Trough 2-D section, the continuous colour shows the maturity based on the model, for comparison, the ovals show the measured VR data at the wells.
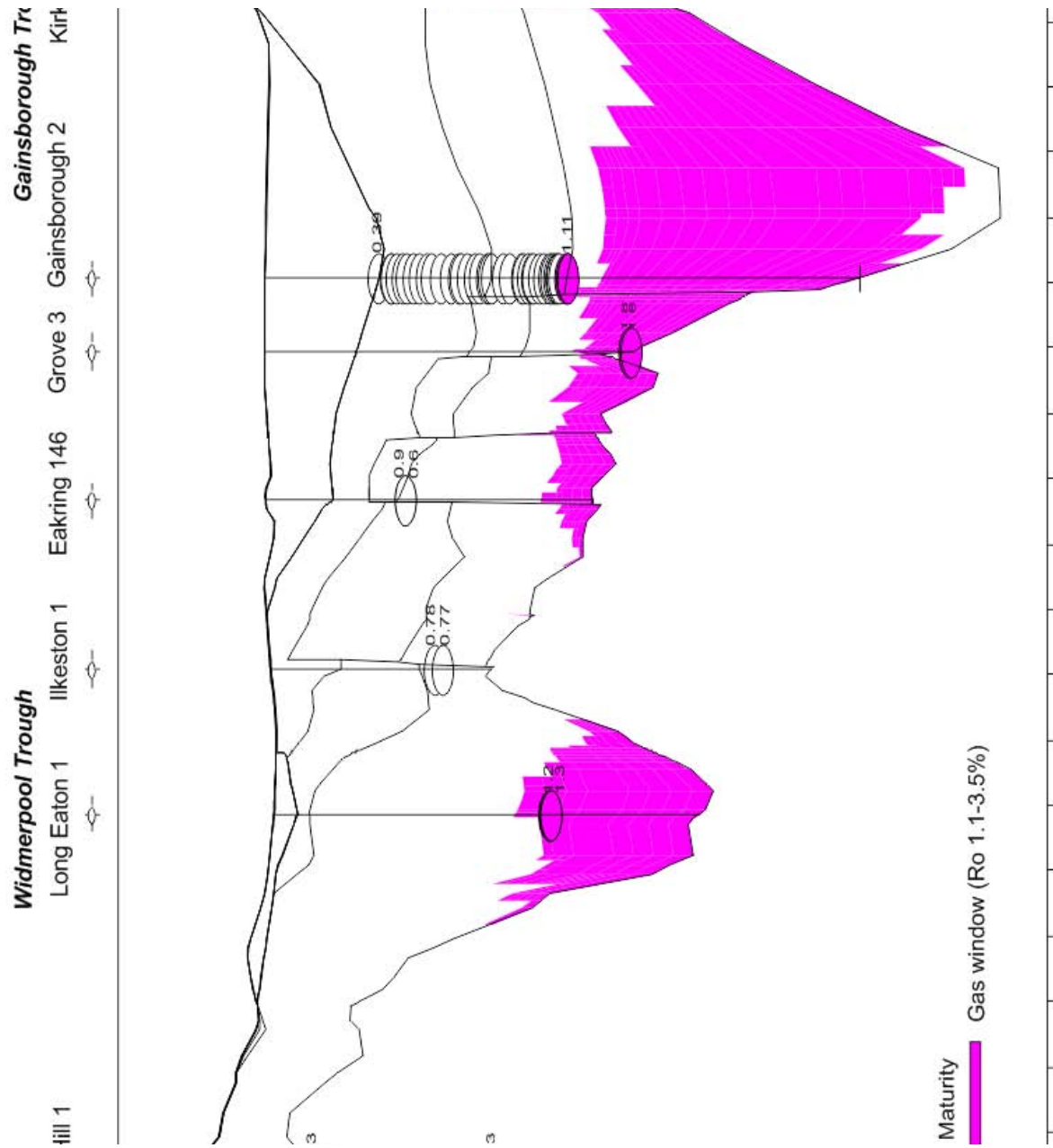
Figure 25. Present day gas window for the Widmerpool Trough - Gainsborough Trough 2-D section model.
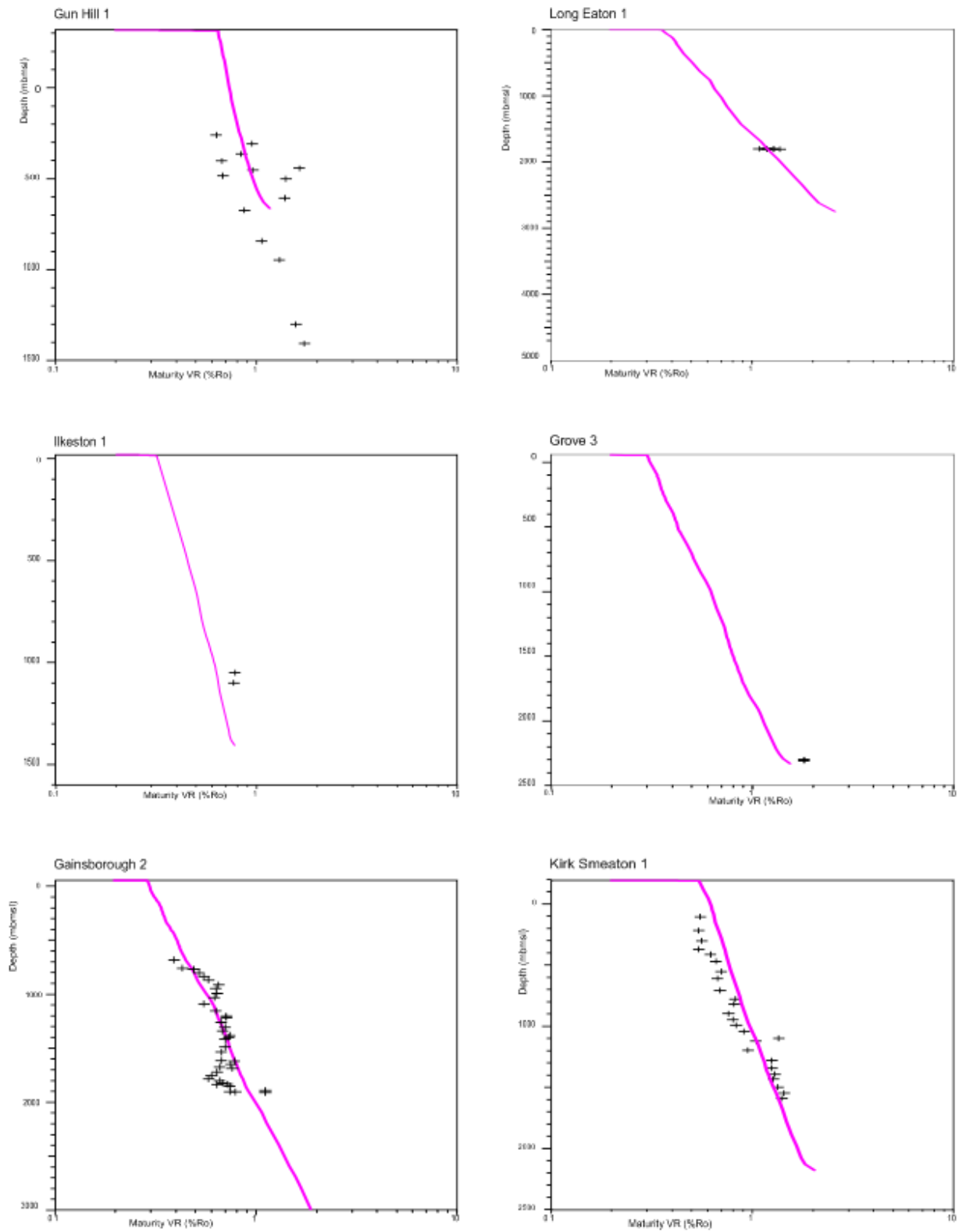
Figure 26. Maturity model at borehole locations across the Widmerpool Trough - Gainsborough Trough 2-D section. Pink line shows the modelled maturity, black crosses show VR data.

Glossary

LBS   Lower Bowland Shale

MG   Millstone Grit Group

MMG   Mercia Mudstone Group

SSG   Sherwood Sandstone Group

UBS   Upper Bowland Shale

VR   Vitrinite reflectance

References

British Geological Survey holds most of the references listed below, and copies may be obtained via the library service subject to copyright legislation (contact libuser@bgs.ac.uk for details). The library catalogue is available at: http://geolib.bgs.ac.uk.

AITKENHEAD, N., BARCLAY, W. J., BRANDON, A., CHADWICK., R. A., CHISHOLM, J, I., COOPER, A. H. AND JOHNSON, E. W. 2002. British Regional Geology. The Pennines and adjacent areas. Fourth Edition. *British Geological Survey, Nottingham*

BGS 2009, Geological Time Chart, version 6 March 2009

BURLEY, A. J., EDMUNDS. W. M. AND GALE. I. N. 1984. Investigation of the geothermal potential of the UK. Catalogue of geothermal data for the land area of the United Kingdom. Second revision*. British Geological Survey, Nottingham*

DOWNING, R. A. AND GRAY, D. A. (EDITORS) 1986. Geothermal Energy – the potential of the United Kingdom. *Her Majesty's Stationary Office, London*

GRADSTEIN., F. M., OGG., J. G. AND SMITH, A. G. (EDITORS) 2004. A geologic time scale. *Cambridge University Press, Cambridge*.

HAINS, B. A. AND HORTON, A. 1969. British Regional Geology. Central England (Third Edition). *Her Majesty's Stationary Office, London*

INTERNATIONAL COMMISSION ON STRATIGRAPHY (ICS), 2006. International Stratigraphic Chart 2006. www.**stratigraphy**.org/

JARVIS, G. T. AND MCKENZIE, D. P. 1980. Sedimentary Basin Formation with Finite Extension Rates. *Earth and Planetary Science Letters* **48,** *42-52.*

LEWIS. C. L. E., GREEN, P. F., CARTER, A. AND HURFORD A. J. 1992. Elevated K/T palaeotemperatures throughout Northwest England: three kilometres of Tertiary erosion? *Earth and Planetary Science Letters* **112,** *131-145.*

PEARSON, M. J., AND RUSSELL, M. A. 2000. Subsidence and erosion in the Pennine Carboniferous Basin, England: lithological and thermal constraints on maturity modelling. *J. Geol. Soc. Lond. Vol* **157,** *471-482.*

PHARAOH, T. C., VINCENT, C. J., BENTHAM, M. S., HULBERT, A., WATERS, C. N. AND SMITH N. J. P. 2011. Structure and evolution of the East Midlands Region of the Pennine Basin. British Geological Survey Subsurface Memoir. *BGS, Keyworth* 144pp

PLANT, J. A., JONES, D. G. AND HASLAM, H. W. (ed.) 1999. The Cheshire Basin. Basin evolution, fluid movement and mineral resources in a Permo-Trias rift setting. *Keyworth, Nottingham: British Geological Survey*.

ROWLEY, E. & WHITE, N. 1998 Inverse modelling of extension and denudation in the East Irish Sea and surrounding areas. *Earth and Planetary Science Letters* **161,** 57–71.

SCLATER, J. G. AND CHRISTIE, P. A. F. 1980. Continental Stretching: An Explanation of the post-mid-Cretaceous Subsidence of the Central North Sea Basin. *J. Gephys. Res. 85, 3711-3739.*

SMITH, N., VANE, C. & MOSS-HAYES, V. 2012. Rock-Eval geochemical analysis of 109 samples from the Carboniferous of the Pennine Basin, including the Bowland-Hodder unit. Appendix to DECC final report.

STACH, E., MACKOWSKY, M.TH., TEICHMULLER, M.,TAYLOR, G. H., CHANDRA, D., TEICHMULLER, R. 1982. Stach's Textbook of Coal Petrology (3rd ed.) *Gebruder Borntraeger, Berlin, Stuttgart*

VINCENT, C. J. AND MERRIMAN, R. J. 2002. Thermal Modelling of the Cheshire Basin using BasinMod™. *British Geological Survey Internal Report*, IR/03/092. 223pp.

C.J. Vincent & I.J. Andrews